

Republic of Iraq
Ministry of Higher Education
And Scientific Research
Al-Nahrain University
College of Science
Department of Physics



Development and Optimization of Stand off Explosive Material Detection System

A Dissertation

Submitted to the College of Science Al-Nahrain University in Partial
Fulfillment of the Requirements for the Degree of Doctor of Philosophy in
Physics

By

Wildan Mohammed Awad

B.Sc. Physics/College of Science for Women /Baghdad University (1999)

M.Sc. Physics/College of Science for Women /Baghdad University (2004)

Supervised by

Dr. Suha Mousa Khorsheed
(Assistance Professor)

Dr. Kamal Husain Lateef
(Chief Researchers)

October 2016

Muharram 1437

بِسْمِ اللَّهِ الرَّحْمَنِ الرَّحِيمِ

﴿يَرْفَعُ اللَّهُ الَّذِينَ آمَنُوا مِنْكُمْ وَالَّذِينَ أُوتُوا

الْعِلْمَ دَرَجَاتٍ وَاللَّهُ بِمَا تَعْمَلُونَ خَبِيرٌ﴾

صَدَقَ اللَّهُ الْعَظِيمُ

{سورة المجادلة * الآية ١١ *}

Supervisors' Certification


We certify that this thesis entitled "**Development and Optimization of Standoff Explosive Material Detection System**" was prepared by *Wildan Mohammed Awad* under our supervision at the College of Science/Al-Nahrain University in partial fulfillment of the requirements for the Degree of Doctor of Philosophy in Physics.

Signature: 

Name: **Dr. Suha Mousa Khorsheed**

Title: Assistant Professor

Date: *28 / 3 / 2017*

Signature: 

Name: **Dr. Kamal Husain Lateef**

Title: Chief Researchers

Date: / / 2017

In view of the available recommendations, I forward this thesis for the debate by the examination committee.

Signature: 

Name: **Dr. Saad Naji Abood**


Title: Professor


Address: Head of physics Department

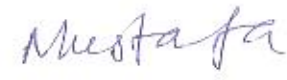
Date: *28 / 3 / 2017*


Committee Certification


We examination committee certify that we have read the Thesis entitled "Development and optimization of standoff Explosive Material Detection System", and examined the student "Wildan Mohammed Awad" in its contents and that in our opinion; it is accepted for the Degree of Doctor of Philosophy in Physics.


Signature: 
Name: *Dr. Ahmed Farhan Atwan*
Title: Professor
Address: College of Education, Al -Mustansiriyah University
Date: 28/3 /2017
(Chairman)


Signature: 
Name: *Dr. Thamir Abdul-Jebbar Jumah*
Title: Assistant Professor
Address: College of Science, Al-Nahrain University
Date: 28/3 /2017
(Member)

Signature: 
Name: *Dr. Mustafa Kamil Jassim*
Title: Assistant Professor
Address: College of Education Ibn Al Haitham, Baghdad University
Date: 28/3 /2017
(Member)

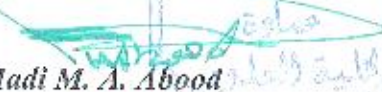
Signature: 
Name: *Dr. Abdulhussain K. Eltayef*
Title: Chief of Researchers
Address: Ministry of Science and Technology
Date: / /2017
(Member)

Signature: 
Name: *Dr. Anwaar A. Al-Derguzly*
Title: Assistant Professor
Address: College of engineering, Al-Nahrain University.
Date: / /2017
(Member)

Signature: 
Name: *Dr. Suha Mousa Khorsheed*
Title: Assistant Professor
Address: College of Science, Al-Nahrain University
Date: 28/3 /2017
(Member/Supervisor)

Signature: 
Name: *Dr. Kamal Husain Lateef*
Title: Chief Researchers
Address: Ministry of Science and Technology
Date: 28/3 /2017
(Member/Supervisor)

I, hereby certify upon the decision of the examining committee.

Signature: 
Name: *Dr. Hadi M. A. Abood*
Title: Professor
Address: Dean of College of Science
Date: 11 / 4 /2017



Dedication

*Firstly, I dedicate my work.... to Iraq
Who create, letters and numbers
Which, without, no sun, have been rise on civil,
To all, I present this work.*

Then,

I dedicate my work to...

*My Advisor Dr. Kamal H. Lateef
Who gave me the knowledge in my research and who
guided me to complete my work.*

Acknowledgements

I am extremely grateful to my supervisor Dr. Kamal H. Lateef and Dr. Suha Mousa Khorsheed, for their patient, motivation and knowledge that helped me at various stages of my research.

Special thanks to the head and the staff of the physics department specially Dr. Ahmad K. Ahmad .

I would like to thank Dr. Alaa Husain for his advice to me during the research and I am also thankful to Ghaidaah Hamza and Noon Kadim for introducing the help to me along the time of the practical work, and big “thank you” to everybody who participated in this study.

Wildan Mohammed

Abstract

In order to develop a effected method to reveal the presence of explosive, numerous detection techniques have been studied that are capable of detecting explosives, The current study provides an overview of the present techniques like LIBS which is an atomic spectroscopy, and examined a new technique for detecting called laser induced fluorescence (LIF).

LIF essentially measures the optical emission of the excited energetic materials by laser. The use of LIF has led to the discovery of unreported optical characteristics of some compounds that are exclusive to the individual material, like the phase shift and the modulation depth of the fluorescence signals.

A high resolution spectrometer is used to record the fluorescence emission wave length for three types of explosive materials, These optical characteristics consist of fluorescence shoulders of the three samples in the wave length between (300 -370) nm .

Using fast rise time photo multiplier and spatial amplification for the fluorescence signal enable us to detect the time domain fluorescence spectrum for three types of explosive materials (AN), (TNT),(C4) and other non-explosive material, this method used Carefully for 8m standoff detection, different type of substrate is examined to simulate the real scan, both the time domain and frequency domain is measured for efficient LIF spectroscopy that give us a total configuration of the tested sample.

A library of a total time configuration for different type of material s spectrum enables us to develop a algorithms to distinguish between explosive and non-explosive material. Used to develop a recognition program to achieve high sensitive detection system.

Table of Contents

Chapter One Introduction		
	Table of Content	ii
	List of Table	ix
	List of Abbreviation	x
	List of samples	xii
1.1	Overview	1
1.2	Literatures Survey	2
1.2.1	LIBS Previous Studies.	3
1.2.2	LIF Previous Studies	5
1.3	Aim of the Work	6

Chapter Two- Theoretical Background		
2.1	Explosive detection	7
2.1.1	Non-Standoff Explosive Detection	7
	A. Ion Mobility Spectrometry	7
	B. Fluorimetric And Colorimetric	8
2.1.2	Standoff Explosive Detection	9
	A. Bulk Detection	10
	1. Backscatter X-Ray	10
	2. Infrared	11
	3. Terahertz	11
	4. Neutron And Gamma-Ray Explosive Detection	12

	B. Trace Detection	13
	C. Optical Detection	14
	1- LIDAR, DIAL, and DURL	16
	2- LIBS technique	17
	3- Laser-Induced Fluorescence Spectroscopy (LIF)	19
	4- Raman spectroscopy (RS)	20
	5- UV Raman spectroscopy (UVRS)	21
2.2	Energetic Materials and Their Characteristics	28
2.1.1	Common types of Energetic Materials	28
	1. (TNT)	28
	2. (RDX)	30
	3. (AN)	31
2.2.2	Chemical Properties of Energetic Materials	32
2.2.3	Extinction Spectra of Explosives Martials	34
2..2.4	Ultraviolet and Visible Range (180-750nm)	35
2.3	Absorption and Emission Light by Atoms and Molecules	36
2.4	Principles of LIBS	40
2.4.1	Energy Source	41
2.4.2	Plasma Formation and Post-Breakdown Phenomena On Solid Targets	42
2.4.3	LIBS of Explosives	45
2.5	LIF Technique	48
2.5.1	Fluorescence Emission	49
2.5.2	Fluorescence Spectra	50

2.5.3	LIF of Explosives	52
Chapter Three Experimental set up		
3.1	LIBS Experimental set up	54
3.1.1	Experimental instrument	55
	A. The Laser System (Nd-YAG)	56
	B. Plasma emission analysis system	57
3.1.2	Measuring of Laser Beam Diameter	58
3.1.3	The energy rate calculation	59
3.2	LIF Experimental set up	60
3.2.1	Experimental Instrument .	61
	A. The Laser System	61
	B. Optical Filters	62
	B. UV Detector	63
3.2.2	Fluorescence Measurements	64
3.3	Explosive Material Samples	64
3.3.1	Sample Positioning System	65
3.3.2	Sample Preparation	65
3.3.3	Substrate	65

Chapter Four Analytical and Experimental Result		
4.1	Experimental Results	66
4.1.1	LIBS Results	66
	A. TNT Sample	67
	B. Ammonium Nitrate (AN) Sample	69
	C. C4 Sample	74
4.1.2	Fluorescence Results	74

	A. Frequency Domain Results	74
	1. TNT Sample	75
	2. (AN) Sample.	75
	3. C4 Sample	76
	B. Time Domain Results	77
	1. TNT Sample	77
	2. (AN) Sample	78
	3. C4 Sample	79
	C. Simulated Samples Test	83
	1. Car Paint	83
	2. Glass	86
	D. LIF Peak Calculations	91
	1. C4 Fluorescence Spectrum Analysis	91
	2. AN Fluorescence Spectrum Analysis	92
	3. TNT Fluorescence Spectrum Analysis	93
	E- Explosive Detection Program	94

Chapter Five conclusions and Suggestions of Future Work		
5.1	Conclusions	98
5.2	Suggestions for Future Work	99

List of Figures

	Chapter 2	
2.1	Ion Mobility Spectrometry	8
2.2	fluorescence quenching explosive sensor	9
2.3	Terahertz Scanner	12
2.4	The laser setup for the LIDAR UVLIF bio-aerosol detection system	17
2.5	Laser Induced Breakdown Spectroscopy (LIBS) system	18
2.6	Laser-Induced Fluorescence Spectroscopy (LIF)	20
2.7	Raman Spectroscopy.	20
2.8	Schematic diagram of UV Raman LIDAR instrument	23
2.9	The structure of the hybrid sensor system that uses Raman spectroscopy and laser-induced breakdown spectroscopy (LIBS)	24
2.10	TNT Molecular structure	31
2.11	RDX Molecular structure	32
2.12	AN Molecular structure	33
2.13	Typical absorption spectra for explosives	36
2.14	Nuclear Configuration	39
2.15	Nomenclature for electron spin pairing in molecular electronic states	40
2.16	Triplet excited state	40
2.17	Diagram of a typical LIBS experiment	41
2.18	Schematic Energy Levels of an Nd:YAG Laser	43
2.19	Illustration Of Plasma Shielding Effect	44
2.20	Ionization by multiphoton absorption	45
2.21	LIBS spectra of some energetic materials	47
2.22	The excited and the florescence pulses	53

	Chapter 3	
3.1	Structure of LIBS Experimental	55
3.2	Experimental setup of LIBS system	56
3.3	Structure of Spectrometer Device	57
3.4	The structure of fluorescence Experimental	60
3.5	LIF laboratory experimental setup	61
3.6	QUANTEL – Brilliant / Brilliant B Laser System	61
3.7	Optical Filters Spectrum	63
3.8	Explosive samples	65
	Chapter 4	
4.1	LIBS spectrum of TNT material	67
4.2	LIBS spectrum analysis of TNT material in air	68
4.3	LIBS spectrum of AN material ...	70
4.4	LIBS spectrum analysis of AN material in air	71
4.5	LIBS spectrum of C4 material	72
4.6	LIBS spectrum analysis of C4	73
4.7	Fluorescence spectrum of TNT material	75
4.8	Fluorescence spectrum of AN material	75
4.9	Fluorescence spectrum of C4 material	76
4.10	Fluorescence spectrum in time domain of TNT	77
4.11	Fluorescence spectrum in time domain of AN	78
4.12	Fluorescence spectrum in time domain of C4	80
4.13	Diagram shows the relation between frequency domain and time	83
4.14	Fluorescence spectrum of car paint	84
4.15	Fluorescence spectrum of car paint with AN on it	85
4.16	Fluorescence spectrum of car paint with C4 on it	86

4.17	Fluorescence spectrum of glass	87
4.18	Fluorescence spectrum of glass with AN on it	88
4.19	Fluorescence spectrum of glass with C4 on it	89
4.20	Comparison between fluorescence spectrums of C4	90
4.21	Comparison between fluorescence spectrums of AN	90
4.22	Fluorescence spectrum analyzes of C4	92
4.23	Fluorescence spectrum analyzes of AN	93
4.24	Fluorescence spectrum analyzes of TNT	94
4.25	Algorithm scheme of explosive detection program	95
4.26	Explosive detection program UI	96
4.27	Explosive detection program result	97

List of Table

2.1	Physical and chemical properties of common explosives	34
3.1	QUANTEL – Brilliant / Brilliant B Laser System Specification	62
4.1	Spectral Transition in the LIBS spectrum of TNT with assignment	69
4.2	Spectral Transition in the LIBS spectrum of AN with assignment	71
4.3	Spectral Transition in the LIBS spectrum of C4 with assignment	73

List of Abbreviation

Abbreviation	Description
AN	Ammonium nitrate
ANFO	Ammonium Nitrate Fuel Oil
CCD	Charge-Coupled Device
CW	Continuous Wave
DIAL	Differential Absorption LIDAR
DIRL	Differential Reflectance LIDAR
DNT	Dinitrotoluene
EGDN	Ethylene Glycol Denigrate
EVP	Explosive Vapors Pressure
FPDs	Flat Panel Detectors
fS	Femtosecond (10^{-15} Second)
HMEs	Homemade Explosive
HMTD	Hexa methylenetriperoxidediamine
HMX	Cyclotetramethylenetetranitramine
ICCD	Intensified Charge-Coupled Device
IED	Improvised Explosive Device
IMS	Ion Mobility Spectrometry
IR	Infrared
ITMS	Ion Trap Mobility Spectrometer
kcal	Kilo calorie Per Mole
LIBS	Laser Induced Breakdown Spectroscopy
LIDAR	Light Detection And Ranging
LIF	Laser Induced Fluorescence
NG	Nitro-Glycerine
ns	Nanosecond (10^{-9} Second)
PETN	Penta erithrylte tranitrate
PF	Photo- Fragmentation
PFNA	Pulsed Fast Neutron Analysis
PMT	Photomultiplier Tube
ppb	Parts-Per-Billion, 10^{-9}
ppm	Parts-Per-million, 10^{-6}
ppt	Parts-Per-Trillion, 10^{-12}
RDX	(Research Department explosive) or (Royal Demolition explosive) – Cyclotri methylene trinitramine
RSL	Raman scattered light
SERS	Surface Enhanced Raman Scattering
SNR	signal-to-noise ratio

SORS	Spatially offset Raman spectroscopy
TATP	Tri acetone tri peroxide
TFT	Thin Film Transistors
THz	Terahertz
TNA	Thermal Neutron Activation
TNT	Tri nitro toluene
UN	Urea Nitrate
UV	Ultraviolet
UVRS	UV Raman spectroscopy
VIS	Visible
VRS	Visibly Raman spectroscopy
μJ	Micro joule (10^{-6} Joule)

List of samples

Sample	Description
K^+	Potassium Ions
NH_4NO_3	Ammonium nitrate
KNO_3	Potassium Nitrate
$NaNO_3$	Sodium Nitrate
NO_2	Nitrites
NO	Nitric Oxide
C_3H_8	Propane
CH_4	Methane
$KClO_3$	Potassium Chlorate
$NaClO_3$	Sodium Chlorate
$Pb(N_3)_2$	Lead Azide
AgN_3	Silver Azide
HN_3	ammonia
C–N	Carbon–Nitrogen Bond
O–N	Oxygen –Nitrogen Bond
N–N	Nitrogen–Nitrogen Bond
O–O	Oxygen – Oxygen
A	Absorbance
C	Concentration of the Absorbing Species in the Sample
ℓ	Path Length
ϵ	Molar Extinction Coefficient
E	Photon Energy
h	Planck's Constant
ν	Frequency
c	Speed of Light
λ	Wavelength
T	Transmittance

I	Intensity of the Light Coming Out of the Sample
I_0	Intensity of the Incident Light
T1	triplet excited state
m_e	Electron Mass
ω	Frequency of the Laser Radiation
e	Electron Charge
S1	Singlet excited state
Hg	Mercury
Xe	Xenon

Chapter One

Introduction

1.1 Overview

Recently, terrorist attacks in several places have elevated national and international security concerns. Work has quickly been done to create an effective sensor and ways for the detection of explosives which have been ongoing for the past few decades. Having an impact in both national security and environmental safety, the need for a sensitive and selective detection method is still relevant as the acts of terrorism continue and landmines remain undiscovered [1,2].

There are several kinds of explosives which have a variety of trinitrotoluene (TNT), pentaerithrityltetranitrate (PETN), cyclotrimethylene trinitramine (RDX), and cyclotetramethylene tetranitramine (HMX). Military explosive chemicals usually consist of: N-NO₂ in nitramines such as (RDX and HMX), O-NO₂ in nitrate esters [EGDN (ethylene glycol dinitrate), PETN and NG (nitro-glycerine)], and C-NO₂ in nitro aromatics such as (TNT) [3].

Nitro glycerine is commonly used in solid rocket propellants. The Nitro glycerine and the Ethylene Glycol Dinitrate are glutinous liquid explosives which can be mixed to use in dynamites. The NH₄NO₃ (Ammonium nitrate), which is a widespread fertilizer, is usually employed to fabricate the (HMEs) homemade explosive. The solid rocket propellants usually use an oxidizer that is ammonium perchlorate [NH₄ClO₄ (AP)]. Plastic explosives such as Semtex-H (made up of PETN and RDX) and C₄ (made up of plasticizers and RDX) have

become widely used in fabric terrorist bombings. The sodium nitrate (NaNO_3) and potassium nitrate (KNO_3) are commonly used in fabricating the black powder. The peroxide based explosives, including hexamethylene triperoxide diamine (HMTD) and triacetone triperoxide (TATP), also became widely used by terrorists in the past few years since they are easily created from available materials, They are extremely unstable with rapid oxidized bond (O-O) that makes them easy to explode and initiate [4].

The explosive materials usually have smaller vapour pressures (ppb) which make them hard to detect. Techniques for detecting the vapour should have the ability to detect very little concentrations and/or large volume samples. Moreover, packaging and wrapping the explosives (for example inside a plastic bag) should certainly minimize the efficient vapour pressure by a number of orders of magnitude, which makes the explosive vapour detection be very difficult. Explosive analyses, which have typically low vapor pressures, present many difficulties in the field of detection, requiring innovated ideas for improvement. Varying approaches have been considered to solve the problem of undetected explosives [5].

1.2 Literatures Survey

The recent years have seen a rapid growth of explosive detection solutions. Several explosive detection techniques exist based on a wide variety of current and developing technologies. An ideal explosive detection technique would classify all explosive samples as explosives and would not misclassify any non-explosive sample as explosive. In this thesis, we exploit the previous results derived from the works of several research groups investigating standoff LIF and LIBS to further

improve the ability to detect high explosives at standoff distances by evaluating the possible gains achievable using LIF, LIBS to detect explosives. At first we have focused on the study of the molecules property of the explosive material and studied the optical absorption with the chemical property of the TNT material, the absorption of that material lies in the UV region. Also, we studied the absorption spectrum of a different type of explosive materials and compared the Previous Studies concerning the UV-VIS LIF to detect explosive molecules.

1.2.1 LIBS Previous Studies

Many standoff LIBS devices for the detection of explosives have been demonstrated in the last decade. Some focused on improved system, detection of explosive materials, another study examined the environmental factors, the instrumental parameters, the chemical and physical properties of the sample that significantly affected the analytical performance.

In 2000, Anzano et al [6], used LIBS to see if linear correlation techniques would allow sorting of a variety of plastics, including polystyrene and high-density polyethylene. Subtle differences in the carbon and hydrogen intensities enabled successful identification 90% to 99% of the time. Portnov et al. 2003 [7], used LIBS to investigate the spectral signatures of Nitro aromatic and polycyclic aromatic hydrocarbon samples. They observed the atomic emission lines associated with C, H, N, and O.

In 2006, Ferioli and Buckley [8] used LIBS to study hydrocarbon mixtures (C_3H_8 , CH_4 , and CO_2 in the air). The strength of the C, N, and O atomic emission lines was investigated in relation to the concentration

of carbon and hydrogen in the samples. In the same year, Lopez-Moreno et al. 2006 [9], presented a mobile cart-sized LIBS system that can detect C4, RDX, and TNT placed on a car door from 30 m away. This study focused on the challenge that field measurements may be faced by using the LIBS technique for unknown samples and determine the capability to recognize explosive spectral signatures in the existence of additional emitting interferes. The authors designed a spectral analysis technique as a flowchart which they utilized to detect the existence of explosives.

Gondal et al. (2007-2008) [10, 11] studied the relationship of signal intensity and laser pulse energy, and the results showed that signal intensity linearly increased with increasing pulse energy from 10 mJ to 30 mJ.

In 2008, Dennis et al [12], studied the enhancement of the LIBS technique by using 10.6 micron CO₂ laser and 1.064 micron Nd:YAG laser, enabling one or two orders of magnitude enhancement factor, depending upon the emission lines observed and the target composition.

Gottfried et al. 2009 [13], researched and designed a principle component analysis and partial least squares chemo-metric software to assist the recognition of explosive spectral signatures in the existence of other emitting interferes on several substrate materials. In same year González et al. [14], discovered that they are able to employ LIBS to determine TNT and C₄ positioned behind transparent sheets of glass and plastic.

In the field of hybrid Raman and LIBS spectroscopy in a single device to be able to measure both molecular and elemental information of the sample, Moros et al. 2011 [15], designed a hybrid Raman&LIBS instrument that used a single 532nm laser pulse to produce both Raman scattering and LIBS plasma, that had been collected by the telescope and redirected into 2 individual spectrometers to be able to collect both spectra at the same time. TNT, DNT, PETN, NH_4NO_3 , RDX, KClO_3 and NaClO_3 were all tested at 20 m distance. In 2013, Lucena et al. [16], lately created an image LIBS system that can image explosive molecules fingerprints to a 30 m distance.

1.2.2 LIF Previous studies

In 2001, Abel et al. [17], studied the NO molecule excitation process and the threshold of the vibrational rotational energy distribution. They detected the emission spectrum of the NO fragment resulted from the interaction between the explosive materials and single UV laser with a wavelength in the absorption rang of the molecule.

many method for increasing the fluorescence signal intensity by studying the effect of the examined molecule state, the soluble explosive increasing fluorescence signals, but the spectrum was shifted according to the solvent type and concentration. To improve the fluorescence process different type of substrate was used with many explosive materials. Tonghun et al. 2007 [18], studied the NO molecule and, the temperature and pressure effect on the fluorescence process and laser wavelength. In 2008, Charles et al. [19], developed a standoff fluorescence based technique to detect trace amounts of explosives by

using (236nm) laser, where the amount of standoff distance is 30cm. Another attempt of their work was to increase the distance for 10s of meters detection of trace explosive residues. They designed a standoff system for detection using 226nm laser to study a different type of explosive material as a solution, the detection limits of the solution are 100ppb. Shiou j. et al. 2012 [20], briefly introduced the principle of Explosive detection using fluorescence polymers and design of the spatial setup to capture the fluorescence signal, the detection data where static and time dependent spectral signature.

1.3 Aim of the Work

The aim of this thesis is to develop and optimize a detection program which has the potential for rapid standoff detection of small amounts of the energetic materials using their distinct and unique optical fluorescence spectrum in the frequency domain and the time domain.

Chapter Two

Theoretical Background

This chapter provides a comprehensive introduction to the detection techniques of the explosives, the types of energetic materials and their chemical, physical and optical characteristics, also elucidates the basic principles of the two techniques used in this research, namely, LIBS and LIF techniques.

2.1 Explosive Detection

There are two approaches fields in the explosive detection: Non-Standoff Explosive Detection and Standoff Explosive Detection. The discussion below summarizes some techniques that have been used, or might be used, for non-standoff and standoff detection of explosive material [21,22]:

2.1.1 Non-Standoff Explosive Detection

Many non-standoff techniques are usually used by military and personnel. Below some of the non-standoff techniques:

A. Ion Mobility Spectrometry (IMS)

It is an analytic procedure, which is commonly used in airports to detect an explosive material. The IMS technology is relatively mature that make it possible for development in a wide field of use. The technique is used surface swabbing to collect samples, then the swab is quickly heated up to evaporate every adsorbed unstable species. The strategy of ‘sniffing’ could also be used where air is taken directly into the Ion Mobility Spectrometry to be tested. The samples added inside the IMS is usually preconcentrated prior to being ionized through radioactive

^{63}Ni , corona discharge, photo-ionization, or electrospray ionization, among other techniques. The ions will be added into a drift tube in addition to a carrier gas that generally purifies air. The electrical field applied over the entire drift tube propels ions via the field at various characteristic velocities that depend upon its charge, mass and collision cross sections prior to being detected (fig. 2.1) [23].

The limits of detection of explosive molecules quickly reach to the Pico gram level. The IMS is largely used as a method for explosive detection since it has become commercialized as being easy to use and having small instruments that create results due in a few seconds. Yet, there are many challenges of IMS technique; this is to the analyzed molecules that should be physically driven to the spectrometer, so it hinders the use of IMS for standoff detection. The need for handling the physical samples will hinder the screening of large objects and also hinder the automated screening.

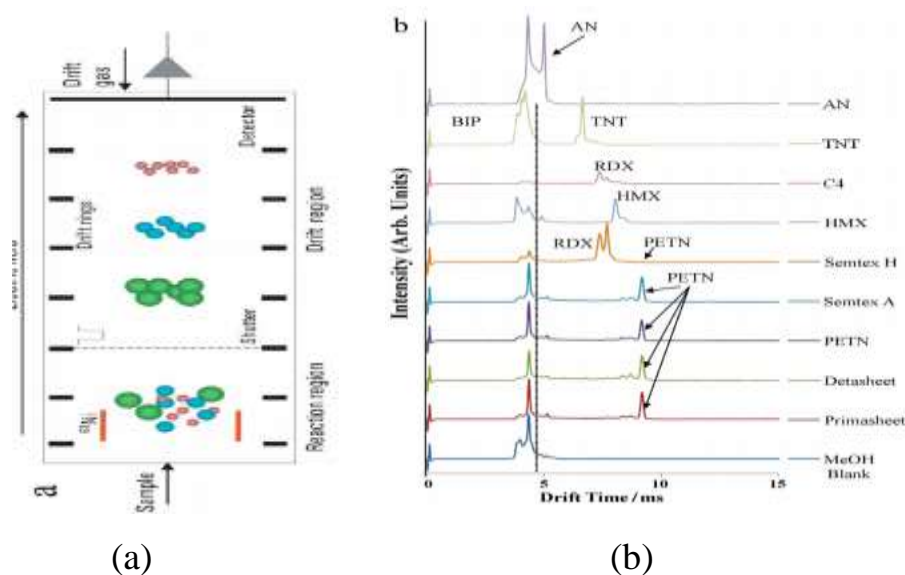


Figure 2.1: Ion Mobility Spectrometry (a) Example of IMS measurement (b) Example spectra of several explosives detected by an ion mobility spectrometer [5].

B. Fluorimetric and Colorimetric

Fluorimetry generate spectral changes via interactions with explosive analyses. The techniques of color-based are simple to understand, and low cost detection that could be done even by untrained personnel in the field. Three wide types of color-based explosive detection exist: fluorescence activation, fluorescence quenching shown in fig 2.2, and colorimetric. The wider challenge facing color-based sensors is usually that every sensor is made to sense a single type and a certain explosive of interest. Therefore, several sensors will be required for the field detection of explosives. These types of techniques are not agreeable to standoff detection [23].

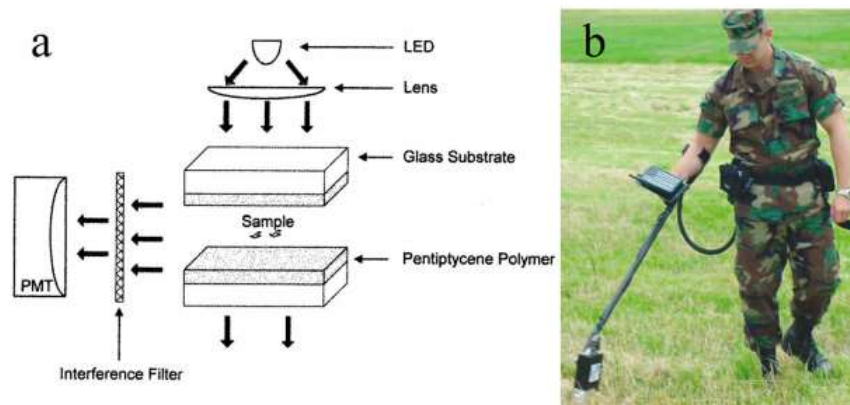


Figure 2.2: fluorescence quenching explosive sensor (a) Schematic of the sensor (b) A fluorescence device [5].

In addition to the prior techniques, there are several different other techniques which have been researched with regards to explosives detection. These techniques involve neutron and mass spectrometry techniques for the explosive identification [24,25]

2.1.2 Standoff Explosive Detection

The non - standoff is extremely undesirable from a safety standpoint, so development focused on standoff techniques to determine the

structure of the sample at a low risk range to help keep both operator and device from damage if an explosion happens. There are many approaches were developed to achieve the standoff explosive detection that can be described as follows

A. Bulk Detection

The scanning methodology is the primary strategy for standoff detection situations. Almost all bombs have unique spatial characteristics and exclusively shaped metal elements like wires, batteries and detonators. Explosive dielectric constants give a minimum of limited discrimination through the background for microwave and X-ray imaging strategies. The scattering, absorption and reflection for several explosives in a number of spectral bands are usually classified, and that info can be utilized for image analysis. This part explains many imaging techniques utilizing radiation with wavelengths covering ranges from radio waves to gamma rays. The majority of the bulk detection approaches which have the possibility of standoff detection include imaging [26].

1. Backscatter X-Ray

It has a good possibility of standoff detection for a distance reaching to 15 meters. Its benefits are great image resolution in addition to limited discrimination approximately explosives and background objects. The drawbacks of X-ray imaging include the identified medical issues that occur due to ionizing radiation along with the legal and cultural issues that occur while imaging people through their clothing. The X-rays standoff distance is a problem, however, the size and cost and of X-ray recognition systems will also be a concern. Sizing is very important in military cases when the movements are so important [27].

2. Infrared

In IR method which is a spectral range between one and ten microns, the explosive packages, clothing, and many other items are impermeable to radiation. Yet, the human body or any other object, near the room temperature passively emits thermal IR radiation, which can be easily recognized by using basic, pretty cheap IR imaging cameras. The objects which slightly differ in their surface temperature can be easily recognized, even for temperature variations under a surface. Studying IR spectral range is required to study the spectroscopic properties such as: thermal emissivity vs. wavelength of clothing, human skin, and other related materials. These details would lead to differential spectroscopic approaches that can enhance IR imaging for explosive detection, which has advantages such as: real-time response, sensitivity and readily, which are accessible technologies for the image patterns that are usual in suicide bomber cases. But it doesn't have the ability to specify explosive type [28].

3. Terahertz

Millimeter wave imaging (1 THz = 0.3 mm wavelength) is currently being developed for imaging of bombs concealed on people. This technique is perhaps better suited than X-ray imaging for personal screening because the radiation involved is non- ionizing, and the technique can even be passive, i.e. one can simply monitor the radiation emitted from the human body to look for anomalies, rather than actively irradiating a test subject. However, the non-ionizing nature of the radiation makes this technology problematic for vehicle screening, because radiation in this wavelength range will not penetrate metal and thus it is impossible to image what is inside a vehicle cargo hold. Furthermore, like X-ray imaging, this technique will only produce an

image that contains possible anomalies it will not specifically identify explosive materials. Standoff imaging of personnel has recently been demonstrated at distances up to 25 feet [25].



Figure 2.3: Terahertz Scanner (a) Visible man holding newspaper, (b) terahertz images displays this man holding a knife concealed in a newspaper and a gun inside the pants [26].

4. Neutron and Gamma-Ray Explosive Detection

The explosive detection by both neutron and Gamma-Ray has problems with a variety of sensitivity limitations and the health hazards for standoff detection. Probing neutron technologies such as thermal neutron activation (TNA) and pulsed fast neutron analysis (PFNA) can be used to inspect the contents of vehicle cargo holds. Neutrons are used to irradiate a vehicle being screened, and gamma rays emitted by nuclei inside the vehicle are detected. In contrast to X-ray imaging, these techniques provide some material specificity, (TNA) identifies nitrogen-rich materials and (PFNA) being capable of characterizing the amounts of several lighter elements in a target material. However, the use of this

technology for standoff detection is problematic for several reasons. Most notably, there is the same $1/r^4$ dependence of the signal intensity as there is in X-ray imaging. In a mode, it is much like that utilized for X-rays. Similar to neutrons, health issues will reduce the scenarios of interest, The main disadvantage of Gamma-ray procedures is usually that the sources used to produce the gamma-ray flux needed for standoff cases are often costly and huge. Studying this field seems to be a lot less promising for standoff detection compared to other techniques [23].

B. Trace Detection

The detection of trace at standoff distances is a very difficult challenge. The pressure of saturated vapour for several popular explosives are extremely low, about (10 ppb) for PETN, RDX and TNT. In several cases the environment volume, including the explosive is big, the minimum is in the size of a big room. Gas diffusion in a huge air volume will ultimately generate a saturation vapour pressure, however this will require several hours. Generally, in many explosives detection cases, the air currents will charge the explosive molecules and the adsorption close to surfaces determine the real explosive molecule concentration. Although the molecules probability of sticking the surfaces could be far less than (1ppm), the area of surface is large. Several explosive molecules are highly electrone gative (for example, they have a very high probability of appending an electron and being charged). Each large electric field and air currents in the air will form explosive molecules plumes in the local airspace close to the explosive, similar to smoke moving from a cigarette or perfume from a rose. The specific concentration of molecules during these plumes could be easily 100 to 10,000 times less than that expected by the saturated vapour pressure. As a result, the explosive vapours detection has a massive challenge [29].

Several trace detection techniques depend on stimulating flux increment of particles or molecules for the explosive instrument (i.e. laser defragmentation or ablation and turbulent airstreams are used to raise the trace material presented for analysis). With regards to dogs, exciting the local environment with the foot, head, and body the motion might give rise to sensitivity. Concentrators are one other popular sampling method for detecting the trace explosive. As an example, a vacuum system close to a portal could be used to collect a big air sample from where explosive molecules could be gathered by filters. The dog's nose is operating on a similar principle. A dog breathes in air and collects molecules and particles through the amazingly large area in the nose, within the range of 10m^2 . There is still a wish for researchers to get a method to fabricate optical, biological, electronic, or chemical "noses" which will be similar or exceed the dog's nose.

The explosive molecules produce a special identifier for every explosive because there are fairly sharp spectral absorption lines due to the electronic transitions within the vibration and ultraviolet absorption lines in the terahertz and IR ranges. As explained previously there is a challenge because of the very low concentrations found in the gas phase. When the molecules are absorbed on surfaces or are integrated into tiny granular particles, the molecular absorption lines are significantly extended and their benefits for specific recognition using optical spectroscopy are reduced. This is often more of a challenge for the terahertz and IR torsional, vibrational, and bending spectral lines[30].

C- Optical Detection

Optical absorption techniques use the UV electronic and infrared vibrational resonances to identify explosive molecules. Such techniques usually require expensive and breakable apparatus to capture and analyze

large samples in order to raise the signal-to-noise ratio (SNR) to the preferred level. Likewise, the cavity ring-down spectroscopy and SERS (surface enhanced Raman scattering) spectroscopy can detect lower molecular concentrations in the (ppt) rang. The disadvantage of these methods is that big samples need to be obtained and analysed with comparatively costly and fragile equipment [31].

Techniques involving optical fluorescence have been used for standoff explosive detection. A laser is used to induce fluorescence in the explosive particles in the (VIS and UV) wavelengths where they highly decompose and absorb into fragments which exhibit fluorescence properties. These patterns can then be captured at standoff distance and used for detection. The insufficient high level of sensitivity and issues of eliminating the fluorescence with contaminants of environmental are the major disadvantages of this technique.

Spectroscopic approaches are often highly selective and could be used to identify a variety of analyses of interest. Laser based spectroscopies may also be utilized in chemical imaging techniques to acquire spatially resolved chemical structure details. Standoff spectroscopic techniques face important challenges. As the distance between tests object and collection optics increases, the quantity of collecting light will probably be reduced by the Inverse Square of the distance. For this reason, the measurements at Long-distance usually need the use of a big telescope to get high laser powers, efficient spectrometers, light collection, and long accumulation times. The intensity of collecting signal will be increasing with the excitation power; nevertheless, skin-safe and eye field detection needs low laser powers. Some of the fields of researches in optical approaches as in follow [26,32]:

1- LIDAR, DIAL, and DIRM

LIDAR is generally used in the studies of polluting the environment and in chemical substance plume detection. They are based on the principle where the radiation is backscattered from a pulsed illuminating source to a detector. The molecules of an explosive material that is in the pulsed laser illuminating beam could be absorbed once the light source is tuned into a molecular resonance (usually a vibrational resonance in the infrared spectral range). This kind of absorption attenuates the backscattered beam, so it permits the explosive detection. Backscatter might occur from particulates in the air. With a range in between (10- to 30-m) standoff distances, the lower molecular concentrations feature of explosive molecules lead to limiting in the level of sensitivity of these laser ranging methods. Probably the other optical methods may be used to raise the SNR. These methods are usually used in a sensing instead of an imaging mode. For the sensing mode, it can identify the distance and direction of a target, but it is unable to image it. Imaging can be done through scanning a scene and mapping the returned signal. A study in this field is required to have the comprehensive characteristics of both spectral reflectance of explosive particles (of various particle sizes) and spectral absorption of explosive vapors. This would help in selecting the proper spectral bands for executing differential reflectance or absorption LIDAR. Rather than utilizing particles in the air for the needed backscattering, it is possible to make use of retro-reflectors much like those seen on highway signs. As a type of using low-cost remote device. Using retro-reflectors could reduce this system to portal scenarios [33].

Imaging that used DIRM or DIAL method is a type of dual-spectral image. Even though these methods include two laser wavelengths for illumination, it is possible to use the same method of illumination using a

broadband source and observing with two narrow-band filters. Currently, there is one particular "similar" explosive imaging system, which uses imaging system and solar illumination with two rotating IR filters and is built to identify adhered particles of a no nitrate explosive [26].

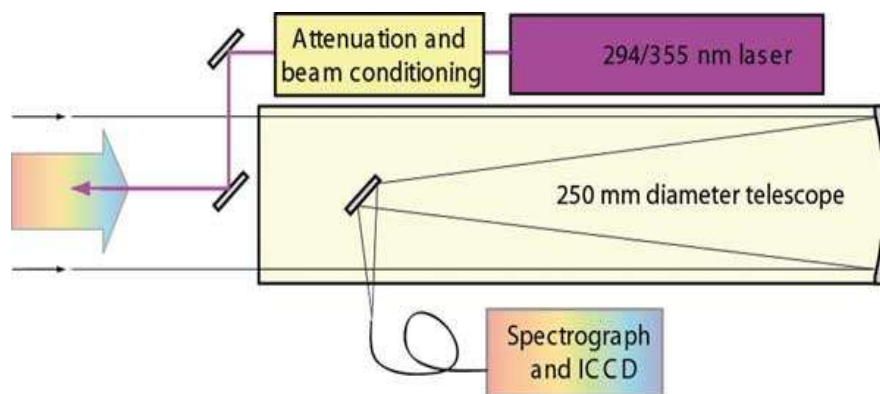


Figure 2.4: Laser setup of the LIDAR UVLIF bio aerosol detection system

Another technique utilizes a gas sample to be discovered like a filter in one channel of laser beam and electro optic changing from filters to unfiltered channel. The system of dual spectral that mentioned previously is a unique case of multi spectral or hyper imaging. These methods need to be researched for detecting surface-adhered or airborne explosive molecules. This needs to get full information of spectroscopic characteristics, ranging from ultraviolet to the millimeter wave, of the explosive in different forms (particulate and gaseous of diverse size). In addition, the banded spectroscopy coupled with imaging should be also researched more. The challenge of these hyper or multi spectral methods is to get “processed” images in real time [5].

2- LIBS Technique

LIBS nowadays have been developed to be a spectroscopic method of standoff explosive detection. It uses high, short peak power laser

pulses to generate a dielectric breakdown of the sample surface, causing fast heating and plasma formation. When plasma spark generated, the materials will be ablated and break down into several smaller ionic, atomic, and molecular species, which are excited via plasma and emitted photons of aspect wavelengths. The ratios of intensity of the atomic emission lines from H, C, O, and N could be used to infer an original molecular construct stoichiometry through comparing the collected spectra with typical spectra obtained from identified compounds within identical experimental conditions. It has been recently utilized on standoff explosive sensing since it affords the chance of a long standoff ranges, larger signal, in addition to low times of spectral accumulation with no needs for sample preparation. The biggest challenge facing the LIBS implementation to detect the explosive materials is that the LIBS spectra highly depends on the comprehensive experimental conditions [34].

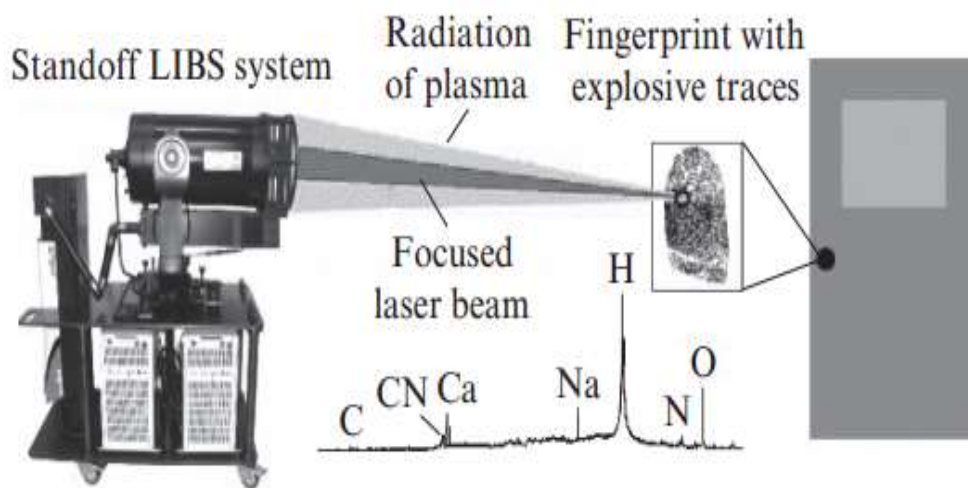


Figure 2.5: LIBS system sent laser light from Nd: YAG laser generates pulses of 1064nm light and received LIBS spectrum through high resolution ICCD spectrograph system [35].

Medium effects such as the atomic emission with the surrounding atmosphere may complicate the analytic recognition. Moreover, organics inside of the plasma could be reacting to form new types with many other spectral emissions. In addition to the incident laser pulse wavelength, energy, and width affect the quantitative analyses, complicating qualitative and excited plasma [35].

3- Laser-Induced Fluorescence Spectroscopy (LIF)

Laser Induced Fluorescence (LIF), belongs to spectroscopic diagnose technology, is a new method of flow visualization and measurement which obtains real-time distribution information via non-intervention, and undertakes quantitative measurement of concentration field, temperature field, pressure field and velocity field. Laser induced fluorescence measurements (LIF) are a common way to sensitively detect small traces in several media such as bulk materials, liquids or gases [36].

LIF used for explosives detection is often coupled with photo-fragmentation (PF) so as to photo dissociates a target molecule and consequently identify the fluorescence of the produced photo fragments. The fluorescence intensity of the NO generated by (PF) is strong, allowing to detect even low concentrations of explosives. This technique provides the benefit of being very sensitive and easily applied for in situ measurements [23].

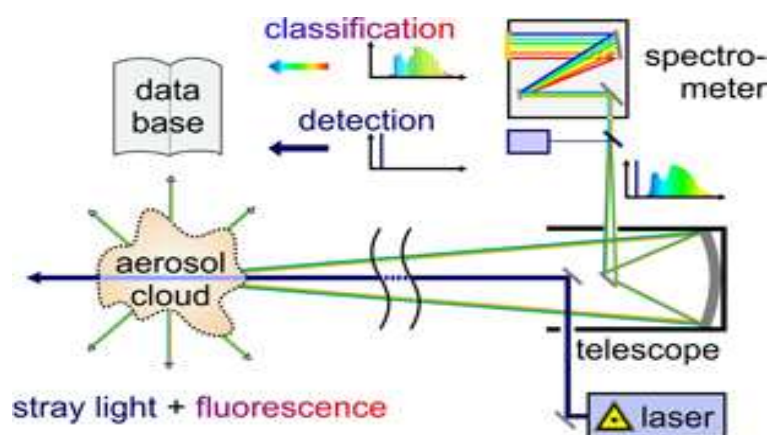


Figure 2.6: Laser-Induced Fluorescence Spectroscopy operation with explosive materials.

4- Raman spectroscopy (RS)

It has become commonly employed for standoff detection. Raman spectra originates from exciting the sample using a monochromatic source of light, usually a laser. Raman spectra details the intensity in- elastically scattered light as a function of the frequency variation compared to the excitation light. These spectra details both the environment and the structure of the scattering molecule. Therefore, Raman spectra work as specific and sensitive fingerprints which can be used to find the chemical structure of illuminated samples, which have a benefit that is non-destructive, standoff, eye-safe, highly specific monitor of molecular structure [37].

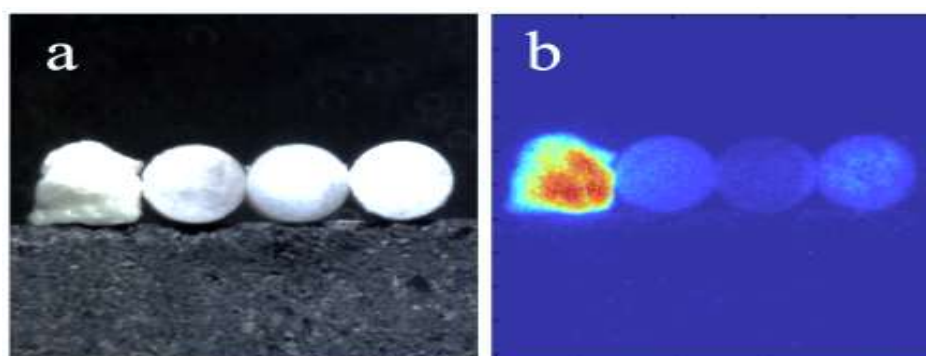


Figure 2.7: Raman spectroscopy (a) normal picture taken (b) Image of Raman spectral [5].

The Spatially offset Raman spectroscopy (SORS) operates on the spatial offset between the spot of laser excitation and the one in which the collection optic focuses so that it can decrease the Raman bands contribution from the container walls, which raises the Raman bands relative intensities of the container contents. The key to regard spatially offset Raman spectroscopy is that Raman scattered light (RSL) produced by a strongly scattering sample powder within a container is much more prone to propagate laterally prior to it exits the container, in contrast to Raman light produced by the container wall. Thus, since the collection optic is pointed beyond the laser excitation, extra RSL from the container material are discovered in accordance with that from the container wall [5].

The standoff Visibly Raman spectroscopy (VRS) is challenged via impurity and sample fluorescence that usually happens in a similar spectral region as the Raman bands of interest. The Intense fluorescence could break down spectral SNR, which limits analyze detection. Gated detection and Pulsed laser excitation could be used to lower contributions from fluorescence [38, 39].

5- *UV Raman spectroscopy (UVRS)*

However, VRS has been used efficiently for the standoff detection of bulk quantities of explosives. For trace explosives detection, visible or near-IR excitation will be difficult because of small cross sections of both near IR and visible Raman which cause low sensitivity. Moreover, visible and near-IR excitation cannot be utilized to uniquely improve the resonance Raman spectra of explosives. In case of visible excitation, Raman bands of explosives have cross sections like that from substrates

and interference. This degrades a chance to spectrally separate between interference and explosive analyses. On the other hand, the excitation in the deep UV (less than 260nm) leads to a heightened sensitivity and selectivity of standoff Raman because of resonance improvement, the V^4 dependency upon scattered intensity, whilst the deep UV interference lacks fluorescence. Resonance improvement leads to improved Raman intensities from molecules that absorb at or near the excitation wavelength. This absorption reduces the depth of penetration of the excitation beam. The excitation of visible wavelength leads to higher Raman intensities regarding thicker explosive samples and that has a minimal absorption of the excitation beam. The visible excitation generates Raman scattering from the significantly higher depth of a thick sample since the beam of laser is not highly attenuated. Near-IR and Visible wavelength excitation is effective for transparent and thick samples that are unlikely to become experienced in the field. UV excitation is effective for trace explosive detection, which usually requires thin samples. UV excitation will also be good for standoff instrumentation considering that higher eye exposure limit for deep UV light permits the usage of higher laser powers in comparison with visible excitation. Developments in UV Raman instrumentation are assisting enhancing standoff UV Raman techniques for trace explosive detection. However, near-IR and visible Rayleigh rejection optical filter technique is older and somewhat low-cost, Commercialized deep Rayleigh rejection filters have a lot of losses performance with minimal out of band transmitting, [5, 19, 39].

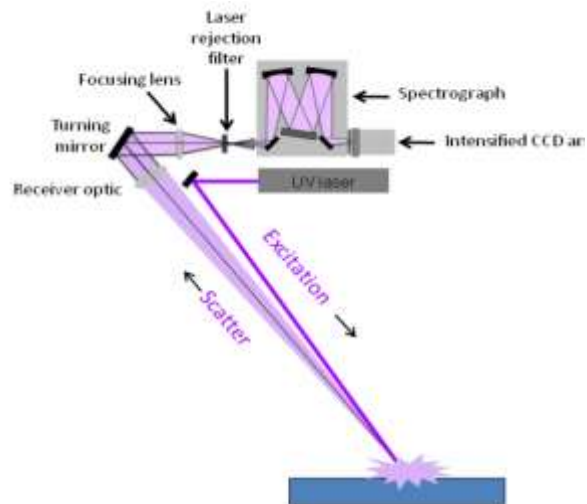


Figure 2.8: Schematic diagram of UV Raman LIDAR instrument.

In addition to the previous techniques, there are many approaches to hybrid two techniques, such as project at the University of Málaga, where researchers have demonstrated a novel hybrid sensor system that uses Raman spectroscopy and laser-induced breakdown spectroscopy (LIBS) simultaneously for instant and remote standoff analysis of explosives. Combining the atomic sensing of the former with the vibrational spectroscopy of the latter could facilitate the standoff detection of explosives residue in trace quantities – left, for instance, by human fingerprints on car door handles – at distances of up to 50 m [40].

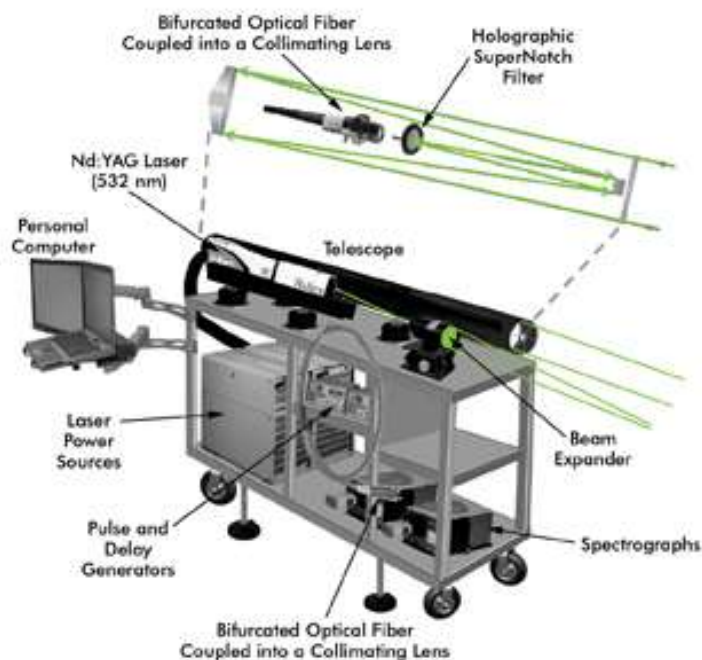


Figure 2. 9: Structure of the hybrid sensor system that uses Raman spectroscopy and laser-induced breakdown spectroscopy (LIBS) [40].

The system integrates a pair of Andor Shamrock SR303i

spectrometers, each fitted with a I Star intensified CCD, a Cassegrain telescope and a Quantel Brilliant Twins Q-switched 532-nm Nd:YAG laser. The Raman and LIBS hybrid system have spectra for a variety of explosives, including C4 and H15 (both plastic explosives) and Goma2-ECO. The hybrid sensor offers an extremely fast response and can operate at relatively long distances, and the tests approved it can detect explosives through the car glass as well as through warehouse windows [40].

Another successful hybrid system is the area novel sensor done the US Department of Energy's Oak Ridge National Laboratory in Tennessee, where the researchers developed a device that takes advantage of the nonlinearity associated with Nano scale mechanical oscillators. The device uses microscale resonators, which also have been

explored for mass- and force-sensing applications. By measuring these changes, researchers can determine the mass of the trace amounts of substances, including explosives, biological agents and narcotics that hit the micro cantilevers. The challenge of this technique comes with trying to measure and analyze oscillation amplitudes as small as a hydrogen atom. Conventional approaches seek to achieve this use of a sophisticated system of low-noise electronic components, which adds both cost and complexity to a device. The Oak Ridge team instead of pumping energy into the system, it produces considerably larger amplitudes. With this approach, the relationship between frequency and amplitude changes is no longer described by a simple bell-shaped resonance curve. The system can view the amplitude changing more abruptly and will be able to detect considerably smaller amounts of explosives than with currently available chemical sensors with the ability to measure trace amounts of explosives in real time [40].

From our study in the explosive detection background and approaches, we have focused on developing standoff methodologies for two selective methods which are LIBS and LIF. This approach appeared to be the most suitable to our purposes. We believe that using the fluorescence spectra with time resolving techniques can be more encouraging for stand-off detection for the following reasons:

- 1- The standoff explosive detection has a very important advantage than Non-standoff explosive detection that the safe distance helps keep each operator and device from danger, while our technique can give safer distance than others.
- 2- Laser induced fluorescence is very sensitive where many atoms and radical can be detected.

3- The fluorescence spectrum can give more details, true and reliable results. A spectroscopic detection capability may provide additional information by measuring the fluorescence time parameters with the wave length [20].

2.2 Energetic Materials and Their Characteristics

Explosives are part of a group of materials termed "energetic materials". These classes of material receive their name from a large amount of energy that is stored within the molecules and originates from the molecules thermodynamic properties. Every molecule requires a defined amount of energy in order to form, termed the heat of formation. For energetic materials, the molecular formation reaction is endothermic, meaning it gains heat or energy from the exterior environment. The larger the heat of formation, the greater amount of energy stored within the molecule. The explosion of a material is caused by the spontaneous release of energy upon decomposition, called heat of decomposition. The heat of decomposition is simply the energy from the exothermic reaction where the molecule decomposes to smaller molecules. It is equal in absolute value, but opposite in sign, to the heat of formation if the material decomposes to the same molecules from which it was originally formed. If the material decomposes to different molecules, then the heat of decomposition may be larger or smaller than the heat of formation. The decomposition chemistry of the explosive materials has become widely researched with far effort still going on. In this thesis, we focus on the chemical and physical properties of explosives which are important on their characterization and detection [41].

2.2.1 Common types of Energetic Materials:

Explosives may be broken down into two general classes: nitro/nitrate-based and non-nitro/ nitrate-based. Non-nitro/nitrate based

explosives are derived from materials such as peroxides, e.g., triacetone triperoxide (TATP), perchlorates, and azides. While these explosives clearly pose a threat, our studies focused upon the more common nitro-based explosives. In the following description of the most common explosive materials used by terrorists in explosive cars, explosive belts, and improvised explosive devices (IED), etc. [19].

1. Trinitrotoluene (TNT)

TNT is a pale yellow, solid organic nitrogen compound used chiefly as an explosive, prepared by stepwise nitration of toluene. Because TNT melts at 82° C (178° F) and does not explode below 240° C (464° F), it can be melted in steam-heated vessels and poured into casings. It is relatively insensitive to shock and cannot be exploded without a detonator. One such detonator is lead azide $\text{Pb}(\text{N}_3)_2$, which explodes when struck or if an electric discharge is passed through it. For these reasons, it is the most favored chemical explosive, extensively used in munitions and for demolitions [42].

TNT is an important explosive, since it can very quickly change from a solid into hot expanding gases. Two moles of solid TNT almost instantly change to 15 moles of hot gases plus some powdered carbon, which gives a dark sooty appearance to the explosive. TNT is an explosive for two reasons. First, it contains the elements of carbon, oxygen and nitrogen, which means that when the material burns it produces highly stable substances (CO , CO_2 and N_2) with strong bonds, so releasing a great deal of energy. This is a common feature of most explosives; they invariably consist of many nitrogen or oxygen containing groups (usually in the form of 2, 3 or more nitro-groups), attached to a small and constricted organic backbone. However, explosives like TNT, actually have less potential energy than gasoline,

but it is the high velocity at which this energy is released that produces the blast pressure. This very high speed reaction is called "detonation". TNT has a detonation velocity of 6,940 m/s. The second fact that makes TNT explosive is that it is chemically unstable - the nitro groups are so closely packed that they experience a great deal of strain and hindrance to movement from their neighboring groups. Thus it does not take much of an initiating force to break some of the strained bonds, and the molecule then flies apart. Typically 1 gram of TNT produces about 1 liter of gas, which is a 1000 fold increase in volume. This expanding hot gas can be used to propel a projectile, such as a bullet from a gun, or for demolition purposes [43].

As shown in Figure 2.1, TNT has an aromatic or cyclic molecular structure with one methyl and three nitro groups spaced around the ring. The aromatic structure is based on a benzene ring that contains electrons that are delocalized, that is, the electrons travel freely through all of the orbitals and are not attached to a particular carbon atom. Methyl and nitro groups are considered substituents because they replaced a hydrogen atom on the benzene ring and contribute characteristics to the molecule consistent with their own molecular structure [44]. The methyl group is an electron donating group in that it supplies a partial electron to the benzene structure while the nitro groups are electron withdrawing. The positions of these substituents can vary so that TNT occurs in six different isomers such as 2, 3, 5-, 3, 4, 5-, and 2, 4, 5- but 2, 4, 6 is the symmetric isomer, the most commonly used for explosives, and will be referred to as simply TNT [41].

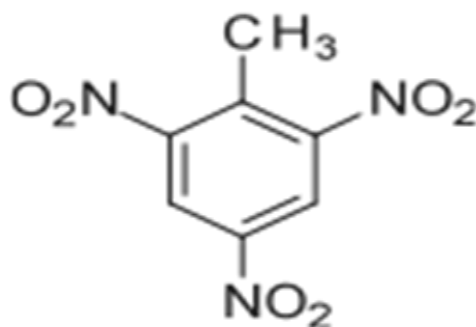


Figure 2.10: TNT Molecular structure.

TNT also can be mixed with RDX or alumina creating different explosive properties and it can increase the explosive power in improvised or homemade explosives made from ammonium nitrate fuel oil (ANFO) and an ignition source [44].

2. RDX

RDX is abbreviation of Research Department Explosive or Royal Demolition Explosive, formally cyclotrimethylene trinitramine, also called cyclonite, hexogen, or T₄. It is a powerful explosive, discovered by Georg Friedrich Henning of Germany and patented in 1898 but not used until World War II [45].

RDX is a hard, white crystalline solid, insoluble in water and only slightly soluble in some other solvents. Sensitive to percussion, its principal nonmilitary use is in blasting caps. It is often mixed with other substances to decrease its sensitivity [46].

The molecule is composed of a ring of alternating carbon and nitrogen atoms with three substituent nitro groups. Unlike the aromatic molecular structure of TNT, the carbons in the ring are saturated, so that the electrons are localized to each bonded atom pair. RDX is considered a tertiary derivative of the ammonia molecule. This suggests that the

chemistry of the molecule is dominated by the nitrogen atom creating the amine and the electron pair located on that nitrogen atom. RDX is solid at room temperature and has to have significant amounts of molecular defects in the form of vacancies which cause dislocations and dislocation pile-ups in the crystal [45].

RDX is the most commonly known and the main component in C-4, and it is a plastic explosive. C-4 is moldable and easily formed into improvised explosive devices. RDX is also often mixed with TNT. Figure 2.2 shows the shape and molecular structure of C-4 [2].

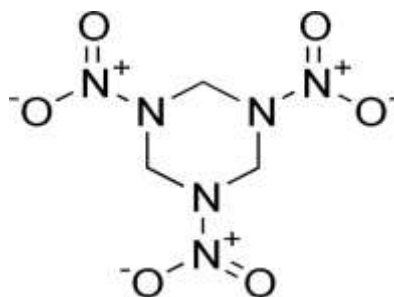


Figure 2.11: RDX Molecular structure [2].

3. Ammonium Nitrate (AN)

Ammonium nitrate, (NH_4NO_3), a salt of ammonia and nitric acid, used widely in fertilizers and explosives. The commercial grade contains about 33.5 % nitrogen, all of which is in forms utilizable by plants. It is the most common nitrogenous component of artificial fertilizers. Ammonium nitrate is also employed to modify the detonation rate of other explosives, such as nitroglycerin in the so-called ammonia dynamites, or as an oxidizing agent in the ammonals, which are mixtures of ammonium nitrate and powdered aluminum. Ammonium nitrate is a colorless, crystalline substance (melting point 169.6°C). It is highly soluble in water, heating of the water solution decomposes the salt to nitrous oxide (laughing gas). Because solid ammonium nitrate can undergo explosive

decomposition when heated in a confined space, government regulations have been imposed on its shipment and storage [47].

The common type of AN is used with fuel oil (ANFO) as a homemade explosive. The ammonium nitrate (fertilizer) contains a nitrogen compound that when mixed with fuel oil (diesel fuel for example), which gives oxygen to the compound, the result is explosive materials. In addition, TNT can increase the power of the (ANFO) explosive or it can be an ignition source to that explosive materials. Figure 2.12 shows the shape and molecular structure of AN [48].

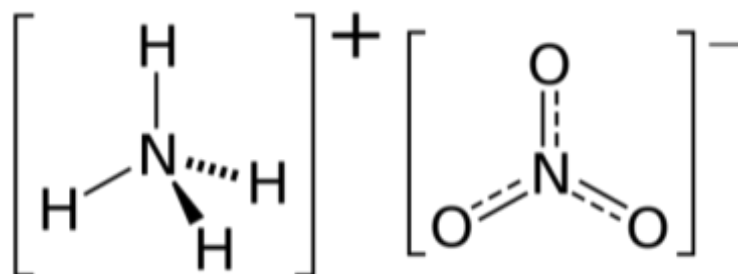


Figure 2.12: AN Molecular structure [48].

2.2.2 chemical Properties of Energetic Materials

Explosive detection techniques based on using Laser need to recording details on the wavelengths and the intensity of the characteristics of absorptions and/or emissions of the samples which could include explosive material. It is the explosives, chemical and physical properties that constrain or control the strategy and techniques of laser-based detection. Several laser-based strategies that focus on the detection of the vapor and/or particle have been developed from the information about spectroscopic signatures and molecular properties of the target. Explosives are classified or distinguished based on their chemical structures. They are often put into the following groups: chloric;

nitramines; salts of nitric, nitric esters, nitro compounds, and; perchloric acids as well as other compounds able to exploding; and mixes. Nitro compounds are recognized via the carbon-nitrogen bond (C-NO₂). The majority of compounds which have 3 or more nitro groups for one benzene ring and some that have two nitro groups (dinitrotoluenes and dinitrobenzenes) are utilized as explosives. Nitric esters are described as the existence of a nitroxy group -C-O-NO₂. This means that nitro group in nitric esters is linked to a carbon atom through an oxygen atom. Nitramines are described by nitro groups linked to carbon atoms through a bridging nitrogen atom -C-N-NO₂. They are generally derivatives of the basic inorganic nitramine NH₂ NO₂, perchloric acids, chloric and salts of nitric can be used as an explosives materail or it can be mixed to be as oxygen carriers. Azides contain materials like silver azide (AgN₃), lead azide (Pb(N₃)₂), and hydrazoic acid (HN₃). Some other materials like diazo and fulminates compounds also come under this category. Mixtures are basically the common explosives mixed to have the requested characteristics. Therefore, many organic compound explosives contain a chemical composition with a bound NO₂ functional group and are divided into atoms connected to that group. Table 2.1 provides the common explosive properties with its properties. Various methods to measuring these properties have led to many different values, specifically for vapor pressures. The methods of vapor detection are limited since the vapor pressures at room-temperature of these explosives are few. There is a great rise in vapor pressure at increased temperatures, but other properties like ignition temperature reduce maximum detection temperature and expose numerous dangers. In addition, explosives go through a variety of physical and/or chemical transformations at these elevated temperatures. Table 2.1 details the equations utilized to compute the vapor pressure for

any given temperature, that have been produced using measurements from the vapor-generator equipment and a least-squares analysis [49-53].

Table 2.1: Chemical and physical properties of popular explosives [50] .

Acronyms	Name	Melting point (°C)	Ignition temperature (°C)	Vapor pressure equation ^a
TNT	2,4,6-Trinitrotoluene	82	300	$\text{Log } P \text{ (ppb)} = 19.37 - 5481/T$
RDX	1,3,5-Trinitro-1,3,5-Triazacyclohexane	204	229	$\text{Log } P \text{ (ppt)} = 22.50 - 6473/T$
HMX	1,3,5,7-Tetranitro-1,3,5,7-Tetrazacyclooctane	278	335	-
PETN	Pentaerythritol tetranitrate	141.3	205	$\text{Log } P \text{ (ppt)} = 25.56 - 7243/T$
NG	Nitroglycerin	13.2	-	$\text{Log } P \text{ (ppb)} = 18.21 - 4602/T$
AN	Ammonium nitrate	169.6	-	$\text{Log } P \text{ (ppb)} = 12.97 - 541.77/T$

ppt, parts per trillion. ^a*T* is in kelvin.

2.2.3 Extinction Spectra of Explosives Martials

Several spectroscopy techniques in the UV region are based on the material's interaction with the electromagnetic radiation by absorption and back scattering. The absorption means that energy transition from the electromagnetic incident photon to an electron in the molecule causing the electron to move to an unoccupied, higher energy state[54], extinction versus the wavelength is shown in figure 2.13.

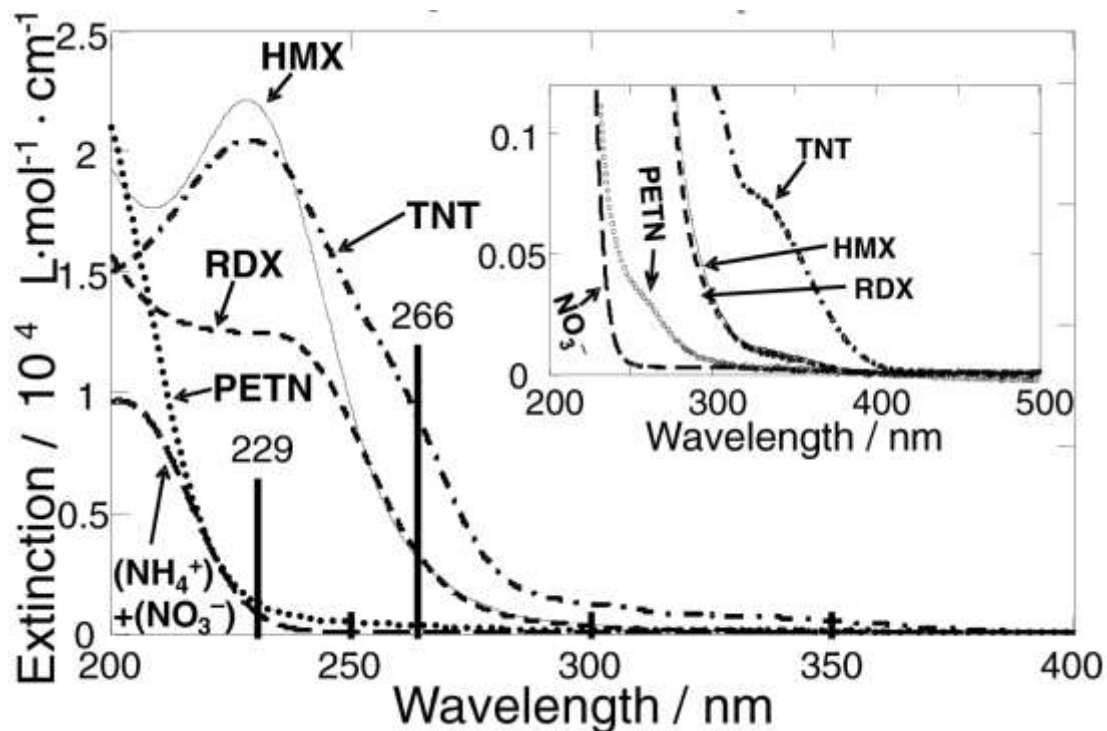


Figure 2.13: Typical extinction spectra for explosives [55].

2.2.4 Ultraviolet and Visible Range (180-750nm)

The ultraviolet (UV) region of the electromagnetic spectrum is commonly defined from 180 nm to 350 nm and the visible region from 350 nm to 750 nm. These two regions are often measured together due to the availability of detectors and light sources that can accommodate both regions. The energy of electromagnetic radiation in this range is in the order of the band gaps or difference in energy levels in those materials. Therefore, several spectroscopy techniques in this region are based on the absorption of the electromagnetic radiation by a material. This absorption is caused by an energy transfer from the incident photon (electromagnetic radiation) to an electron in the sample causing the electron to move to an unoccupied, higher energy state. A spectrometer of this type uses an UV-Visible light source such as a Xe, Hg, or a Deuterium lamp. The light source may also be coupled with a stronger

visible spectrum emitter for example a tungsten halogen lamp that emits predominantly the red part of the spectrum [56, 57].

UV illumination of explosives induces a relatively strong fluorescence signal. However, it is not very specific to explosives, since many materials fluoresce under UV illumination and their fluorescence spectrum is often nonspecific. Thus, this technique does not fulfill the specificity constraint; chemical clutter would be a significant problem. Other techniques generate a reflection signal based on the absorption peaks in explosives. Again, optical clutter appears to be a problem because the spectra are broad and not necessarily unique to explosives. Furthermore, only a very thin layer of material (monolayer) is being interrogated; thus, it will not absorb much light beyond the ultraviolet. Additionally, and perhaps more importantly, the explosives distribution is non-uniform, that much of the reflected signal may not be dominated by the explosives themselves but by the surface upon which they reside. An alternate approach, which removes many of the difficulties associated with the indistinct spectra of the materials themselves, is to dissociate the materials and use instead signals related to their constituents. Laser induced breakdown spectroscopy (LIBS) is one such technique, which in its most common incarnation analyzes the atomic constituents. LIBS uses tightly focused high energy laser pulses to dissociate the materials into their constituent atoms via the formation of micro plasma. The atomic emission spectra allow identification of the atoms and estimation of their relative abundances [58].

2.3. Absorption and Emission Light by Atoms and Molecules

We understand the electromagnetic nature of light, when an atom or a molecule absorbs light, an electron in the outer shell of the molecule is promoted to a greater energy level. The absorbed light energy must be

equal to the energy difference of the two orbital levels involved in this transition. This is because the energy levels of the electrons in a molecule or an atom are discrete and not continuous. The relationship between the photon energy and its frequency is stated by equation [59]:

$$E = h\nu = hc/\lambda \dots\dots (2.1)$$

Where:

h: is Planck's constant (6.63×10^{-34} J.s)

ν : is the frequency at which absorption

c: is the speed of light (3.0×10^8 m/s)

λ : is the wavelength

The absorption Photon can excite one pair or more electrons to higher energy states (singlet or triplet). The absorption processes are followed by the relaxation emitted. The time needed for an electron to relax from unexcited state to ground state is called the "lifetime of the excited state" which is inversely proportional to the transition probability .

The absorbance of a sample is linearly related to the concentration of the absorbtion in the sample. This is described by Beer's law[59].

$$A = -\log T = \epsilon \ell C \dots\dots (2.2)$$

Where

A: is the absorbance (the intensity of certain frequency light absorbed by a molecules),

T: is the transmittance,

ϵ : is the molar absorptivity with units of $L.mol^{-1}.cm^{-1}$,

ℓ : is the path length (cm),

C: is the concentration of the absorbing species ($mol.L^{-1}$)

The transmittance can be defined as the portion of incident light at a particular wavelength that passes through a sample [60]

$$T = I/I_0 \dots\dots\dots (2.3)$$

Where: I_0 is the intensity of the incident light, I is the intensity of the light coming out of the sample.

Lambert-Beer's law shows that only photons with a specific frequency can be absorbed by the molecule. The absorption spectrum should appear as sharp lines. But, the absorption bands in molecules generally appear as broad bands. The explanation for this is given by the Franck-Condon principle. It states that electronic transitions (10^{-15} s) is faster than nuclear motion (10^{-13} s). After the electronic transitions have occurred the nuclear geometry re-adjustment takes place (Figure 2.14). Electronic transitions are vertical with respect to the nuclear geometry, which means the electron is excited to a higher state before the nuclei have had a chance to respond to the new electronic structure. Therefore, the transition from the lowest vibrational level of the ground state to vibrational levels of the excited state occurs before the nuclei geometry re-equilibrates [62].

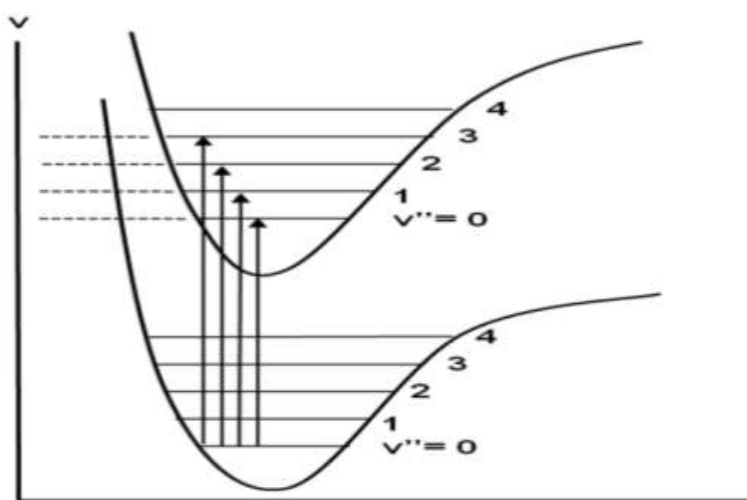


Figure 2.14: Electronic transitions Configuration [61].

The excited molecule in the first excited state first relaxes to the lowest vibrational level by the thermal relaxation. In the ground state, the electrons are paired with an anti parallel spin as in figure 2.15. When the electron is elevated to the excited state, its spin does not change according to spin restrictions.

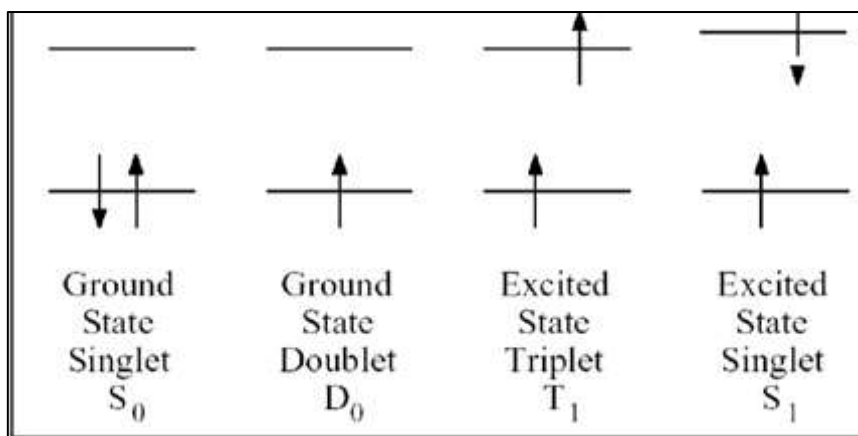


Figure 2.15: Nomenclature for electron spin pairing in molecular electronic states [62].

The excited state formed is called singlet excited state (S_1). If the spin of the excited electron changed, its spin momentum becomes three and this process is called intersystem crossing, the state is called triplet excited state T_1 (as shown in figure 2.16). This process is a forbidden process because of spin restrictions. [64]

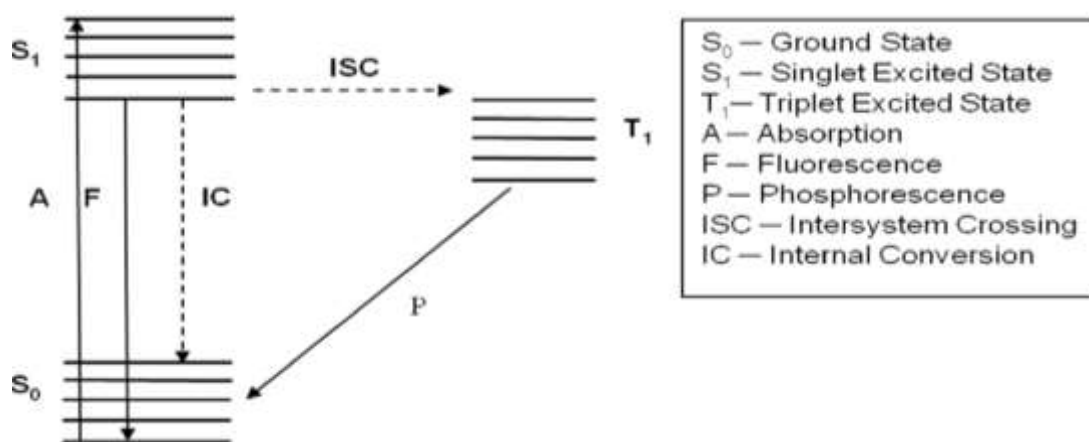


Figure 2.16: Triplet excited state (T_1) [65].

Inorganic material we can excite the valence electrons by absorbing electrons from the external radiation, the results of the relaxation of these electrons are broad spectral bands according to the superposition of overlapping transitions. The Analysis of this spectral gives us information about all the compounds [65].

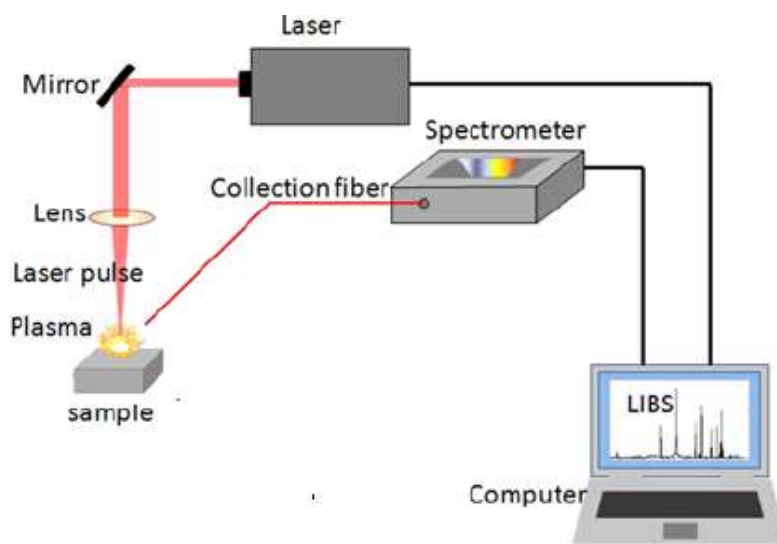


Figure 2.17: Diagram of a typical LIBS experiment.

2.4. Principles of LIBS

Laser-induced breakdown spectroscopy (LIBS) is a Spectro-Chemical technique which uses an intense laser pulse to determine the elemental composition of a sample and the relative quantities of the target's constituent elements. The overall processes that occur during nanosecond LIBS can be summarized in the following basic steps [66]:

1. A short laser pulse is incident on a target material.
2. The incident energy on the sample will vaporize a small amount of the sample. The incoming laser pulse will also interact with the vapor plume to create a high-temperature plasma.
3. An optic (lens or optical fiber) is used to collect light and a spectrometer dispersing element (typically a grating) is used to

disperse the light. The light originates from the spontaneous emission of hot atoms and/or ions in the plasma.

4. The resulting atomic emission peaks are analyzed to determine the elemental constituents of the sample and their relative concentrations[67].

The following sections are the main physical processes that occur.

2.4.1. Energy Source

Many LIBS applications use an Nd:YAG (neodymium-doped yttrium aluminum garnet) pulsed laser with an infrared wavelength of 1064 nm. This laser is the most common type of solid-state laser and is widely used because it is reliable, easy to use, and because of its high peak pulse energies. with a Nd:YAG laser, neodymium ions doped into the amorphous YAG glass act as the gain medium. Nd^{3+} energy levels create a 4-level laser system and its energy schematic is shown in Figure (2.18). The two main pump bands of Nd:YAG take place at wavelengths shorter than 900 nm, specifically at ~730 and 800 nm. These bands are coupled with a fast non radiative transition (d

ecay) to the lower energy level. At this point, the metastable (long life) of that energy level will be occupied and as a result a population inversion is achieved. After that, the laser emission is generated by the transition in at $\lambda = 1064$ nm. And another fast and non-radiate decay cause a transition to the ground state [67].

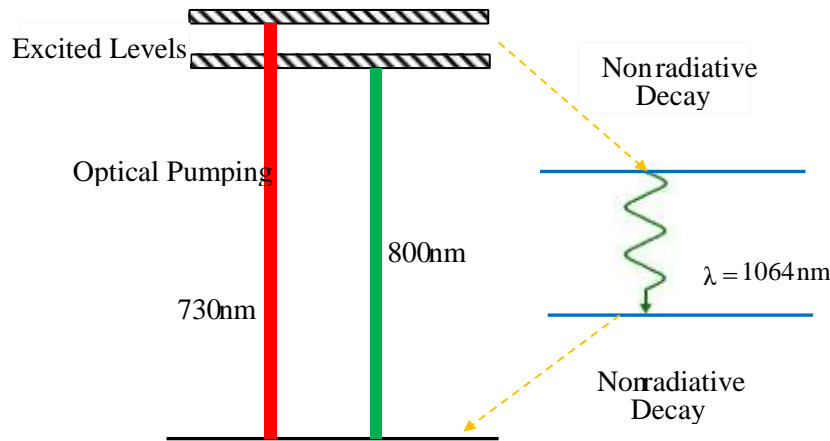


Figure 2.18: Schematic Energy Levels of the Nd:YAG Laser [67].

Nd:YAG lasers are also used at the second and third harmonic wavelengths of $\lambda = 532\text{ nm}$ (visible emission) and 355 nm (ultraviolet emission), respectively. Those harmonics can be generated by inserting a non-linear optical crystal into the path of the 1064 nm laser beam. Moreover, these lasers can be operated in continuous wave (cw) or Q-switched mode (pulse mode). In the case of cw lasers, the energy flows smoothly and constantly with time. Q-switched mode can be achieved by inserting an electro-optical device (i.e. polarizer) inside the laser cavity, specifically between the active medium and the rear mirror, to control when stimulated emission occurs. In this mode, the output of the laser occurs in a series of very short (nanosecond domain) energy pulses that are compressed into concentrated packages. On the other hand, recent LIBS experiments have also been carried out with femtosecond lasers [66].

2.4.2 Plasma Formation and Post-Breakdown Phenomena On Solid Targets

When a Q-switched Nd:YAG laser pulse is focused onto a solid target with sufficient energy, a certain amount of material is vaporized and thus a plasma is formed on the target surface as in figure 2.18.

Reported values of the laser-induced plasma breakdown threshold of a solid target lie between 10^8 W/cm^2 and 10^{10} W/cm^2 . For the work reported here, the maximum Nd:YAG laser pulse energy lay between 600 mJ and 800 mJ, operating at its fundamental wavelength 1064 nm with a 6 ns pulse duration. Focused by a spherical lens with a spot diameter around $100 \mu\text{m}$, the calculated power density approached 10^{12} W/cm^2 , well above the breakdown threshold [68].

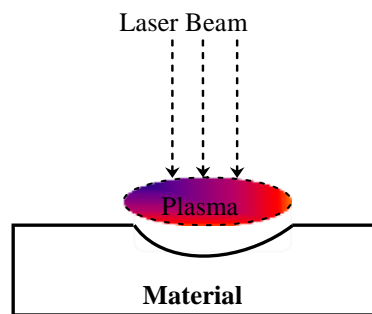


Figure 2.19: Illustration of plasma effect [68].

When the laser irradiance is high enough to initiate a plasma on the sample surface, some of the pulse energy heat, melts and vaporizes material into a plume above the target surface. Almost simultaneously, some seed electrons are produced by one or more processes such as multi photon ionization, laser assisted photo absorption, etc. to form a weakly ionized plasma. These seed electrons allow for further laser radiation absorption by the process of inverse bremsstrahlung which in turn causes further ionization. The process is regenerative and results in avalanche ionization since an increase in ionization rate results in an increase in laser light absorption which in turn results in an increase in ionization rate and so on as in figure 2.20. Eventually, the plasma can become opaque to the laser pulse and the surface is shielded from it. The plasma density at

which the plasma becomes opaque to the incoming laser light is termed as the critical density and can be calculated using equation 2.4 [69].

$$N_c = \frac{m_e \omega^2}{4\pi e^2} = \frac{1.1 \cdot 10^{21}}{[\lambda[\mu m]]^2} \text{ [cm]}^{-3} \dots\dots\dots (2.4)$$

Symbols in the above equation are:

m_e electron mass

ω frequency of the laser radiation

e electron charge

λ laser wavelength measured.

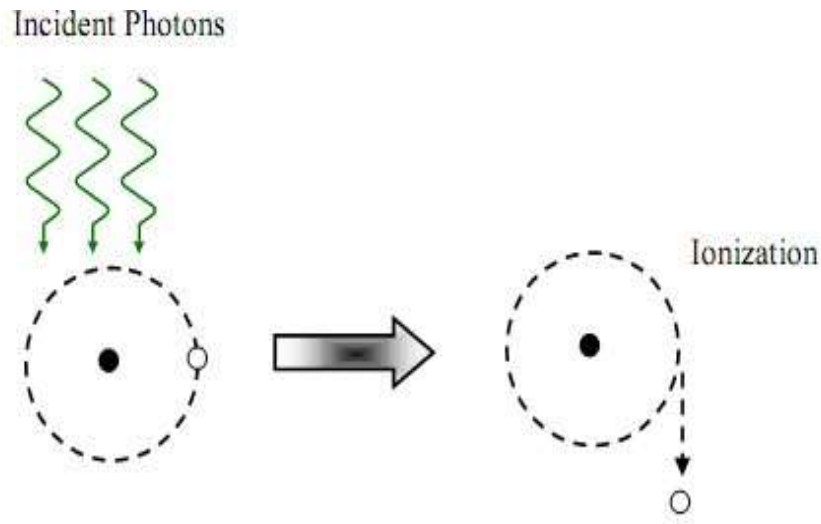


Figure 2.20: Ionization by multi photon absorption [68].

The critical density for the fundamental wavelength (1064 nm \approx 1 μ m) of a Nd:YAG laser is approximately 10^{21} cm^{-3} . When the plasma density reaches the critical value, a large portion of the incident laser energy is reflected by the plasma at and near the critical density zone. At this stage, the plasma starts to expand rapidly from the initial point. The expansion reduces the electron density, the laser light is once again able to pass through the plasma and heat the target. This cyclical process

continues until the termination of the laser pulse(s). After the excitation process, the plasma initiated by the laser pulse expands into vacuum or ambient atmosphere. During the plasma formation and evolution, collisional ionization and recombination processes dominate energy transfer in the plasma [68].

2.4.3 LIBS of Explosives

The success of LIBS for identifying organic compounds, based on atomic emission intensity ratios, led researchers to investigate characteristics of LIBS spectra of explosive compounds. Carbon, hydrogen, oxygen, and nitrogen are found in most military explosives. A common characteristic of most explosives is their high nitrogen and oxygen content relative to the amount of carbon and hydrogen. By tracking the amounts of oxygen and nitrogen in a sample relative to the other elements, it is possible to determine if a compound is energetic or non-energetic. In general, the interference has a much higher carbon and hydrogen content relative to the oxygen and nitrogen than the explosives. Some of the interference contains no nitrogen at all; however, the oxygen content is still low relative to hydrogen and carbon. Furthermore, diesel fuel is a combination of chains of hydrogen and carbon with no oxygen or nitrogen content. These differences can be exploited with LIBS in order to improve the discrimination between energetic and non-energetic materials. Contribution of atmospheric oxygen and nitrogen into the laser-induced plasma complicates the discrimination of energetic and non-energetic materials. Minimizing the oxygen and nitrogen contribution from the atmosphere is necessary to track the true value of oxygen and nitrogen relative to carbon and hydrogen in a LIBS spectrum. The formulation of RDX, for example, has equal amounts of O and N. Air alone has more nitrogen (80%) relative to oxygen (20%). Eliminating

the nitrogen and oxygen contribution from air therefore results in a larger O:N ratio characteristic of an explosive material [70].

The main challenge in cases where using LIBS for the detection of explosives includes a huge amount of chemical elements as well as their substrates which are found in energetic materials which are displayed concurrently in the LIBS spectrum as shown in fig 2-21 This means, the detection of important explosive molecules isn't instantly possible (example of this: the O, H, C, K, N, CN, Ca, Na and C₂ have been created in the plasma from organic molecules which consist of nitrogen) and the other characteristic lines can be found in standard LIBS spectra for explosives as well as non-explosive substances. Another challenge includes the air interference, which is the main component, H₂, O₂, and N₂ that add up to the LIBS spectra. This could be partly removed by directing an argon gas stream onto the sample to displace the air. Yet, it is, not practical in cases where the research of explosives at a large range is desired [34].

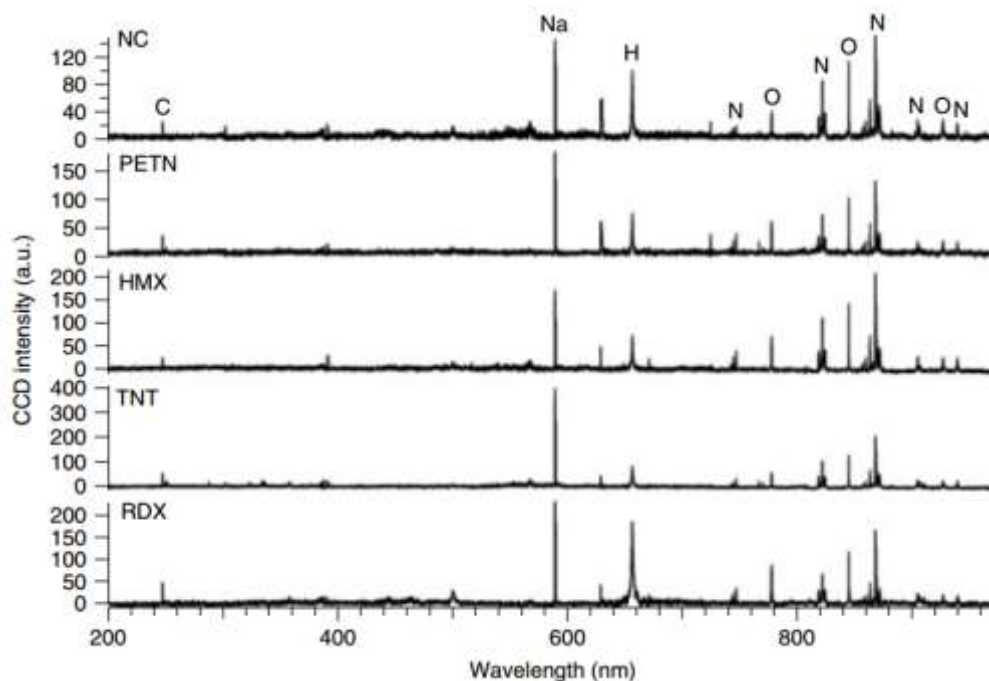


Figure 2.21: LIBS spectra for common energetic materials [34]

Another technique for discriminating the lines is due to the air applies double-pulse LIBS in which the laser is fired double on the same spot inside an interval of some microseconds. This may lead to a heating of the plasma due to the first pulse and absorption of the second pulse. Research made by De Lucia [69], discovered that RDX double pulsation in air boost of the O/N ratio from 2.2 ± 0.2 to 13 ± 5 . On the other hand, the O/C ratio reduced from 28 ± 9 to 3.7 ± 0.6 once the measurement was repeated below an argon atmosphere. The interference via atmospheric nitrogen and oxygen will be reduced (but not removed) through the use of double-pulse LIBS. Lastly, mixes of several samples need a sophisticated algorithm for optimistic detection of the typical explosives [71].

Because the targeted area where the plume is produced is comparatively small, a telescope must be used for a long-range detection, and the target area must be positioned by a wireless range finder. The range between target and laser can be established by LIDAR that measures the position of an object using the time delay a laser pulse, that has been scattered on an object, requires to go back to the emitter.. The investigating wavelength of 1064nm via the Nd:YAG laser offers an eye hazard through light scattering. Therefore, Robert D. W et al. [72] utilized an 80mJ laser, emitting at 266nm for ionization, to reduce harm to the eye, (Even now, damage to the eyes can happen even in this situation if the eye is mistakenly being hit directly via the laser beam.) However, the energy of laser related to the 266nm radiation is usually not strong, and it is sufficient to produce a (weak) LIBS signal. Moreover, it is not easy to focus this laser light closely at standoff distances. Therefore, a CO₂ laser is also used, which will hit the target around 0.5 μ s following the 266nm pulse. A rise of the LIBS signals by a factor of 100-300 is the further advantage of this method (Townsend-effect plasma

spectroscopy) that expands the practical analysis range to 40m. Just, femtosecond (750 fs) fiber-laser-induced LIBS is now applied to recognize explosive materials that have fast scanning about (40 mm.s⁻¹) with repetition rates of 225kHz, and pulse energies of 3μJ and (800 or 1030) nm wavelength. Usually, important components involved O, H, C and N; also, molar emissions from C₂ and CN are discovered. It is known that, unlike nanosecond laser technology, femtosecond fiber lasers generate a lowered interference and lowered contributions from organic compounds and allow developing a stable library for noise discrimination (caused by influence of air and the continuum background) [73].

2.5 LIF Technique

LIF has basically been an optical emission from molecules which have been excited to higher levels of energy through absorption of laser radiation. The fluorescence process is the result of a multistage process that occurs in a certain molecule, The first photon of energy $h\nu$ is supplied by an external source such as laser source the molecule, creating an excited electronic singlet state, second: absorption process, molecule absorbed the energy and rearrange its electronic distribution; a number of vibrational levels of the excited state are populated. These higher vibrational levels of the Molecules then will relax to the lowest vibrational level of the excited state (vibrational relaxation) because the life time of the excited state is short (typically 1–10 ns) From these lowest vibrational levels, several processes can cause the molecule to relax to its ground state:

- 1- Non-radiated relaxation by collisional quenching.

- 2- Phosphorescence: A forbidden transition happens when the molecule relaxes from the triplet excited state to the singlet ground state with the emission of light, the lifetime of the triplet state is long so the phosphorescence is slow.
- 3- Intersystem conversion is the overlapping between the ground and the excited electronic state in the vibronic level or it is a very small energy gap according to the quantum mechanical tunneling, the lifetime of the lowest excited singlet state is (10^{-8} sec) and therefore that process is widely compared to fluorescence in many molecules.
- 4- Fluorescence process or fluorescence Emission.

Other processes, which may participate with fluorescence, are excited state isomerization, photoionization, photodissociation and acid-base equilibrium.

The benefit of utilizing fluorescence detection in comparison with absorption measurements is often the higher level of sensitivity obtained due to the fluorescence signal that has a minimal background. LIF has been used to analyze the electronic construction of molecules and to create quantitative concentrations measurements. The analytical applications of LIF involve monitoring the concentrations of gas-phase in the plasmas, flames, and atmosphere in addition to the remote sensing utilizing light detection[74].

2.5.1 Fluorescence Emission

A photon of energy $h\nu$ is emitted; returning the molecule to its ground state corresponds to the relaxation of the molecule from the singlet excited state to the singlet ground state.

The energy of the emitted light is lower, and therefore of longer wavelength, than the excitation photon ($h\nu_{EX}$). The difference in energy or wavelength represented by $(h\nu_{EX} - h\nu_{EM})$ is called the "Stokes shift". The Stokes shift is fundamental to the sensitivity of fluorescence techniques because it allows emission photons to be detected against a low background, isolated from excitation photons [52].

2.5.2. Fluorescence Spectra

Fluorescence emission is a cyclical process if the phenomenon (photo bleaching) does not exist, The same molecule can be repeatedly excited and detected. In fact, that particular energy level can generate many detectable photons. For those reasons, fluorescence detection techniques are highly sensitive.

The magnitude of the Fluorescence intensity is linearly relative to the following conditions [63].

- 1- The absorbance parameters for the studied material.
- 2- The excitation source intensity.
- 3- The fluorescence emission detector efficiency.

There are two techniques of fluorescence measurement, the frequency domain where the information from a steady-state examination (a plot represents fluorescence wavelengths versus intensity) represents what occurs during the absorption and the emission process for the detected material. The intensity and the wavelength of the fluorescence spectrum can be measured by using a spectrometer, which is very accurate and flexible, providing real time measurements of the emission wavelengths. The angle of recording the emission spectrum is 90° in order to minimize scattering and source contributions [73].

The second technique is the time domain where the fluorescence decay can be measured by using time domain fluorescence measurement which needs short excitation pulses (The shorter the pulse the more information can get from fluorescence data), and fast detection circuits (less than half of an expected fluorescence life time $\sim 500\text{ps}$ at least) in the UV range. To record the photon arrival times at every specific position, A photomultiplier tube (PMT) is very suitable to detect the time of the fluorescence signal, that might be recorded and average the signal using a digital oscilloscope [75].

The pulsed excitation light is at a particular frequency figure (2-21). The emission of the induced fluorescence will mirror this modulation shape and show, because of the fluorescence decay, a time delay as a phase-shift. The difference in time of appearance of the fluorescent pulse from the original laser pulse one of the most important parameter to distinguish between the materials, and the depth of the modulation which represents the difference between the original reflected pulse and the height of the fluorescence pulse which will decrease according to the excitation light, but the average intensity remains constant. The phase-shift and modulation-depth depend on the lifetime of the fluorescence; these three combined spectral parts will give an image of the total behavior of the detected signal, carrying a lot of information to compare and distinguish between materials. It should be noted that the difference between these parameters remains constant for standoff distance [76,77].

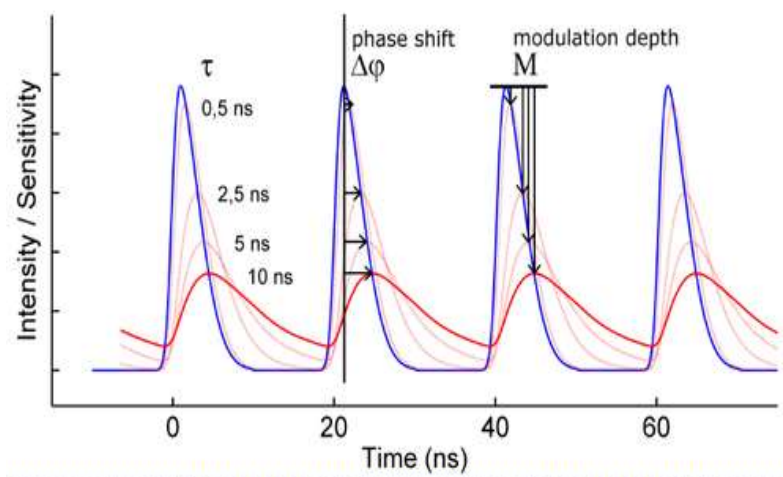


Figure 2.22: The excited and the fluorescence pulses elucidate the modulation depth the phase shift, and the relaxation time and shape[78].

2.5.3. LIF of Explosives

Fluorescence spectroscopy can be used in the explosive materials detection field since the explosive materials are fluorescence spatially with excitation wavelength in the UV region, A spectrum with high sensitivity and specificity may be obtained from the fluorescence of that material [79].

There are many techniques that share the same principle like differential reflectance which depends on the idea that radiation which comes from a pulsed illuminating source will backscatter to the detector from the tested sample. The backscattered radiation is an indicator for the type of explosive material type, but the air particle's scattering spatially at standoff distances and the low molecular concentrations led to sensitivity limits for these lasers ranging techniques [8]. However, most of these techniques need to collect the samples and analyzing them through a time period enough to rise the SNR to the high level.

Optical fluorescence has the probability to exclusively classify Trace amounts of explosive molecules by irradiating samples by a laser in the UV region, which will make them strongly absorbed and fluorescence. The drawbacks of this technique are the very high sensitivity and environmentally offered the benefits are being fast (the detection of a sample can be done on a portion of a second), remote (the detector and the sample can be several meters far), sensitive (more than parts per million), particular (sample can be distinguished by their spectroscopic fingerprint)- User safe (the system can be arranged in few minutes and does not need a specially trained user)[78].

Chapter Three

Experimental setup

This chapter shows a practical side of the work. In order to study the physics of laser induced plasmas, reliable measurements of laser beam power, beam energy, beam diameter, and the intensity distribution of the beam cross-section are needed. The experimental setups are prepared for two parts: LIBS experiment and LIF experiment.

3.1 Setup of LIBS Experimental

The LIBS arrangement used in this work consisted of the following constituents:

- A pulsed laser source which is used to generate the plasma.
- An optic (lens or optical fiber) is used to collect light.
- Spectral analysis system is used to analyze the resulting atomic emission peaks and determined the elemental constituents of the sample and their relative concentrations.
- A computer is used to display and save the results spectrum.

The Nd-YAG laser is used for the ablation of samples material and generation of LIBS plasma. The laser beam is focused onto the sample by using fused silica quartz lens having a focal length of (10 cm) ,the sample placed on a stage with an adjustable height. The optical emission from the plasma is collected and guided to spectrometer via the fiber, to yield information on the material composition. The fiber bundle is positioned at a distance of nearly (1.0-1.5 cm) from the plasma, making an angle 45° to the laser beam. A small lens is mounted at the tip of fiber bundle, the

spectrally dispersed signal from the spectrometer is automatically sent to charge-coupled device (CCD), in-built within the spectrometer, which converts the spectral signal into digital signal. The LIBS spectrometer allows us to acquire laser-induced breakdown spectroscopy (LIBS). Spectrum ranges from (320 to 740 nm). This whole set-up is controlled by a software. By the equipped program with the analyzer, the light intensity as a function of wavelength is recorded in a computer, and the LIBS system is controlled by a computer. figure (3-1) is a schematic diagram of the LIBS system which describes the main components of LIBS set-up[28].

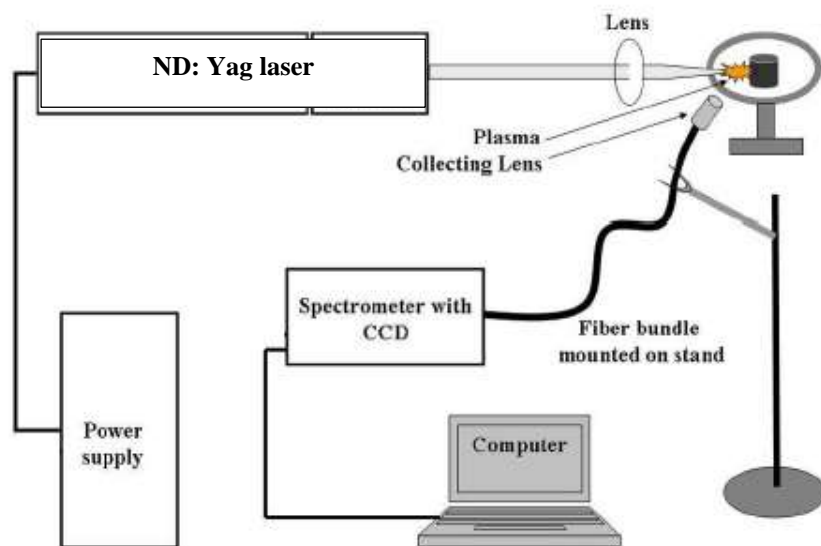


Figure (3.1): Structure of LIBS Experiment

3.1.1 Experimental Instrument:

In the following description of the main instrument and its specification used in LIBS setup

A. The Laser System (Nd-YAG):

The Nd:YAG laser in our lab used is the passive Q-switching (the intracavity loss modulation is performed by a storable absorber, which introduces large losses for low intensities of light and small losses for high intensity) (IR). A laser comprises just an active medium and a resonator will emit a pulse of laser light each time the flash lamp fires. However, the pulse duration will be long, about the same as the flash lamp and its peak power will be low. When a Q-switch is added to the resonator to shorten the pulse, output peak power is raised dramatically; (solid state laser) pulse which delivers pulse energy (300mJ) at 1064 nm, within (9 ns) pulse duration, repetition rate (1 HZ). The laser beam focused using the focusing lens (focal length 10 cm). This laser operates at a fundamental wavelength, the LIBS system set-up is shown in figure (3.2):

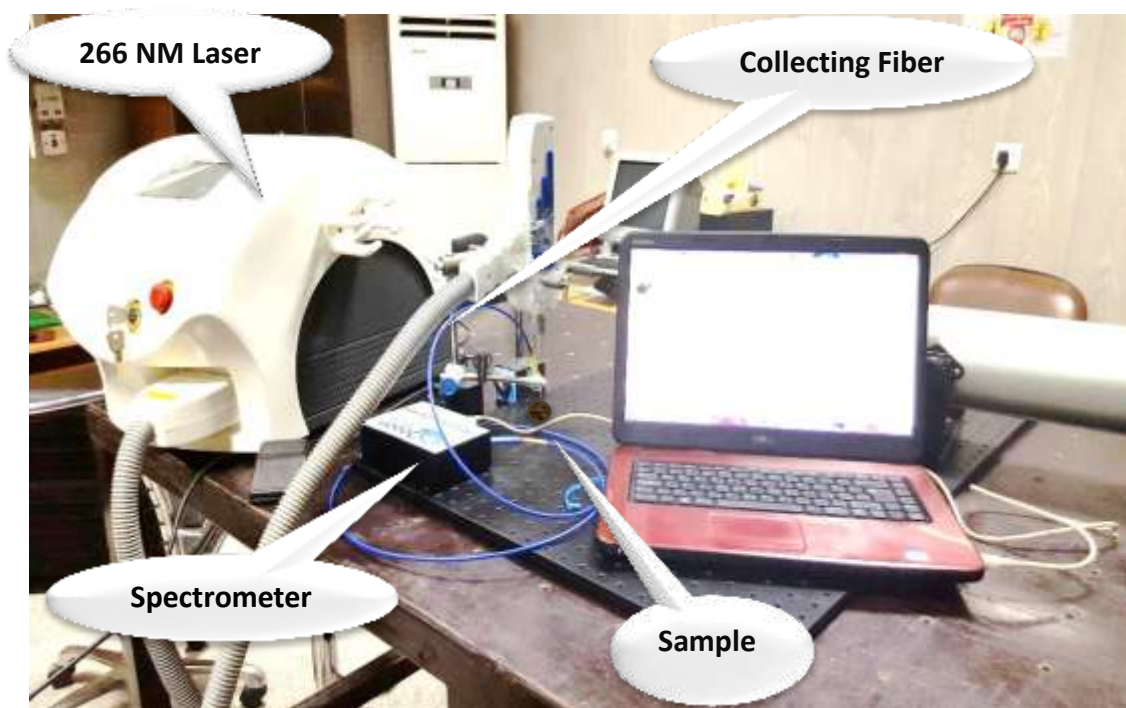


Figure (3.2): Experimental setup of LIBS system.

B. Plasma emission analysis system:

The analysis system of the LIBS technique consists of spectrometer and fiber optic . We have used a spectrometer type Ocean optics (HR 4000 CG-UV-NIR). Below is a diagram of how light moves through the optical bench of a Spectrometer. The optical bench has no moving parts that can wear or break, all the components are fixed in place at the time of measurements.

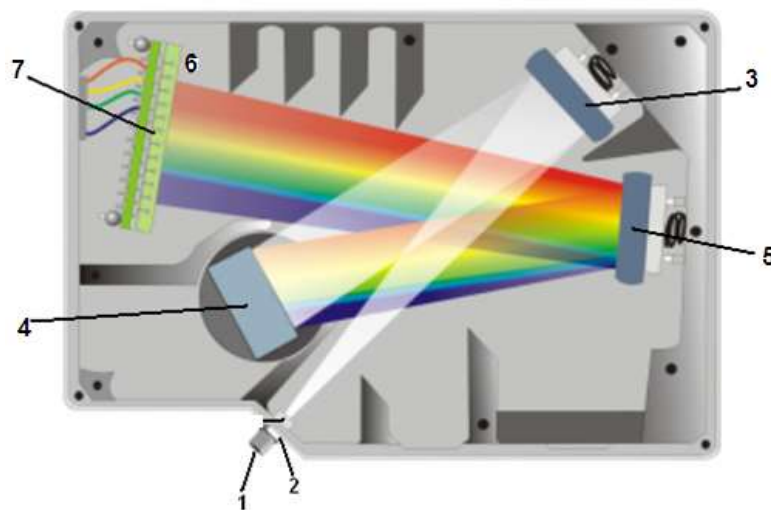


Figure (3.3): Structure of Spectrometer Device

There are explanations of the function of each numbered component in the spectrometer in this diagram:

- 1- SMA Connector: Secures the input fiber to the spectrometer. Light from the input fiber enters the optical bench through this connector.
- 2- Slit: behind the SMA Connector, the size of the aperture regulates the amount of light that enters the optical bench and controls the spectral resolution.
- 3- Collimating Mirror: Focuses light entering the optical bench towards the grating of the spectrometer. Light enters the

- spectrometer, passes through the SMA Connector, Slit, and Filter, and then reflects off the Collimating Mirror onto the Grating.
- 4- Grating: Diffracts light from the Collimating Mirror and directs the diffracted light onto the Focusing Mirror. Gratings are available in different groove densities, allowing to specify wavelength coverage and resolution in the spectrometer.
 - 5- Focusing Mirror: Receives light reflected from the Grating and focuses the light onto the CCD Detector or L2 Detector Collection Lens (depending on the spectrometer configuration).
 - 6- An optional component that attaches to the CCD Detector. It focuses light from a tall slit onto the shorter CCD Detector elements. The L2 Detector Collection Lens should be used with large diameter slits or in applications with low light levels. It also improves efficiency by reducing the effects of stray light.
 - 7- CCD Detector (UV or VIS): Collects the light received from the Focusing Mirror or L2 Detector Collection Lens and converts the optical signal to a digital signal. Each pixel on the CCD Detector responds to the wavelength of light that strikes it, creating a digital response. The spectrometer then transmits the digital signal to be analyzed by a computer program.

3.1.2 Measuring of Laser Beam Diameter

The diameter of the laser beam can be reduced by using a lens, the focal length of the lens was 100 mm. The diameter of the laser beam was 1 mm. The reason of using a lens with 100 mm focal length is to decrease the spot size of the laser beam, which leads to increase the power density of laser. Consequently, the creation of the ionization process will be easier.

3.1.3 The energy rate calculation:

From the measured spot size of the laser beam, we found that the diameter of the laser beam before the lens (D) is (5mm). So the beam diameter can be calculated after the lens by using the following:

$$D^\circ = 1.27 * f * \lambda / D \dots\dots (3.1)$$

Where:

D: the diameter of laser beam before lens.

D°: the diameter of laser beam after lens.

f : focal length of a focusing optic

λ: the wavelength of laser (1064nm).

$$\begin{aligned} D^\circ &= 1.27 * 10 * 10^{-7} * 1064 / 5 * 10^{-1} \\ &= 2.7 * 10^{-3} \text{ cm} \end{aligned}$$

The radius of the spot r is: $r = 1.35 * 10^{-3} \text{ cm}$

The area of the laser spot is:

$$\begin{aligned} A &= \pi * r^2 \dots\dots\dots (3.2) \\ &= 5.72 * 10^{-6} \text{ cm}^2 \end{aligned}$$

Peak power = energy rate / pulse duration (3.3)

$$\begin{aligned} P.P &= 334.7 \text{ mJ} / 9 \text{ ns} \\ &= 37 * 10^6 \text{ J/s} \\ &= 37 \text{ MW} \end{aligned}$$

Intensity = P.P/ area (3.4)

$$I = 6.4 * 10^6 \text{ MW/ cm}^2.$$

3.2 LIF Experimental set up:

The main components in LIF experiments are the excitation laser, the photo detector, the band pass optical filters, and the samples being tested. The schematic diagram is shown in figure 3.4. In our study, the laser was a QUANTEL – Brilliant / Brilliant B system, which is a coherent, collimated monochromatic light source that provides variable laser output from 1064nm, 532, 355, 266 and 213 nm. The laser output was an 6mm^2 beam of 5 ns pulses, emitted at a rate of 1HZ. All wavelengths reported are values in air (approximately 0.03% less than the wavelengths in a vacuum). The fluorescence detection subsystem consisted of a solar-blind (tuned to eliminate the background solar radiation) photomultiplier tube (PMT) in addition to optical filters.

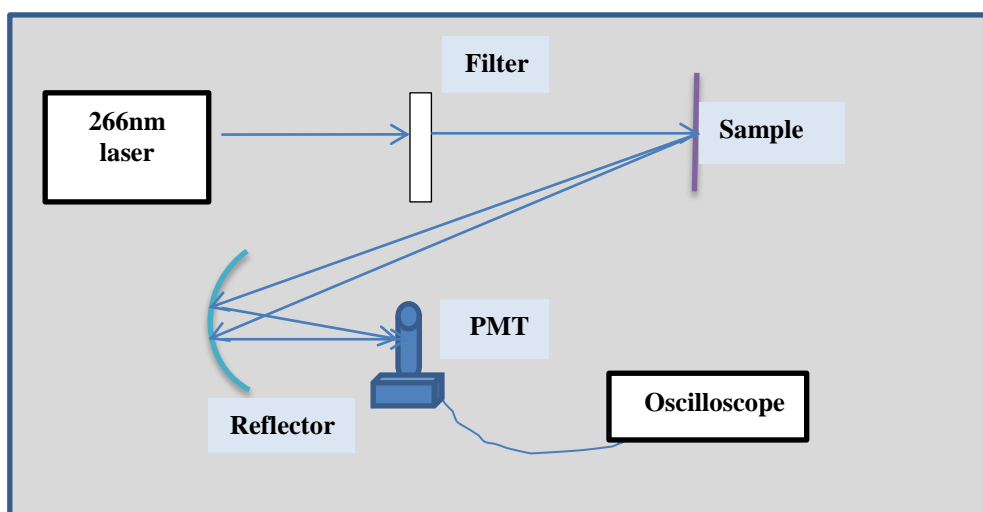


Figure (3.4): Structure of fluorescence Experimental set up

The fluorescence light from the sample is collected by a reflector and directed onto the face of a detector with a spatial filter on the front to removes the unwanted wavelength. The output signal can be observed by an oscilloscope or spectrum analyzer. A reference sample of the solid material is placed in the silver substrate. The LIF system set-up shown in figure (3.5):



Figure (3.5): LIF laboratory experimental setup

3.2.1 Experimental Instrument:

The specification of instruments used in LIF experiment will be stated as follows:

A. The Laser System

The optical source installed in this optical setup for sample fluorescence measurements is a tunable laser source, (Nd:YAG laser from Quantel's laser company Brilliant B series), as shown in figure 3.6.



Figure (3.6): QUANTEL – Brilliant / Brilliant B Laser System

This laser system can be tuned to provide several laser wavelengths infrared, invisible and DUV source in CW and pulse radiation in five wave lengths and five energies as shown in the table below:

Table (3.1): QUANTEL – Brilliant / Brilliant B Laser System Specification

Specification	Brilliant 10Hz
Energy 1064nm	850mJ
Energy 532nm	400mJ
Energy 355nm	225mJ
Energy 266nm	90mJ
Energy 213nm	16mJ
Repetition rate	10Hz
Pulse 1064nm	5ns
Divergence 1064nm	<0.5mrad
Energy stability 1064nm	+/-2%
Beam diameter	6mm

B. Optical Filters

Two types of filters have been used in order to pass only the required wavelength. These filters are: A long pass optical filter from “Chroma” company type (zt266rdc) with an edge at 266 nm is used to block the back scattered light from entering the detector, the second is Laser Line Filter from Newport company type (10LF10-532) which is 25.4 mm diameter, and full width half max of 10 ± 2 nm. It is optimized to block X-ray to Far IR wavelengths.

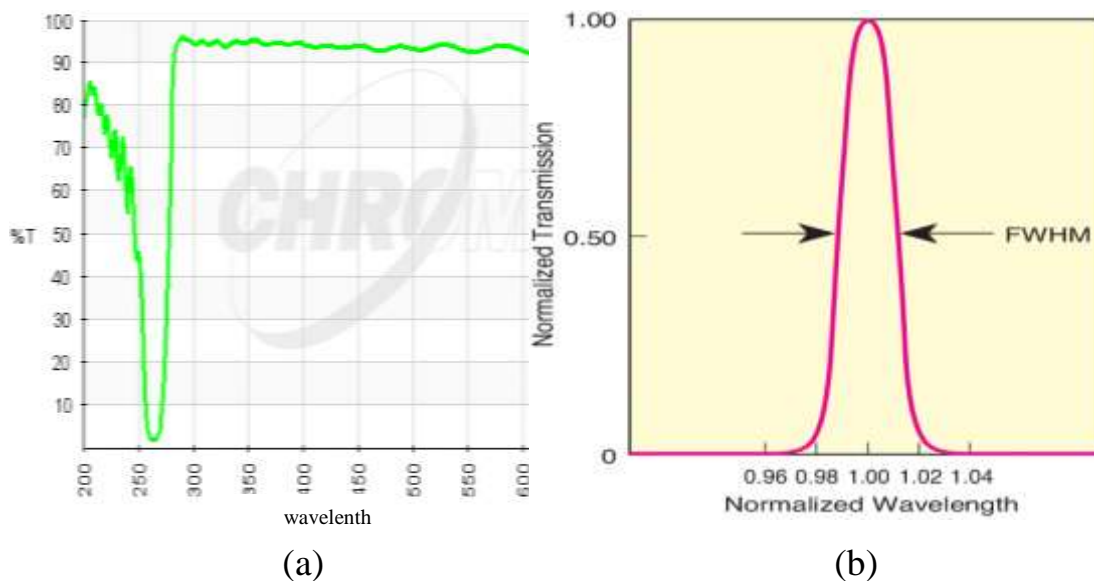


Figure (3.7): Optical Filters Spectrum (a) long pass filter (b) Line Filter

C. UV Detector

The detection elements in this research contain Ocean optics (HR 4000 CG-UV-NIR) spectrum analyzer which was used and Hamamatsu UV photomultiplier tube type R6354 in the range (160-320nm) which was optimized to improve the detection efficiency in the (UV) region, a Tecktronik 500MHZ oscilloscope that was connected to the output of the photomultiplier tube. Generally, many serial measurements were taken for every one sample to ensure the repeatability of the results.

The spectrometer used in this project makes possible real-time imaging of the sample and help to carry out the spectral analysis, by the appropriate choice of the imaging or the spectral modes of operation, the fluorescence spectra of most of the explosives studied was very weak, requiring the highest sensitivity setting available for the detector. High sensitivities, are achieved by a front coated concave reflector with (8cm) Diameter made in our laboratory was used for collecting and focusing the fluorescence signal on to the photomultiplier window. This provides a

high magnification and it led to an effective stand-off distance of more than 6 meter.

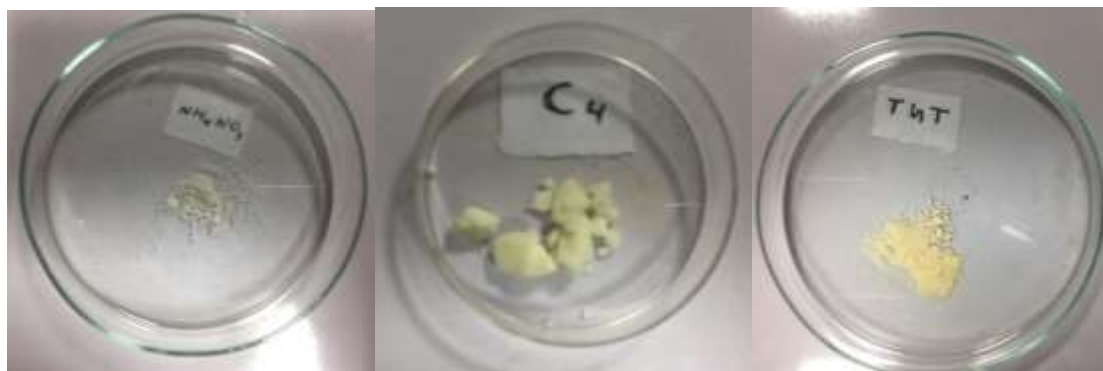
3.2.2 Fluorescence Measurements

Two types of fluorescence measurement were used in the present research; the first was used the spectrometer to record the fluorescence signal as a function of the wavelength and the signal intensities. This method is the simplest and widely used method; it is affected by the environment and the background condition like temperature, light. The excitation beam is delivered onto the sample surface and the scattered signal is rejected by the spatial filter, the filter is placed before the detector window to filter out the elastically scattered light from the signal before entering the slit of the detector that placed at 90° to the incident light beam to minimize the risk of transmitted or reflected incident light reaching the detector

The second method is the use of the fluorescence time domain. The fluorescence process is a spatial process happened in a specific time which is the time of the excited electrons to relaxed, measuring this time to indicate that the fluorescence signal is another method that can be used, a UV photomultiplier tube and oscilloscope are used to record the fluorescence signals as a function of time, with a high amplification by collimating the fluorescence signal on the PMT window using the concave reflectore .

3.3 Explosive Material Samples

Three samples of explosive, which is commonly used, are: NA, C4 and TNT. These samples are brought from the Iraqi Ministry of Interior. Figure 3.8 shows the three explosive material samples.



(a)

(b)

(c)

Figure (3.8): Explosive samples: (a) AN, (b) C4, (c) TNT

3.3.1 Sample Preparation

A thin layer of the solid samples of energetic materials was placed on one side of the substrate. This process can be repeated to insure a better purification as shown in the literature, for experiments requiring these samples was placed an the same sample holder.

3.3.2 Substrate

In order to minimize the amount of fluorescence from interfering, and reduce the substrate backscattered, a suitable type of substrate must be chosen like silver substrate which have high absorption in the UV wavelanght. A metal surface coated with car paint, and glass was selected as an example of a general real- world substrate, the fluorescence of this substrate and many other materials is more intense when a shorter wavelength excitation is used.

Chapter Four

Results and Discussion

This chapter presents the Simulation and Laboratory experimental systems results that have been collected. The 455 systems of the two techniques involving LIBS and optical fluorescence have been proposed and tested to identify the components of different samples.

Mainly there are two concepts in these experimental results. The first concept is about the results of two experimental techniques. The second concept is about the recognition programs that identify the element from the output curves of each technique.

4.1 Experimental Results

As described in chapter 3, the experiments for LIBS and LIF techniques, in following are the results from each experiment.

4.1.1. LIBS Results

In this method, a laser pulses have been shot at different locations on each sample, LIBS spectrum for three different energetic samples (TNT), (C4) and (AN) have been obtained with a spectrum range between (321 nm to 700 nm). This spectrum represents the fingerprint of each sample that contains many emission lines each represents an element and its concentration.

The spectra contain atomic lines coming from oxygen, carbon, hydrogen and nitrogen emissions; the similarity in the constituents of energetic materials results in the emission spectra of these materials sharing the same spectral lines. To analyze the

LIBS spectrum of the samples and determine the element that correspond to each transmission line, NIST (National Institute of Standards and Technology) spectral line database has been used as the reference source of information online position, and on the relative intensities. The emission spectrum of the three samples of explosive has been analyzed as follows:

A. TNT Sample

From the analyzed optical spectrum of the emissions of elements that exist in the TNT sample within the spectrum range (from 321 nm to 700 nm) and optical pumping (1064 nm) by Q-switched Nd:YAG laser of 9 ns pulse width and 1 Hz repetition rate and power 300 mJ), a number of clearly emission lines were appearing as shown in figure 4.1.

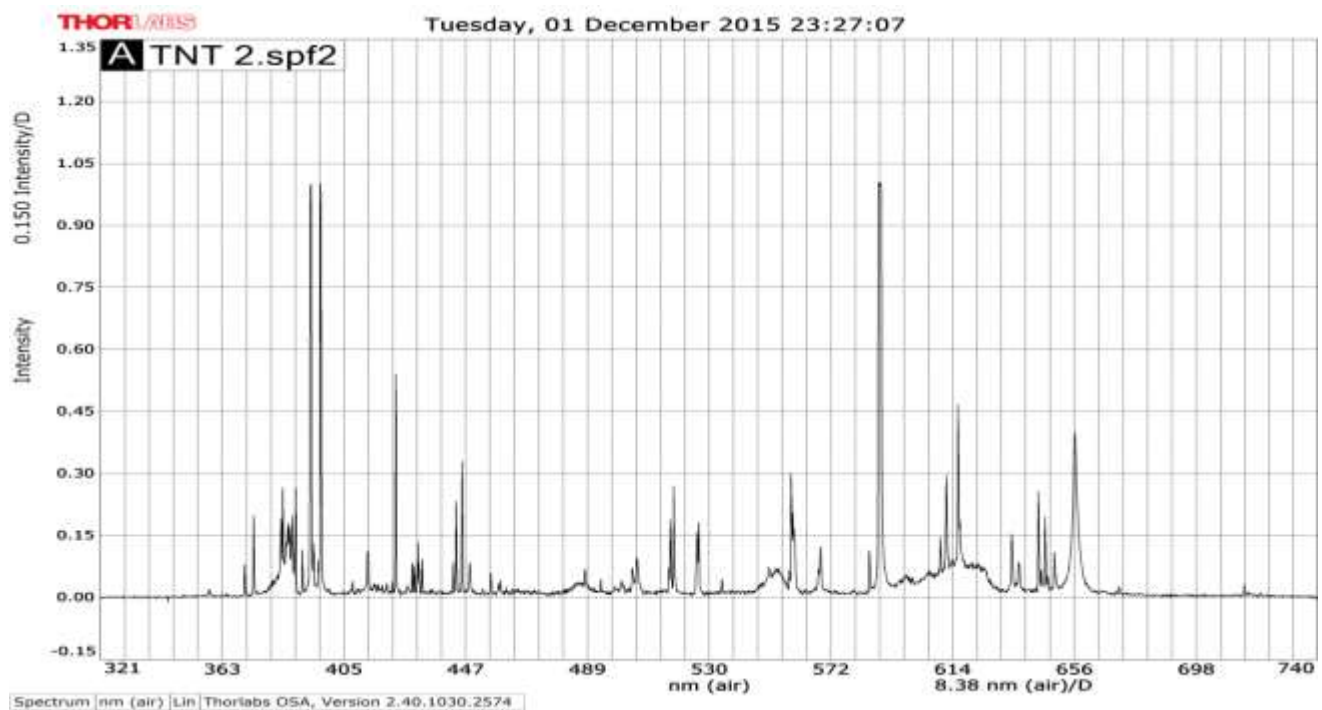


Figure (4.1): LIBS spectrum of TNT material.

When analyzed, these emission lines are compared to NIST database and they showed the existence of the following elements:

- 1- Oxygen Ions: O I, O II, O III and O IV.
- 2- Carbon Ions: C I, C II, C III.
- 3- Nitrogen Ions: N II.
- 4- Hydrogen.

Figure 4.2 shows the position of clearly emission lines and table 4.1 illustrated the corresponding element to particular spectrum lines by comparing with the NIST (atomic spectra database).

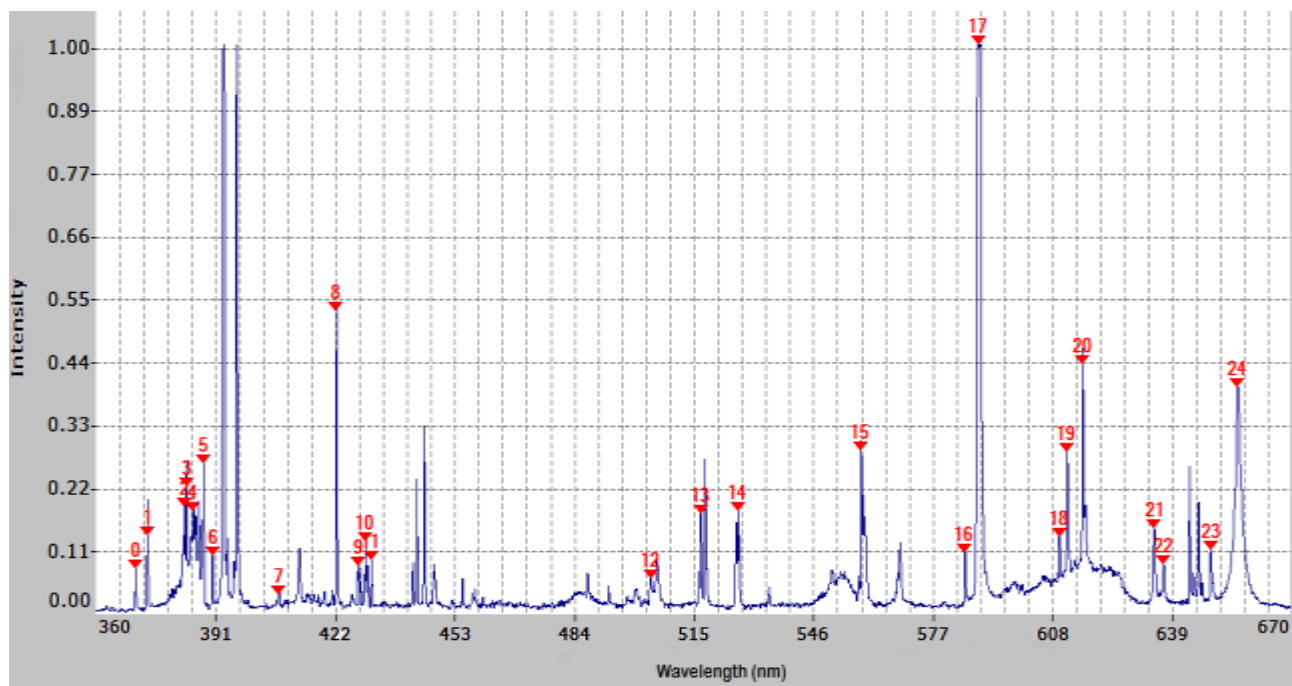


Figure (4.2): LIBS spectrum analysis of TNT material in air.

Table (4.1): Spectral Transition in the LIBS spectrum of TNT with assignment

	Spectral Transition						
	0St	1 St	2St	3St	4St	5St	6St
Spectrum line	370.688	373.804	383.212	383.854	385.637	388.276	390.558
NIST Element Corresponding	370.724 (O III)	373.685 (O IV)	383.307 (O II)	383.837 (N II)	385.613 (O II)	388.244 (O II)	390.63 (O II)
	Spectral Transition						
	7St	8St	9St	10St	11St	12St	13St
Spectrum line	407.761	422.723	428.357	430.247	430.71	504.217	517.212
NIST Element Corresponding	407.771 (O II)	422.774 (N II)	428.372 (O II)	430.285 (O II)	430.758 (C II)	504.197 (O II)	517.581 (C III)
	Spectral Transition						
	14St	15St	16St	17St	18St	19St	20St
Spectrum line	526.867	558.783	585.711	589.262	610.13	612.128	616.147
NIST Element Corresponding	526.894 (C I)	558.323 (O II)	585.834 (C III)	589.202 (C I)	610.338 (O II)	612.081 (C I)	616.001 (C III)
	Spectral Transition						
	21St	22St	23St	24St			
Spectrum line	634.697	637.114	649.321	656.359			
NIST Element Corresponding	635.077 (C III)	637.432 (O I)	649.58 (O II)	656.279 (H)			

B. Ammonium Nitrate (AN)

Through analyzing the optical spectrum of the emissions from elements that exist in the AN sample within spectrum range (from 321 nm to 700 nm) and optical pumping (1064 nm) by Q-switched Nd:YAG laser of 9 ns pulse width and 1 Hz repetition rate and power 300 mJ), a number of clearly emission lines appeared as shown in figure 4.3.

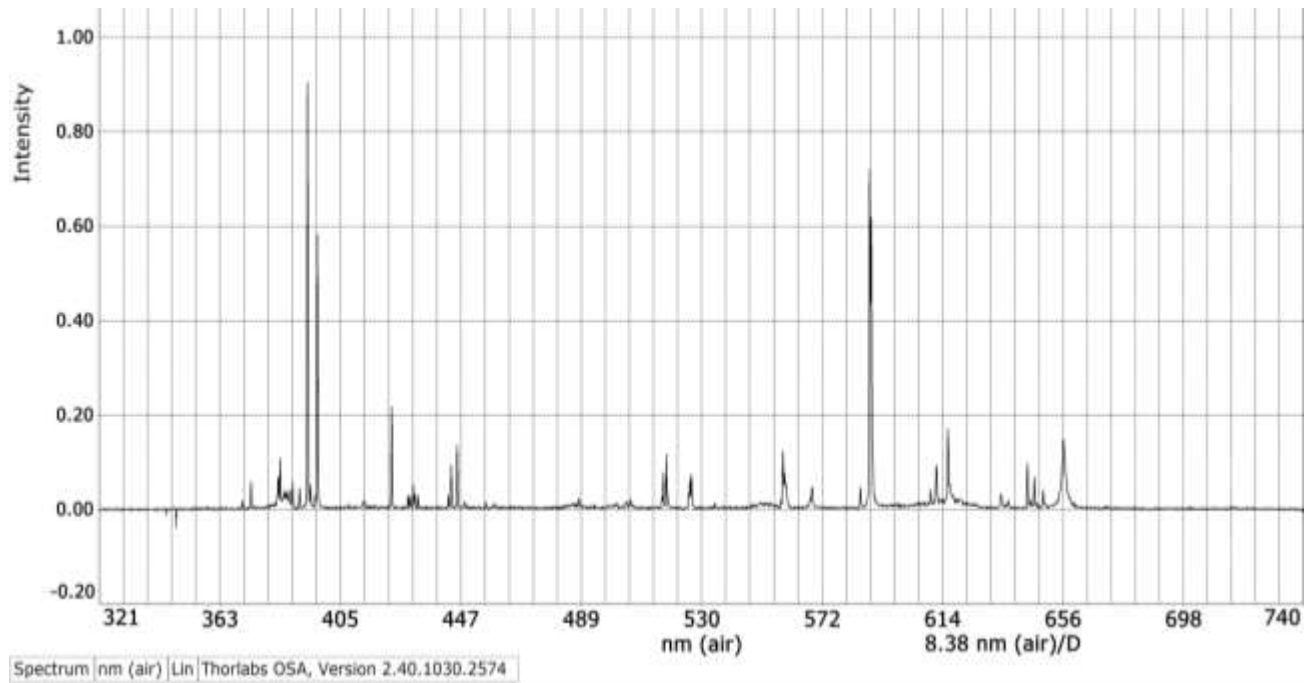


Figure (4.3): LIBS spectrum of AN material.

When these emission lines were analyzed and compared with the NIST database, that showed the existence of the following elements

- 1- Oxygen Ions: O II and O IV.
- 2- Nitrogen Ions: N II.
- 3- Hydrogen.

Figure 4.4 shows the position of clearly emission lines and table 4.2 illustrated the corresponding element of each spectrum line by comparison with the NIST atomic spectra database.

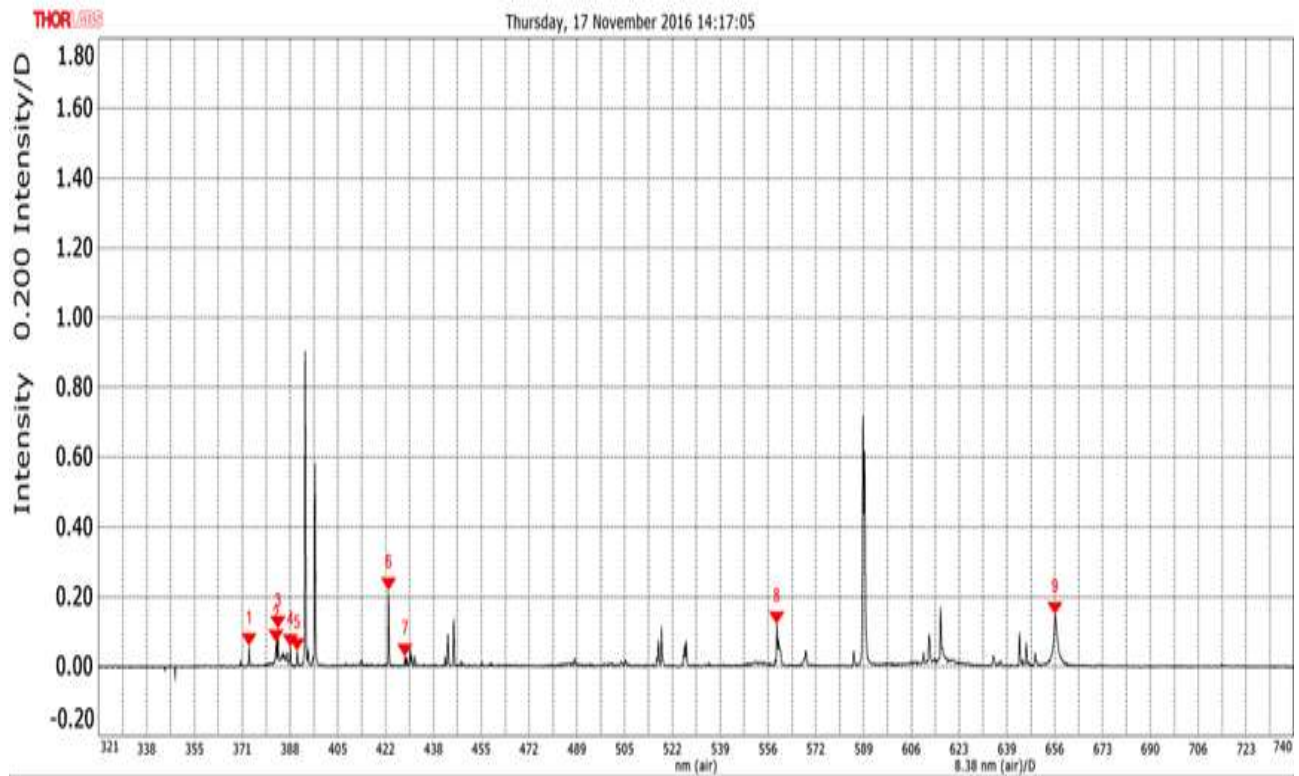


Figure (4.4): LIBS spectrum analysis of AN material in air

Table (4.2): Spectral Transition in the LIBS spectrum of AN with assignment

	Spectral Transition						
	1St	2St	3St	4St	5St	6St	7St
Spectrum line	373.69	383.19	383.859	388.292	390.512	422.719	428.354
NIST Element Corresponding	373.685 (O IV)	383.307 (O II)	383.837 (N II)	388.244 (O II)	390.63 (O II)	422.774 (N II)	428.372 (O II)
	Spectral Transition						
	8St	9st					
Spectrum line	558.73	656.304					
NIST Element Corresponding	558.323 (O II)	656.279 (H)					

C. C4 Sample

Through analyzing the optical spectrum of the emissions from elements that existing in the C4 sample in spectrum range (from 321 nm to 700 nm) and optical pumping (1064 nm) by Q-switched Nd:YAG laser of 9 ns pulse width and 1 Hz repetition rate and power 300 mJ), a number of clearly emission lines appeared as shown in figure 4.5.

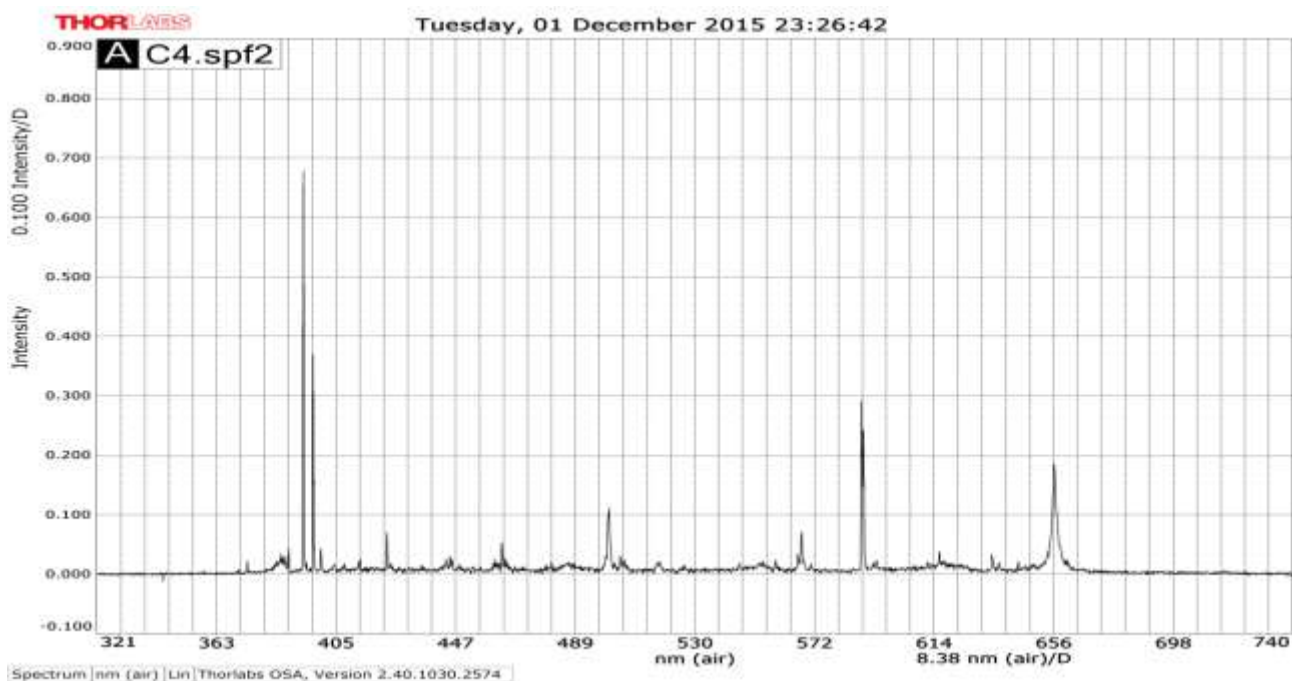


Figure (4.5): LIBS spectrum of C4 material.

When analyzed, these emission lines were compared with the NIST database they showed the existence of the following elements

- 1- Oxygen Ions: O II, and O IV.
- 2- Carbon Ions: C I, C II, C III.
- 3- Nitrogen Ions: N II.
- 4- Hydrogen.

Figure 4.6 shows the position of clearly emission lines of C4 and table 4.3 illustrated the corresponding element of each spectrum line by comparison with the NIST atomic spectra database.

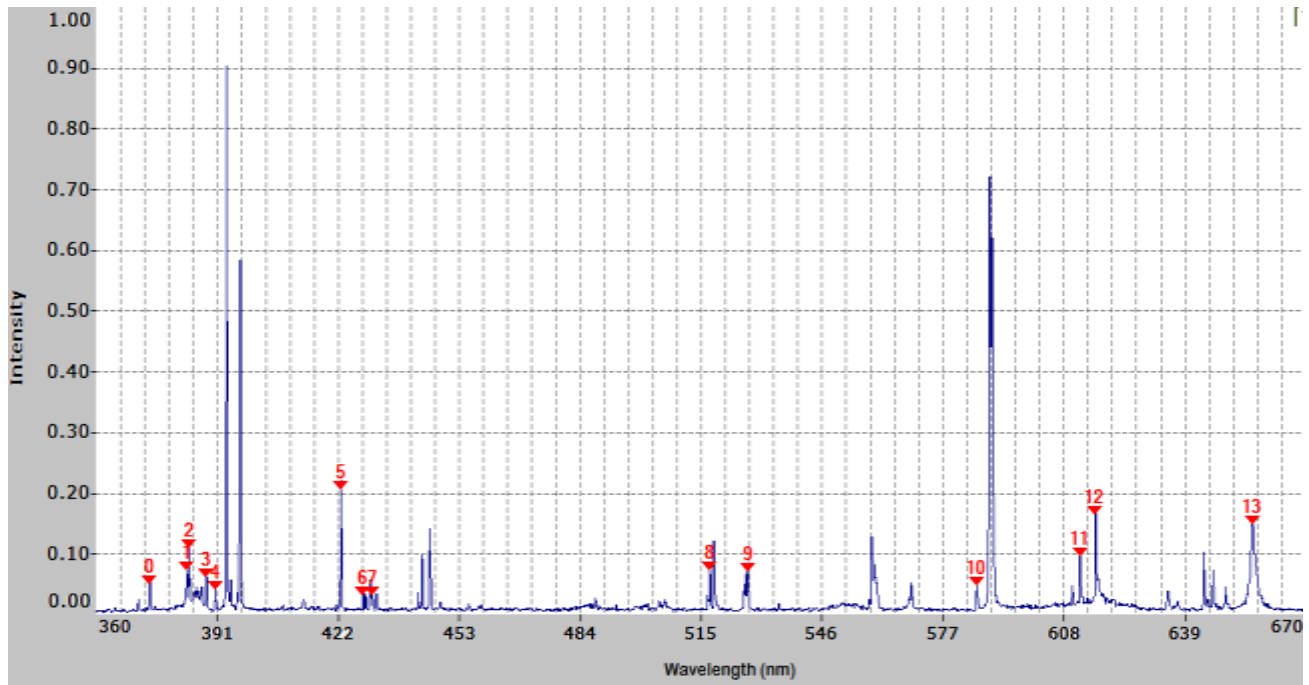


Figure (4.6): LIBS spectrum analysis of C4 material in air.

Table (4.3): Spectral Transition in the LIBS spectrum of C4 with assignment

	Spectral Transition						
	0St	1 St	2St	3St	4St	5St	6St
Spectrum line	373.73	383.279	383.809	388.243	390.592	422.74	428.356
NIST Element Corresponding	373.685 (O IV)	383.307 (O II)	383.837 (N II)	388.244 (O II)	390.63 (O II)	422.774 (N II)	428.372 (O II)
	Spectral Transition						
	7St	8St	9St	10St	11St	12St	13St
Spectrum line	430.71	517.248	526.94	585.731	612.146	616.162	656.358
NIST Element Corresponding	430.758 (C II)	517.581 (C III)	526.894 (C I)	585.834 (CIII)	612.081 (C I)	616.001 (CIII)	656.279 (H)

From spectrum analysis results of three explosive components one can observe that the common elements are: oxygen ions (O II and O IV) that appeared in emission lines at (373.685 nm, 383.307 nm, 388.244 nm, 390.63 nm and 428.372 nm,) nitrogen ion (N II) that appeared in emission lines at (383.837 nm and 422.774 nm) and hydrogen that appeared at(656.279 nm). In addition, carbon ions (C I, C II, C III) are found in emission lines at(430.758,517.581,526.894,585.834,) that for both explosive materials in TNT and C4 but not found in AN. This is due to the organic components presents in C4 and TNT, Other peaks in the explosives spectra are related to the impurities in that sample. The high affected emission lines of LIBS by the background condition and the incapability to gain repeatable data is the reason for the limit LIBS ability to classify trace amounts of energetic materials.

4.1.2 Fluorescence Results

In this part two methods were used: Frequency domain and time domain.

A. Frequency Domain Results

A frequency domain method has been used to record fluorescence spectra from samples after shooting it by laser. At first we have been test three fluorescnce spectra for three different energetic samples (Trinitrotoluene (TNT), C4 and ammonium nitrate (AN)).

1) TNT Sample

Through analyzing the fluorescence spectrum of TNT sample generated by shooting TNT sample by (266nm) laser of (15 mg) energy, the frequency spectrum of TNT is shown in figure 4.7.

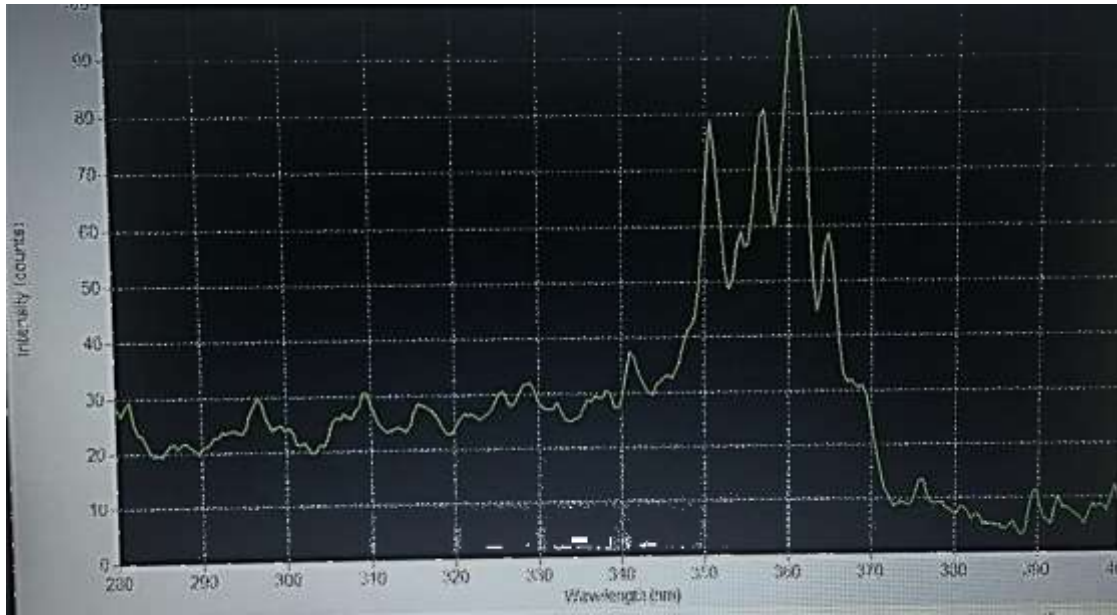


Figure (4.7): Fluorescence spectrum of TNT material by Frequency Domain method

2) Ammonium Nitrate (AN) Sample

Through analyzing the fluorescence spectrum of AN sample generated by shooting AN sample by (266nm) laser of (15 mJ) energy, a clearer AN fluorescence spectrum is shown in figure 4.8.

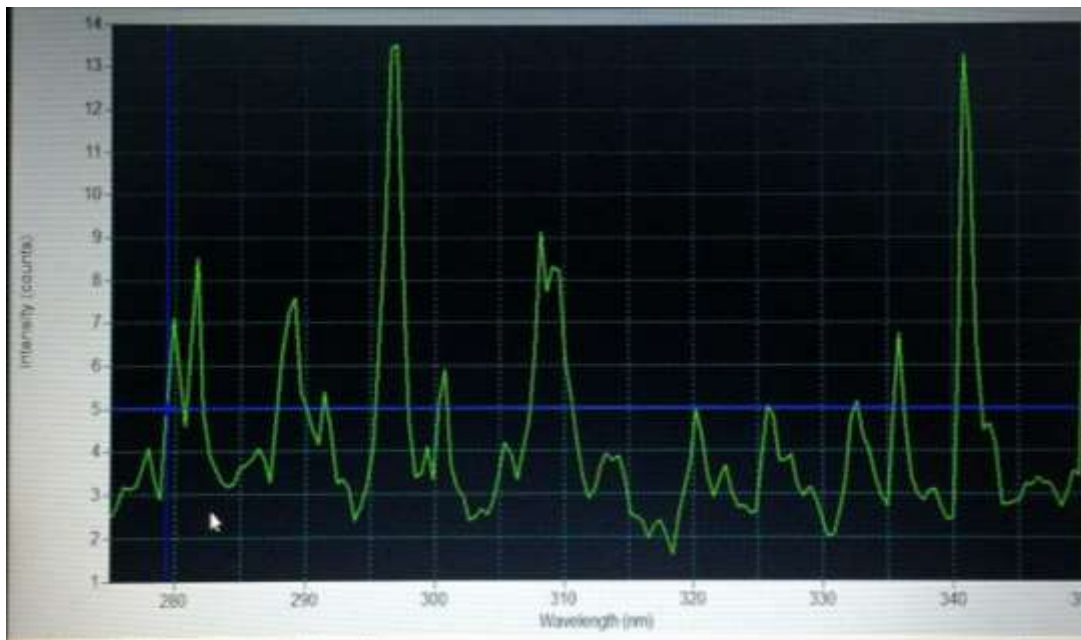


Figure (4.8): Fluorescence spectrum of AN material by Frequency Domain method

3) C4 Sample

Through analyzing the fluorescence spectrum of C4 sample generated by shooting (the same as TNT sample by 266nm) laser of (15 mJ) energy, a clear C4 fluorescence spectrum has been recorded as shown in figure 4.9.

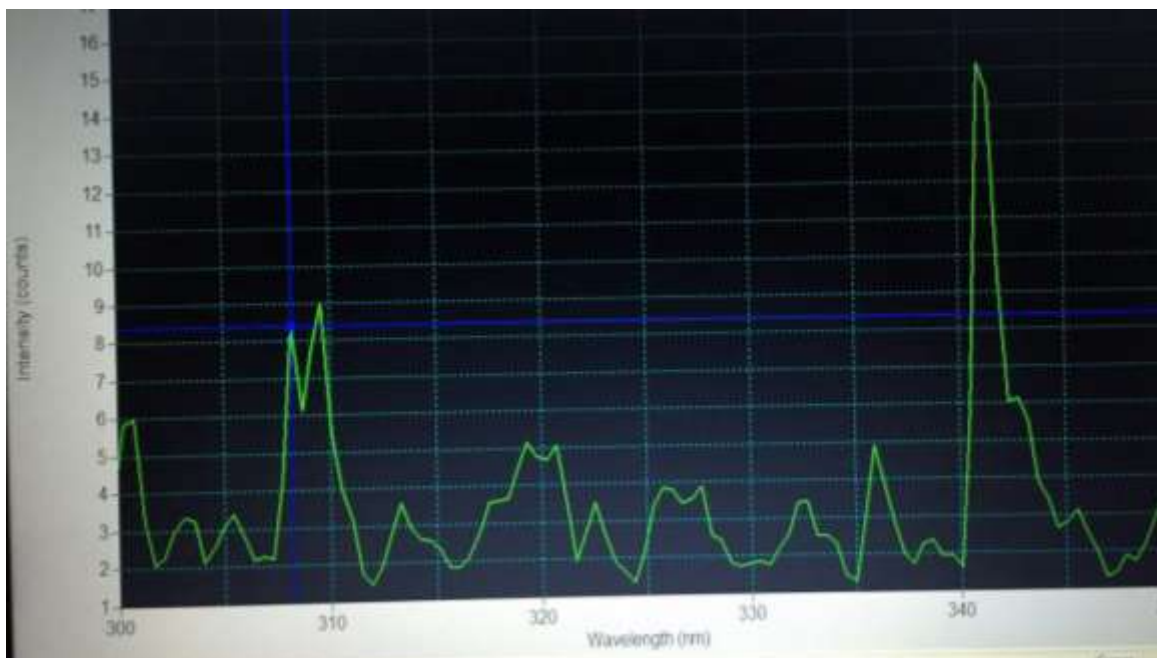


Figure (4.9): Fluorescence spectrum of C4 material by Frequency Domain method

From figure 4.7, 4.8 and 4.9, the fingerprints of energetic material are in the range between (300-370)nm , comparing these results with Sandia laboratory report [21], it is shown that the peaks are similar but the transitions start in a different range. This because we worked with solid materials rather than Sandia work. They used solutions explosive, the reason for this difference is in the solutions. The vibrational collisions transitions with molecules of solvent will appeared more rapid than solid phase, therefore, the vibrational transitions will be in the range of tenths of picoseconds so there will be no transitions of the vibrational levels of the higher electronic excited states to the ground state therefore the spectrum will be Narrower than the spectrum in solution phase.

B. Time Domain Results.

A time domain method has been used to record fluorescence spectra from samples after shooting them by uv-laser pulses. At first, three fluorescence spectra have been tested for three different energetic samples (Trinitrotoluene (TNT), C4 and ammonium nitrate (NH_4NO_3)); the spectrum that got from each of them was used as a reference for simulated tests. Second, we have been simulating the real scanned by but these samples over some expected surfaces such as (car paint, glasses, walls, etc.) then compared it with fluorescence spectrum of pure samples.

1) TNT Sample

Through analyzing the fluorescence spectrum of TNT sample that comes from shooting TNT sample by (266nm) laser (5nsec) laser pulse and (15 mJ) energy which enables us for standoff detection of (8meter), a clear time domain TNT fluorescence spectrum can be shown in figure 4.10.

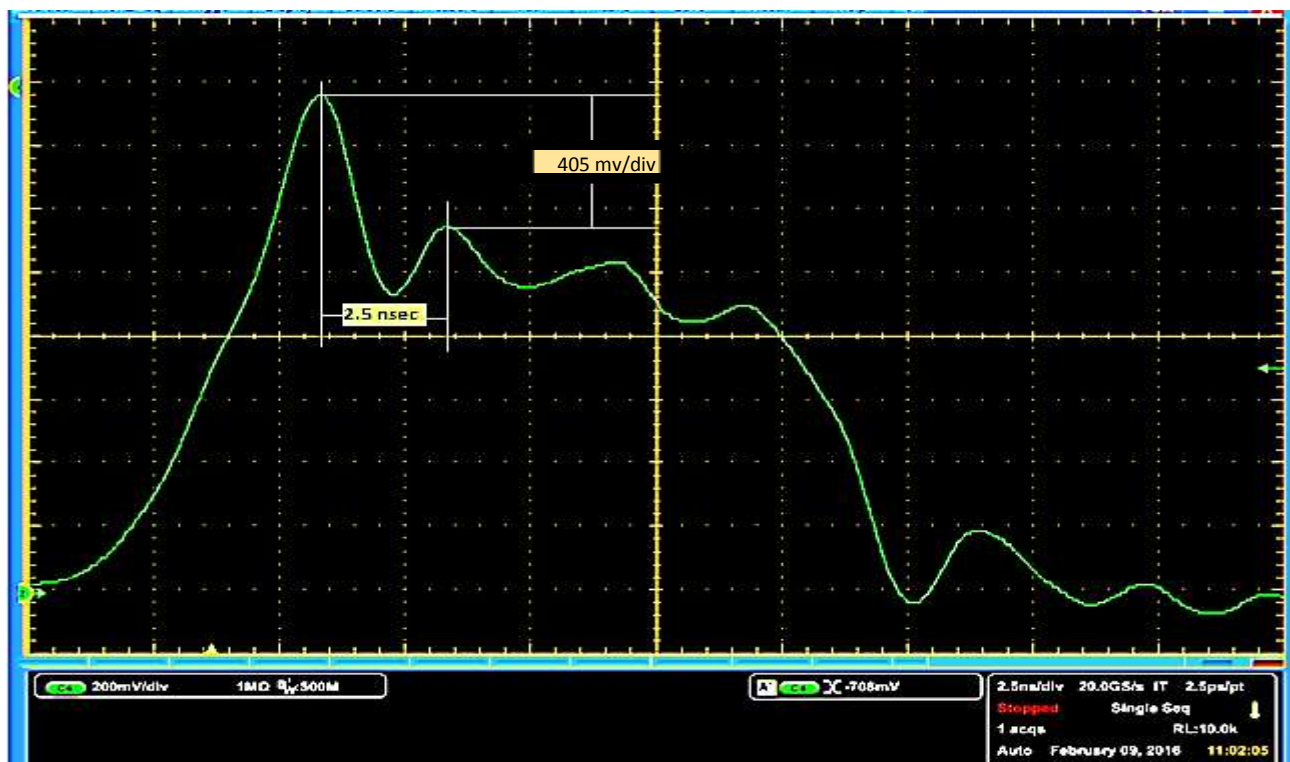


Figure (4.10): Fluorescence spectrum of TNT material (5nsec/ div),200mv/div

From figure 4.10, it seems that the fluorescence of TNT appeared after (10 nsec) after shooting with the laser pulse. The time domain laser-fluorescence pulses for TNT with the following parameters:

a) The fluorescent phase difference:- $\Delta\phi = 2.5nsec \mp 0.2nsec$ which represents the time after impulses the target then the fluorescent spectrum appeared .

b) The modulated difference = $405mv/div \mp 10mv/div$. which represent the height of the fluorescent pulse compared to the impulse laser. The second fluorescence peak appears after 13 nsec

2) Ammonium Nitrate (AN) Sample

Through analyzing the fluorescence spectrum of AN sample comes from shooting AN sample by (266nm) laser (5nsec) laser pulse and (15 mJ) energy, a clear AN fluorescence spectrum is shown in figure 4.11.

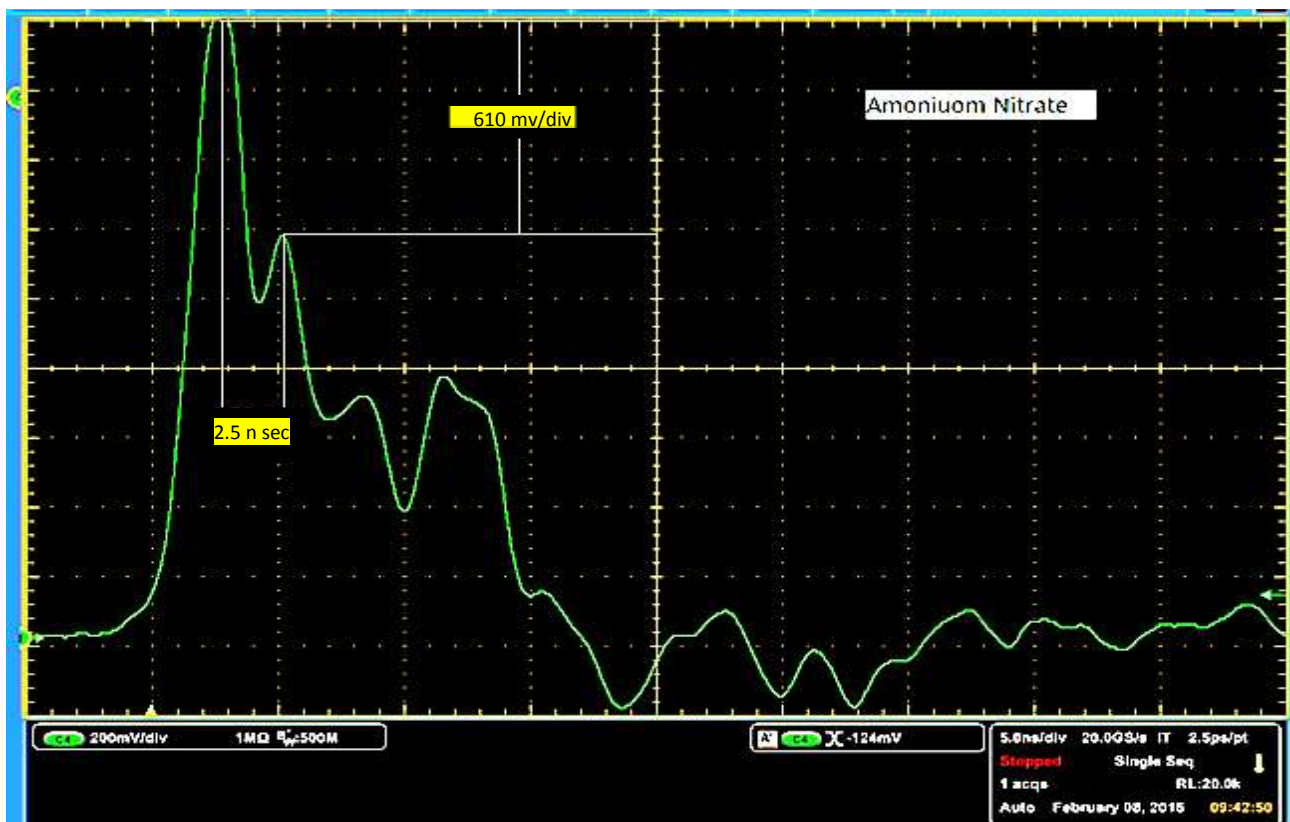


Figure (4.11): Fluorescence spectrum of AN material (5nsec/ div),(200mv/div).

From figure 4.11, it appears that the fluorescence of AN appeared after (10 nsec) after shooting with the laser pulse. The time domain laser-fluorescence pulses for AN with the following parameters:

- a) The fluorescent phase difference:- $\Delta\phi = 2.5 \text{ nsec} \mp 0.2 \text{ nsec}$ which represents the time after impulses the target then the fluorescent spectrum appeared .
- b) The modulated difference = $610 \text{ mv/div} \mp 10 \text{ mv/div}$. Which represent the height of the fluorescent pulse compared to the impulse laser .

As can be seen for the spectral time domain image, we took the first and the sharpest fluorescent pulse appeared after the pumping pulse, this does not mean it is the only line emitted. One can see there still some other peaks very close to each other appeared after some 7 nsec which give AN time domain fluorescent pulse shape.

3) C4 Sample

Through analyzing the fluorescence spectrum of C4 sample that generated by shooting sample by (266nm) laser (5nsec) laser puls and (15 mJ) energy, a clearly C4 fluorescence spectrum has been recorded as shown in figure 4.12.

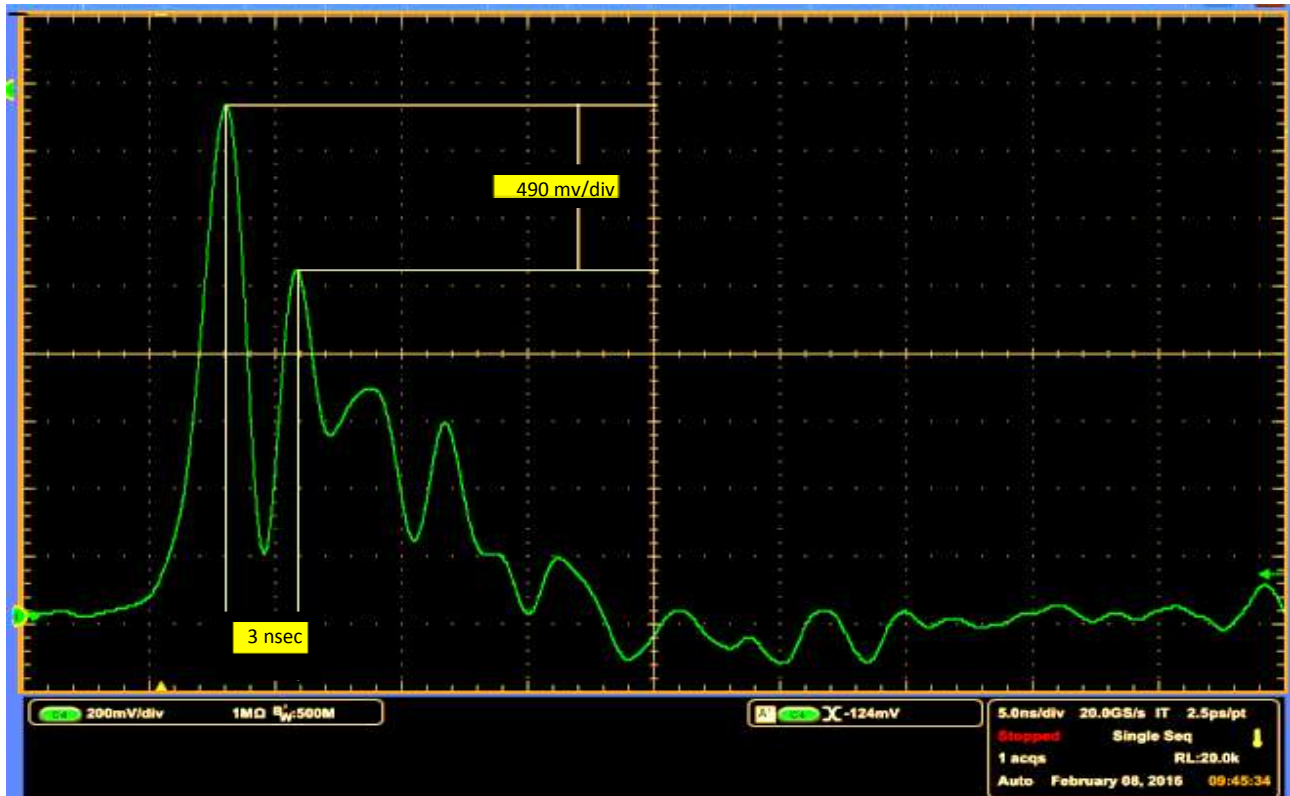


Figure (4.12): Fluorescence spectrum of C4 material (5 nsec/ div), 200mv/div

As can be seen from the above figure, the fluorescence of time domain for C4 where we have the phase difference $\Delta\phi \cong 3nsec \mp 0.2nsec$; and the depth difference of the fluorescence is (490 mv/div) with other pulses appeared after about 6 and 9 nsec respectively.

From figure 4.10, 4.11 and 4.12, the obtained spectra are divided into 3 major parts: the first one is the laser reflection area where the laser pulse after falling on the examined material should be absorbed, but since the used wavelength is located in the end of the absorption spectrum peak for these materials they are not completely absorbed and therefore the major part of the laser beam will be reflected in the expected time of about (5-7ns) as high peak in the signal shown in figures recorded. This is true if we know the low absorption of AN to the used laser wavelength, that is why we see AN has higher modulation depth which means very high reflection can

be appeared Compared with the other explosives. The second part has occurred after a (1-15nsec) represents the response of explosive molecules to the pump laser, it is the fluorescence for every measured point, the spectrum peaks represent transitions between a number of the vibrational levels for the electronic higher states and the ground state of the molecules of the explosive materials due to the energy of the UV laser pulses, The shifted peaks and shoulders show a remarkable response to different explosive materials. Since the radiated lifetime of the first excited state of the these molecules have two transitions, the first appeared after about 20 nsec (with +/- 5 nsec, due to impurities) and the second fluorescence line appeared after 210 nsec(+/- 2nsec).

Therefore, it will be expected to have another temporal pulse appeared far away from the temporal spectrum, which we recorded for each of these explosives as well. The main benefit of using time measurement technique seems to be very promising comparing to the frequency (wavelength)methods that the method of time domain have the ability and well enough reliability to be adopted to detect and amplified the smaller signals using optical amplifying techniques which can easily exclude the electrical pulses from the optical pulses, and simply magnified it by using optical concave reflectore to increase the signal to noise ratio, because weak signal amplitude of the fluorescence will be influenced by the electrical noise that generated in PMT circuits due to dark current. More gained and magnified via optical purposes depends on the energy of the laser pulse and reduces the electrical noise effect.

It is observed that additional peaks compared to normal detect signals will appear by the used of the high gain fitted range PMT, amplification of signals that are otherwise very weak. The difference in time of appearance of the fluorescent pulse from the original laser pulse is one of the most important parameters to distinguish between the materials. Then the modulation depth represents the deference between

the original reflected pulse and the height of the fluorescence pulse. These three combined spectral parts will give an image the total behavior of the detected signal carrying a lot of information to compare and distinguish between materials. It should be noted that this difference remains constant at standoff ranged,

Besides, since we used a limited rise time PMT we faced some difficulties in recognizing the laser pulse ends from the beginning of fluorescent signal which appeared after (1- 5) nsec after the laser pulse, making some convolution (overlap) between the end of the laser pulse and the rise time of the first fluorescent transition that is why we should use a faster PMT in the future.

The peaks obtained for the fluorescence in the time domain can be compared to some other references, in order to prove that it's a fluorescence peak. In addition, we have been drawing a figure (4.13) that shows the phase diagram representing a time of fluorescence, wavelength as a function of intensity (arbitrary unit). It shows the three explosive materials fluorescence wavelength with the time of the fluorescence for each one, that figure can give us a total configuration of the material fluorescence spectrum, and that will minimize the noise effect on the fluorescence measurement.

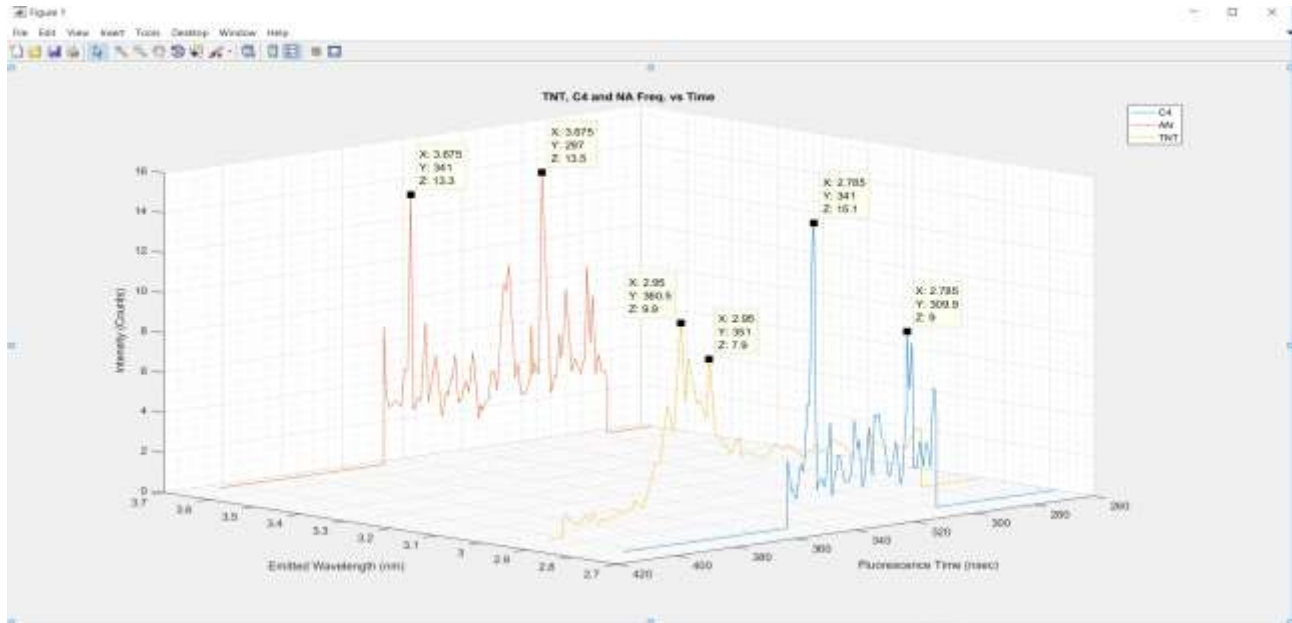


Figure (4.13): The relation between frequency domain and time domain for the three explosive materials.

c. Simulated Samples Test

We have been simulated a real scan of fluorescence technique through putting an explosive material in common surfaces that may be found such as over car paint, glass, wall, iron plates, etc. The fluorescence spectrum of these surfaces has been recorded with no explosive then spectrum recorded after putting the explosive material on it to compare it with a fluorescence spectrum of pure materials to determine the difference in the peak shape.

1) Car Paint

A dyed paint piece of the car has been used as a sample of surface, it has been shot it by (266nm) laser of (5nsec) and (15 mg) energy. The fluorescence spectrum is shown in figure 4.14, and the spectrum was saved in oscilloscope device as a reference.

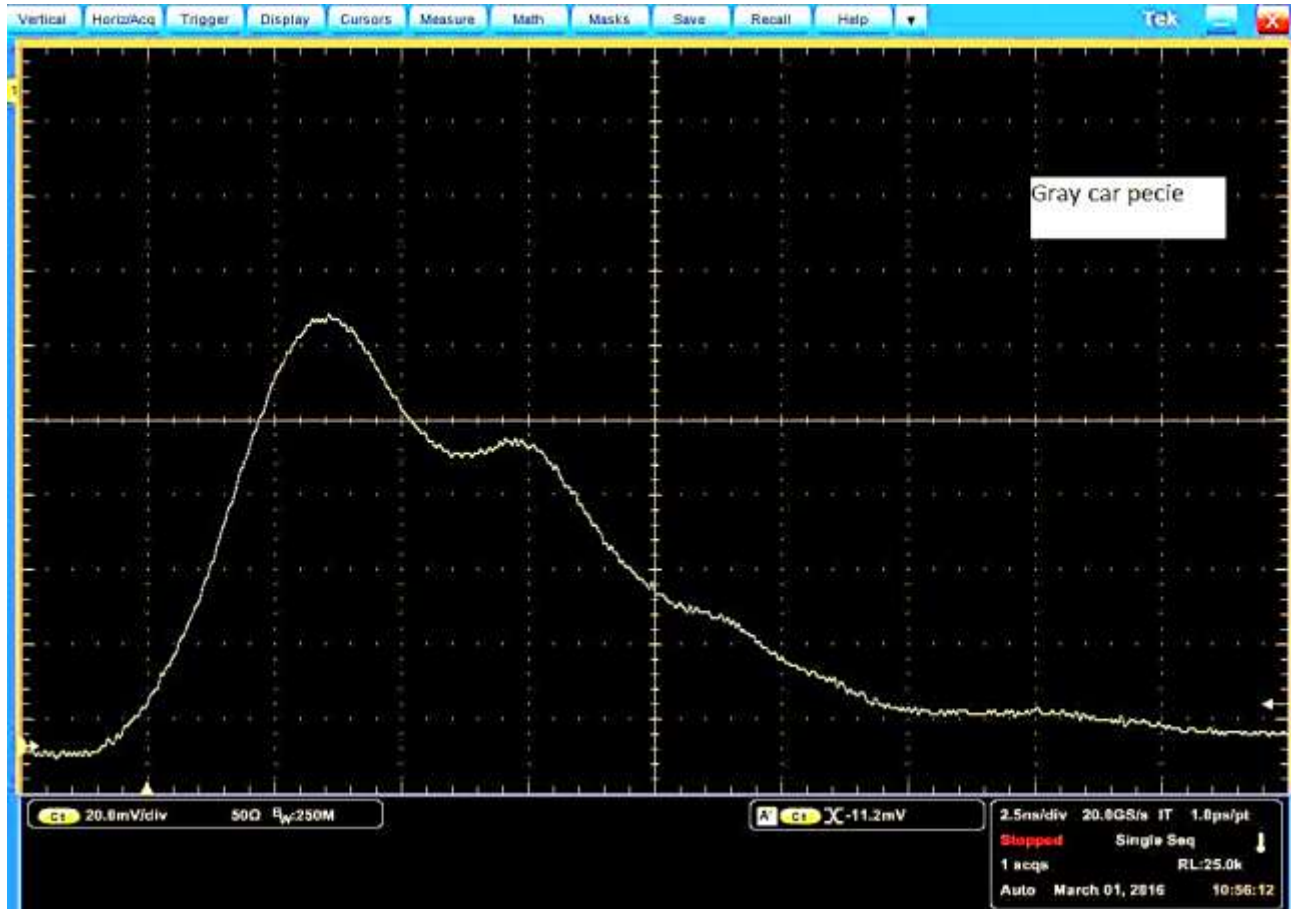


Figure (4.14): Fluorescence spectrum of car paint (2.5nsec/ div), 200mv/div

Then, the first explosive material (AN) was put over it and shot it again, then compared it to the fluoresce spectrum of the car paint. The result is shown in figure 4.15.

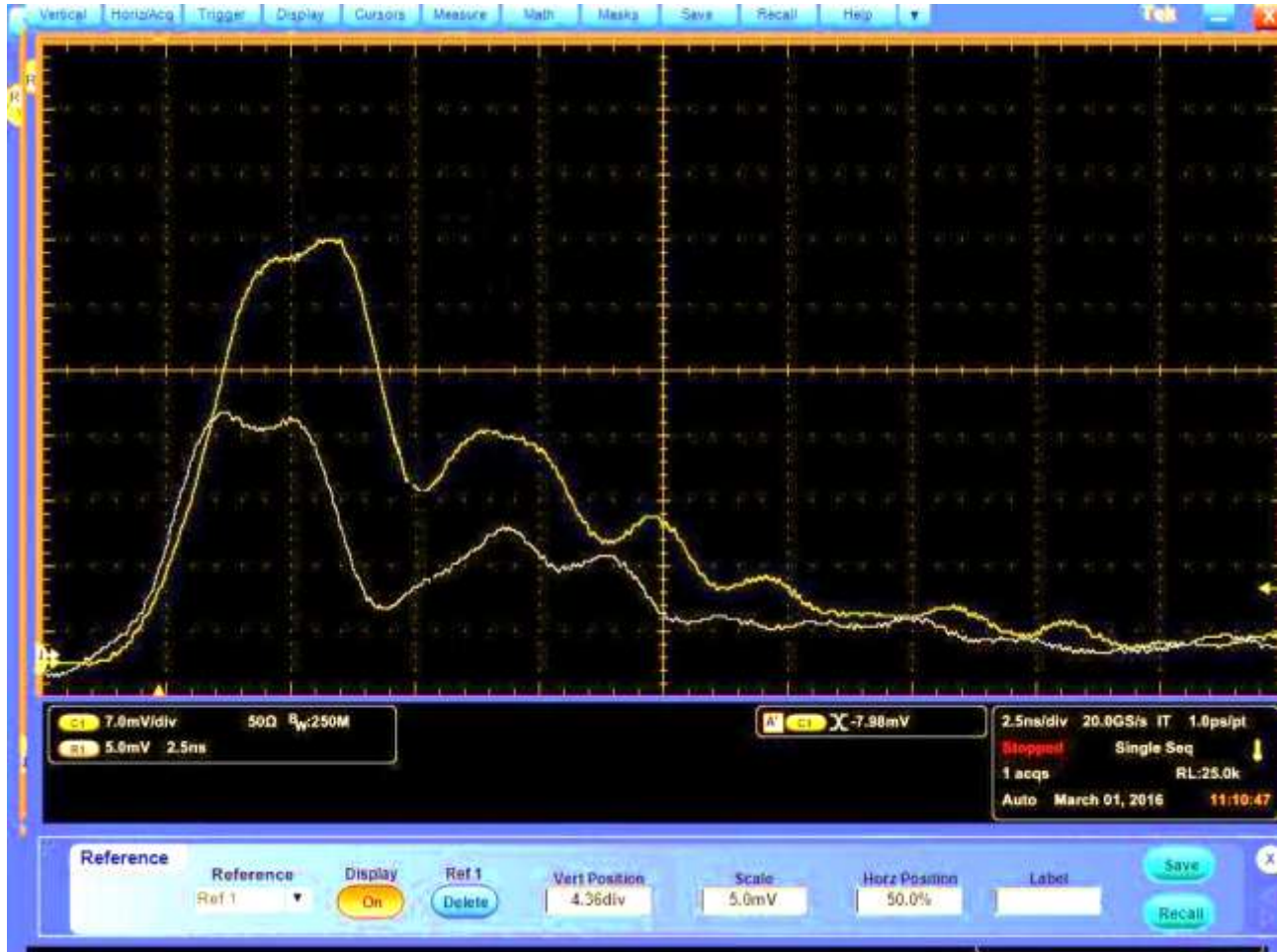


Figure (4.15): Fluorescence spectrum of car paint with AN on it (2.5nsec/ div), 5mv/div, 7mv/div

Second, the C4 explosive material has been put over and shot again, then compared to the fluorescence spectrum of car paint. The result is shown in figure 4.16.

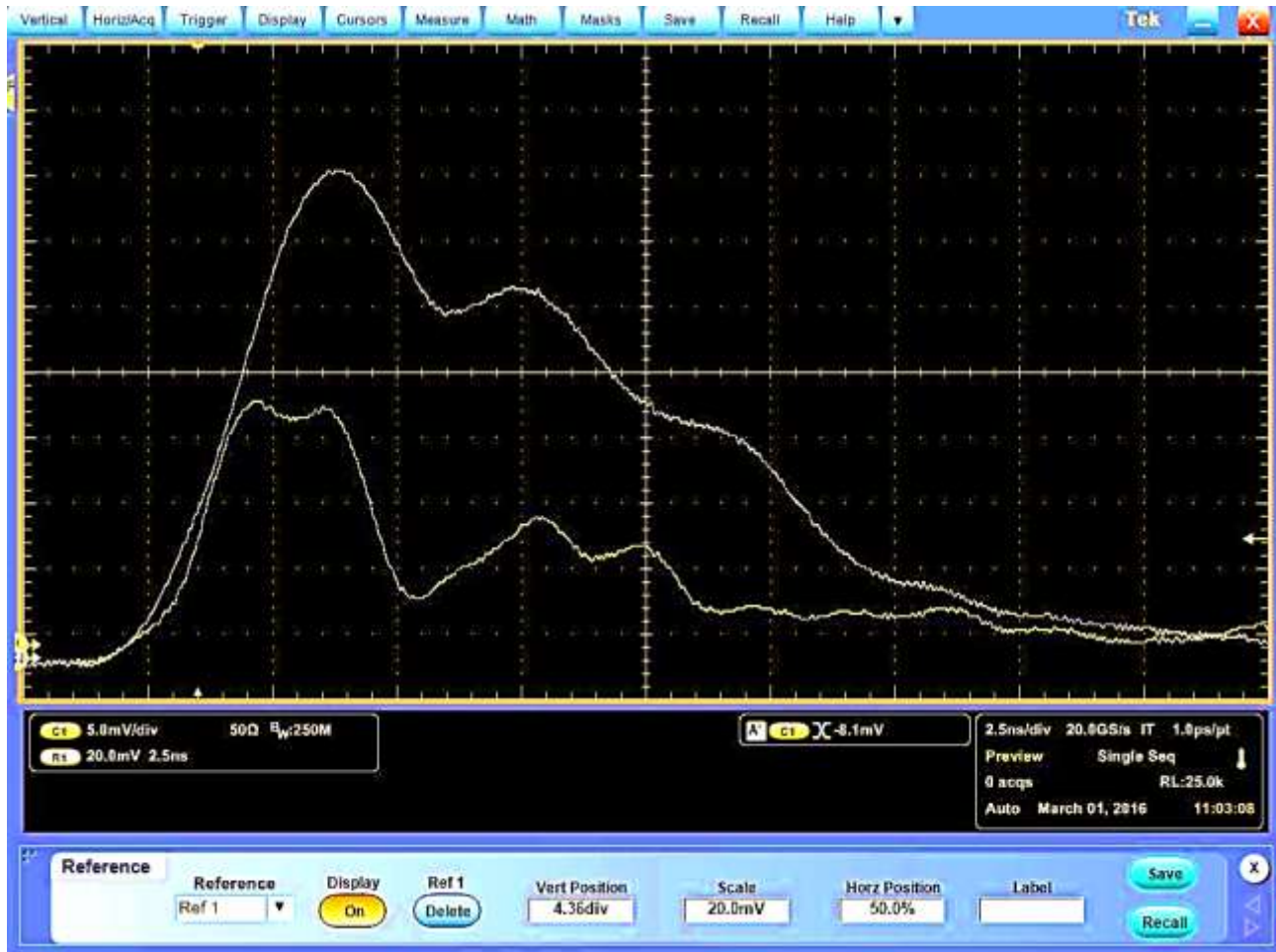


Figure (4.16): Fluorescence spectrum of car paint with C4 trace ($20 \mu\text{g}/\text{cm}^2$) on it (2.5nsec/div) 5mv/div without magnification

From figure 4.14, 4.15 and 4.16 the white signal represents the fluorescence signal from the paint surface with the explosive material and the yellow signal is the paint surface without an explosive.

2) Glass

A piece of glass has been used as a sample of surface, it was shot by (266nm) laser of (5nsec) and (15 mg) energy pulse, the fluorescence spectrum is shown in figure 4.17, and the spectrum was saved in oscilloscope device as a reference.

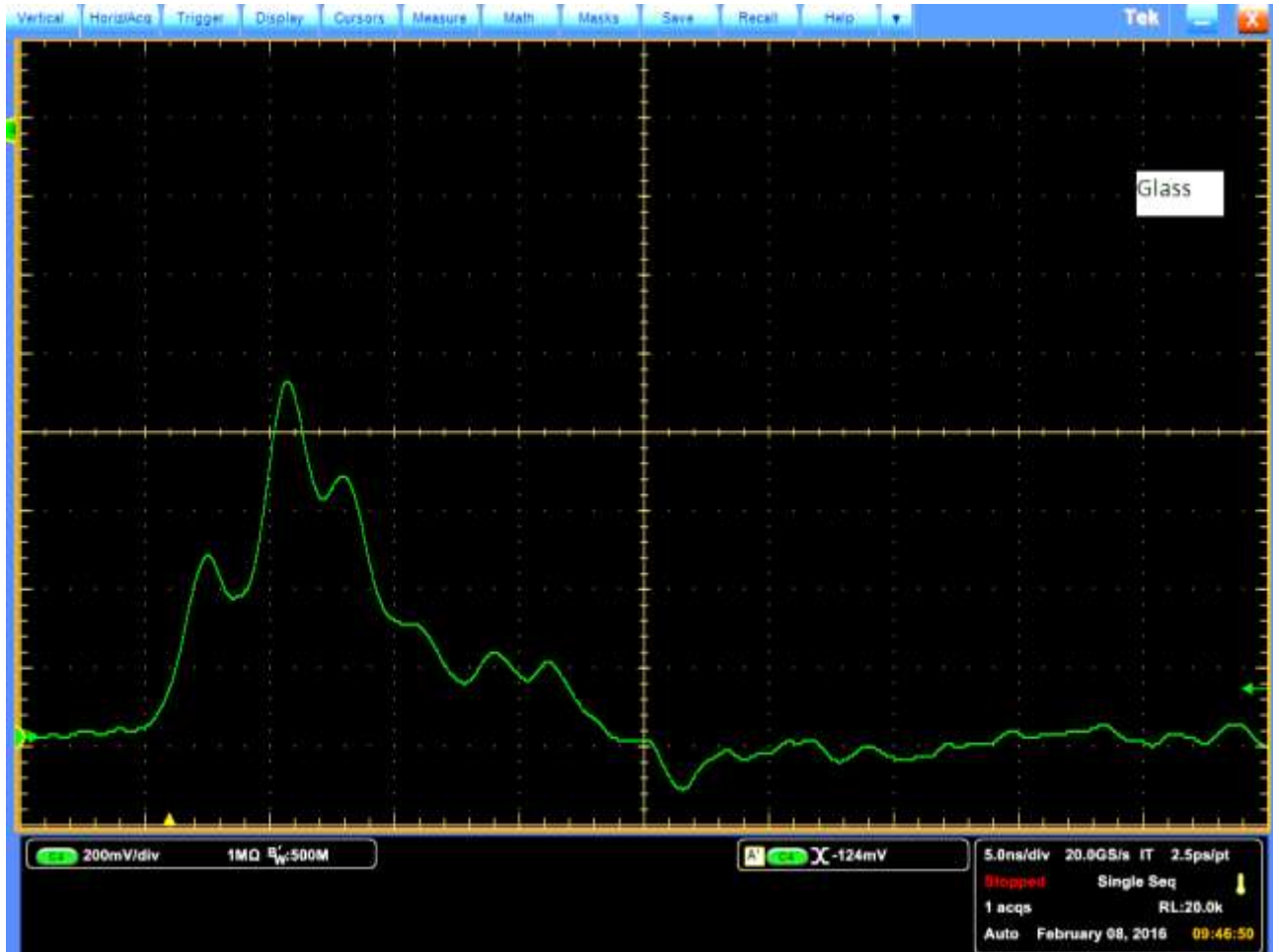


Figure (4.17): Fluorescence spectrum of glass (5nsec/div), 200mv/div

We put first explosive material (AN) over it and shot it again, then compared it with the fluorescence spectrum of car paint. The result is shown in figure 4.18.

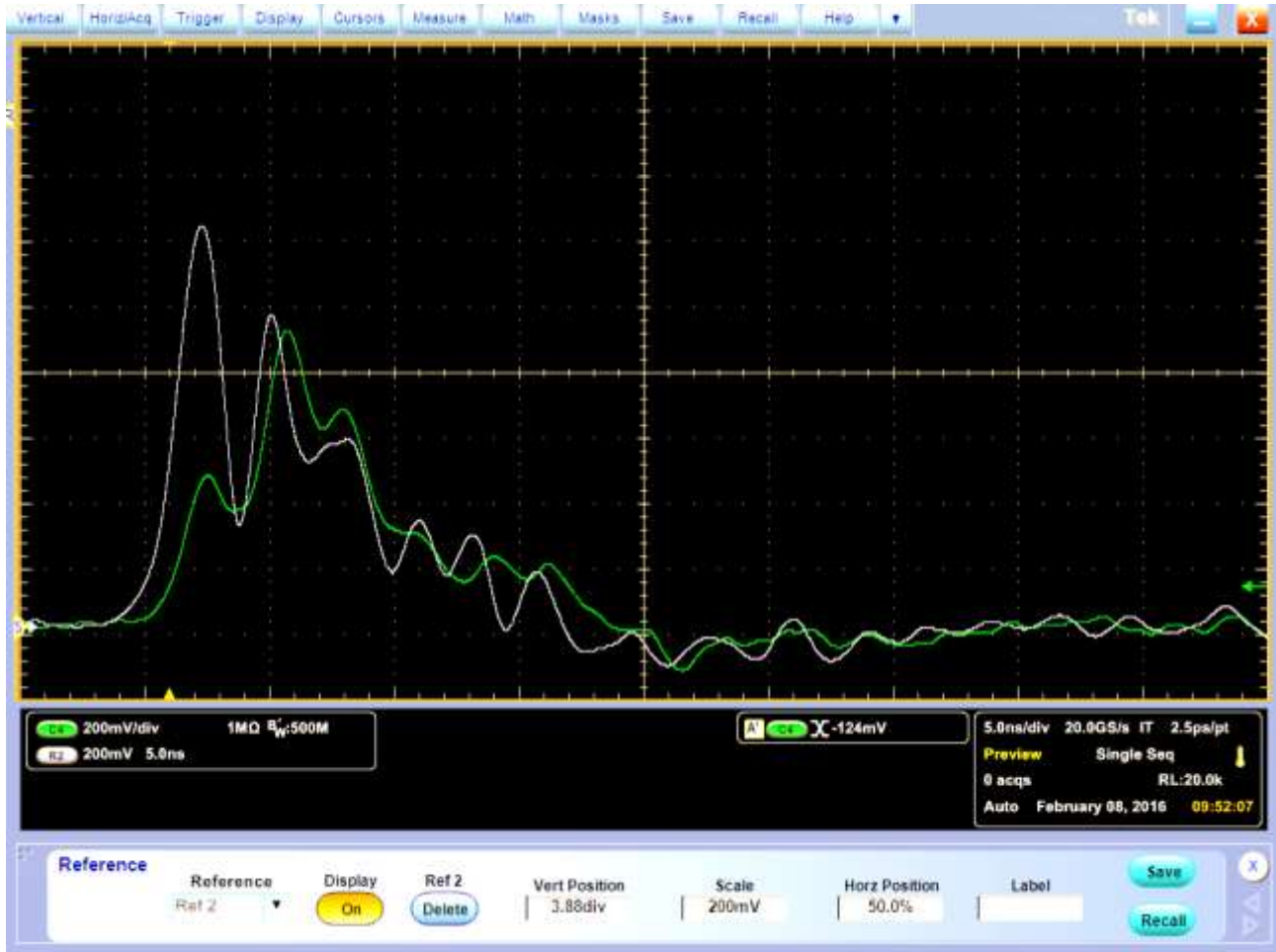


Figure (4.18): Fluorescence spectrum of glass with AN trace on it (5nsec/ div), 200mv/div, the trace amount about $20 \mu\text{g}/\text{cm}^2$ at 10 meters far.

We put the second explosive material (C4) over it and shot it again, then compared it with the fluorescence spectrum of car paint. The result is shown in figure 4.19.

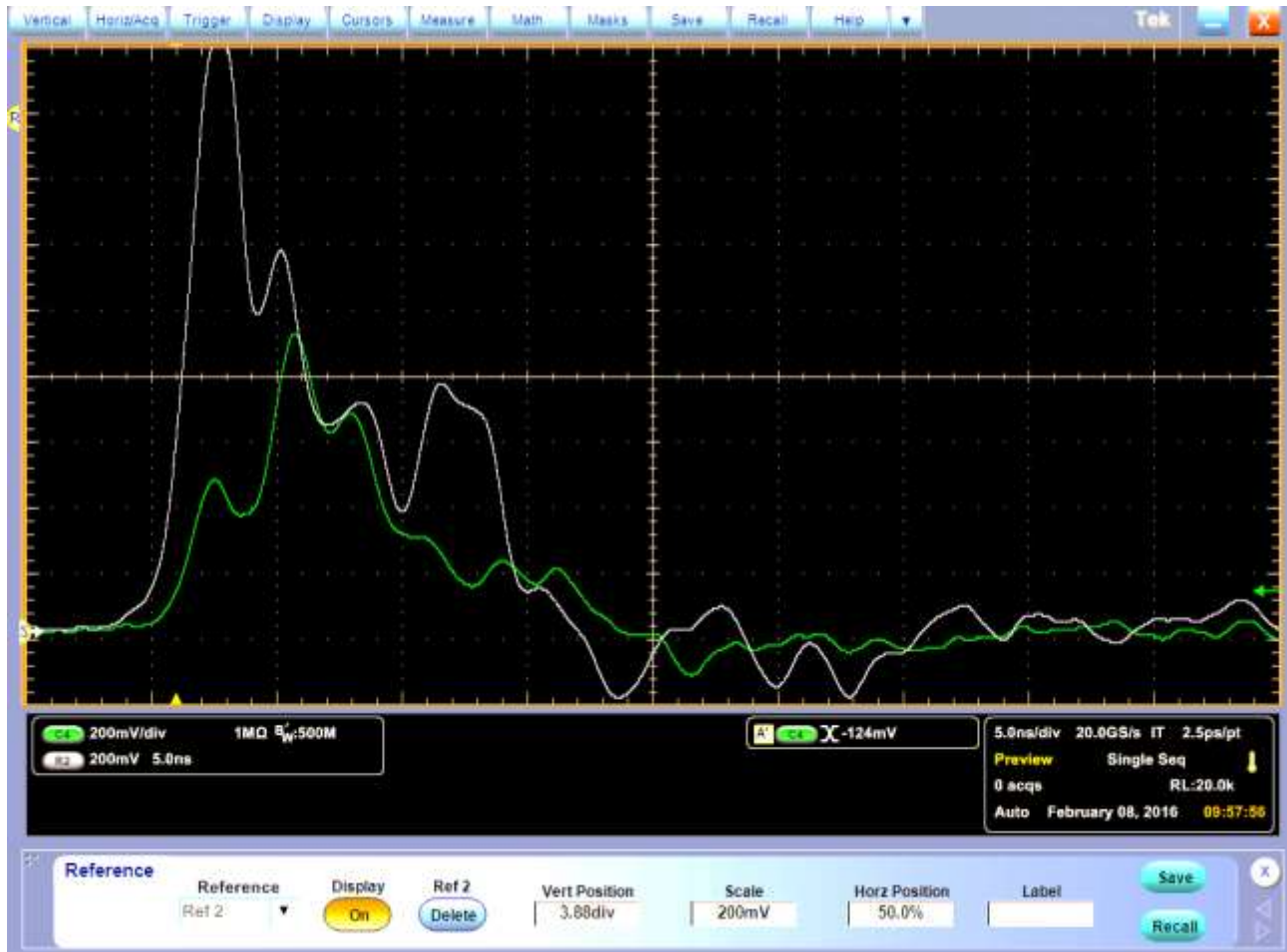


Figure (4.19): Fluorescence spectrum of glass with trace of C4($20\mu\text{g}/\text{cm}^2$) on it (5nsec/div), 200mv/div

The purple signal represents the fluorescence signal from the glass surface with explosive material and the green signal are the glass surface without explosive. By comparing the fluorescence signal of explosive material that on simulated surfaces (paint car or glass) with a fluorescence signal of pure explosive material (AN, C4 and TNT). The similarity of signals can be observed, which prove the ability of this method to detect explosive material efficiently even it covers any other body in traces.

Figure 4.20 and 4.21 show the fluorescence signal of the explosive materials (AN and C4) with fluorescence signal when put over car paint.

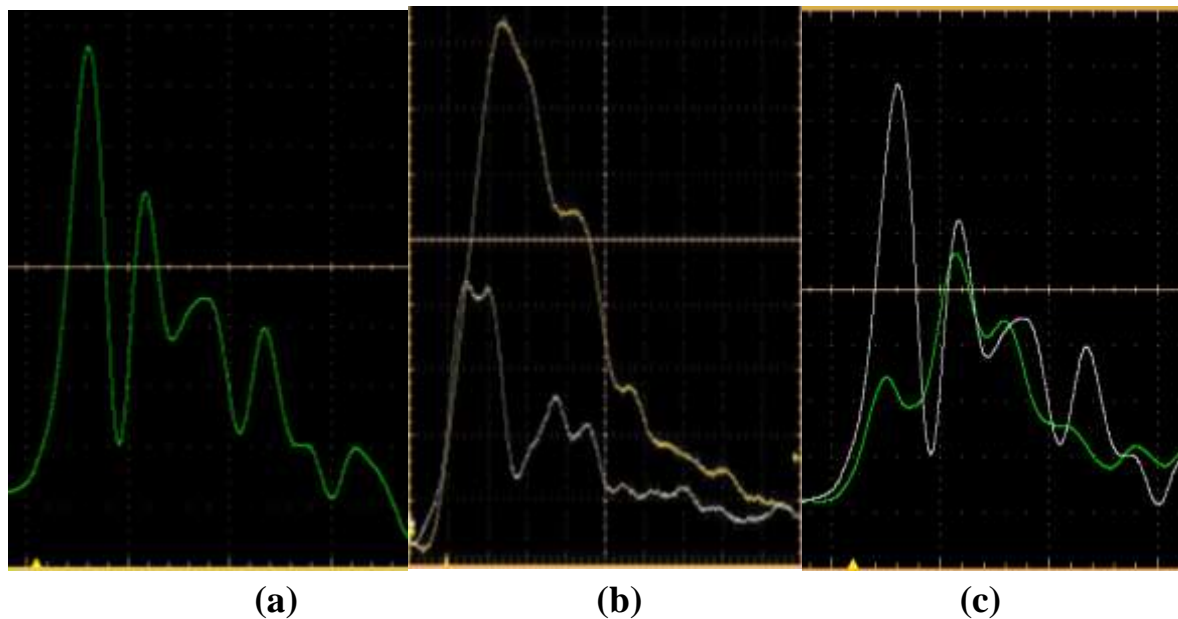


Figure (4.20): Comparison between fluorescence spectrums of C4 where:
a) C4, b) C4 on car paint, c) C4 on glass 5nsec/div

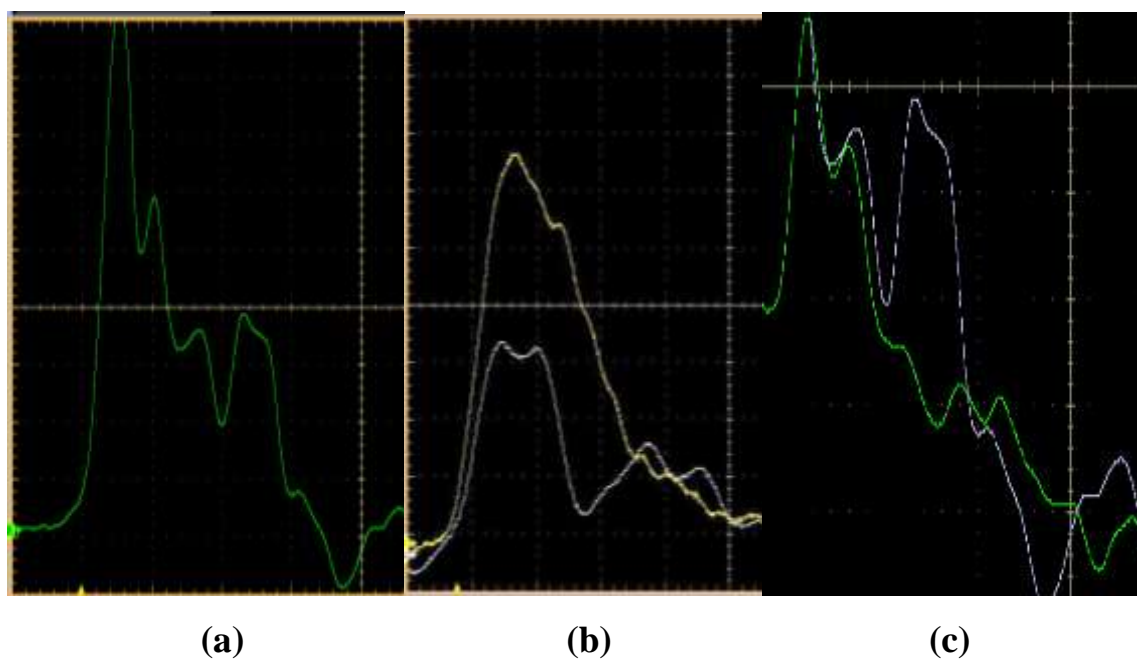


Figure (4.21): Comparison between fluorescence spectrums of AN where:
a) AN, b) AN on car paint, c) AN on glass

D. LIF Peaks Calculations

In this part we have been calculating the fluorescence time, phase difference and modulation depth in order for a design recognition program that is based on the peak specification. The calculation formula is as follows [78-80]:

$$\text{Fluorescence Time } (\tau) = 0.37 T \dots\dots\dots (4.1)$$

$$\text{Phase Difference } (P_d) = \text{Second peak} - \text{First Peak} \dots\dots\dots (4.2)$$

$$\text{Modulation Depth} = L2 - L1 \dots\dots\dots (4.3)$$

1) C4 Fluorescence Spectrum Analysis

From figure 4.22 the first pulse reaches maximum at a time (8.05×10^{-9}) sec and intensity (1.5), while the second pulse reaches maximum at a time (10.84×10^{-9}) sec and intensity (1.016). By applying the formula (4.1, 4.2 and 4.3) we got the following results:

$$\text{Fluorescence Time} = 4.01 \text{ nsec}$$

$$\text{Phase Difference} = 10.84 - 8.05 = 2.785 \text{ nsec}$$

$$\text{Modulation Depth} = 1.5 - 1.016 = 0.49$$

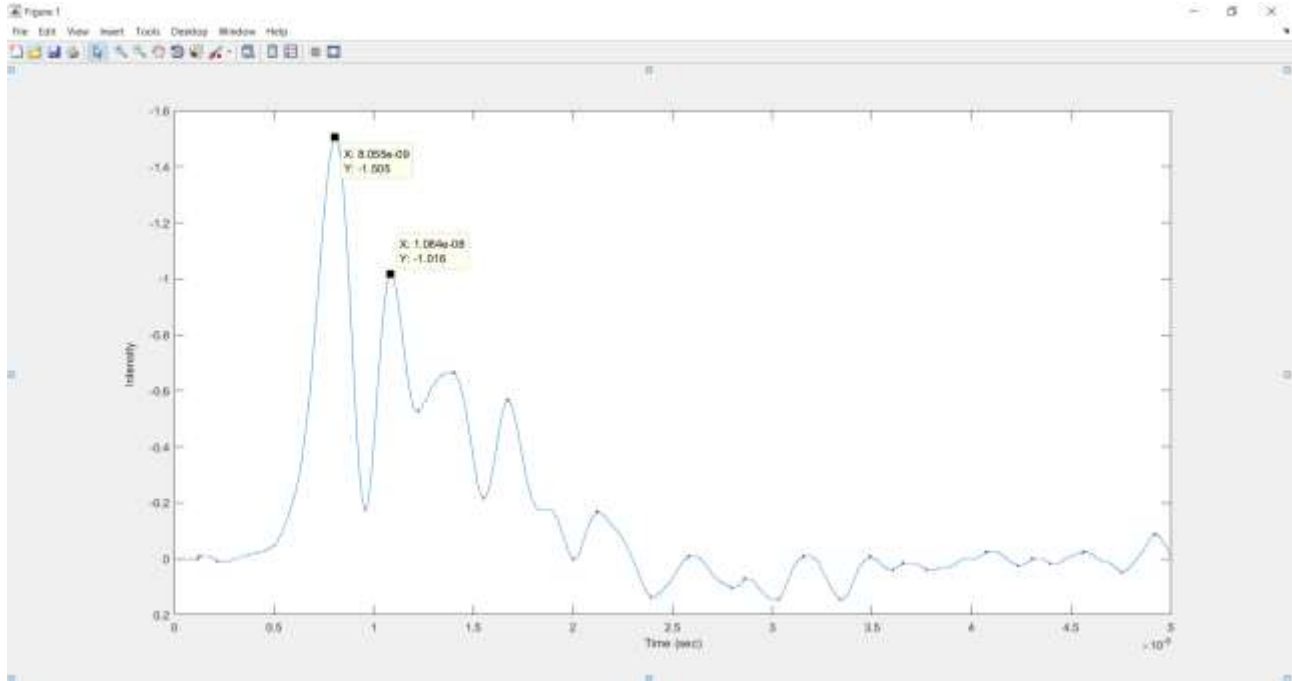


Figure (4.22): Fluorescence spectrum analyzes of C4

2) AN Fluorescence Spectrum Analysis

From figure 4.23, the first pulse reaches maximum at a time (8.415×10^{-9}) and intensity (0.049), while the second pulse reaches maximum at a time (12.01×10^{-9}) and intensity (0.0405). By applying the formula (4.1, 4.2 and 4.3) we got the following results:

$$\text{Fluorescence Time} = 4.44 \text{ nsec}$$

$$\text{Phase Difference} = 12.01 - 8.415 = 3.595 \text{ nsec}$$

$$\text{Modulation Depth} = 0.049 - 0.0406 = 0.00199$$

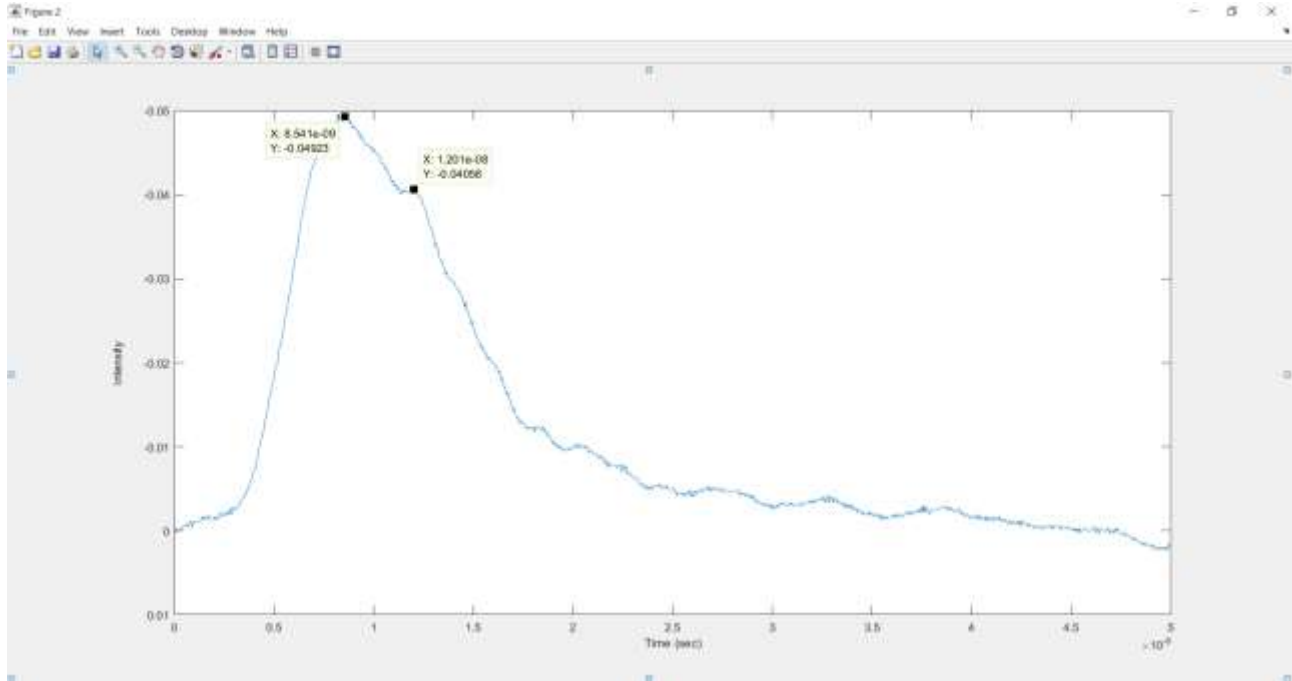


Figure (4.23): Fluorescence spectrum analyzes of AN

3) TNT Fluorescence Spectrum Analysis

From figure 4.24, the first pulse reaches maximum at a time (5.3×10^{-9}) sec and intensity (1.2), while the second pulse reaches maximum at a time (8×10^{-9}) sec and intensity (0.92). By applying the formula (4.1, 4.2 and 4.3) we got the following results:

$$\text{Fluorescence Time} = 2.69 \text{ sec}$$

$$\text{Phase Difference} = 8 - 5.3 = 2.7 \text{ nsec}$$

$$\text{Modulation Depth} = 1.2 - 0.92 = 0.28$$

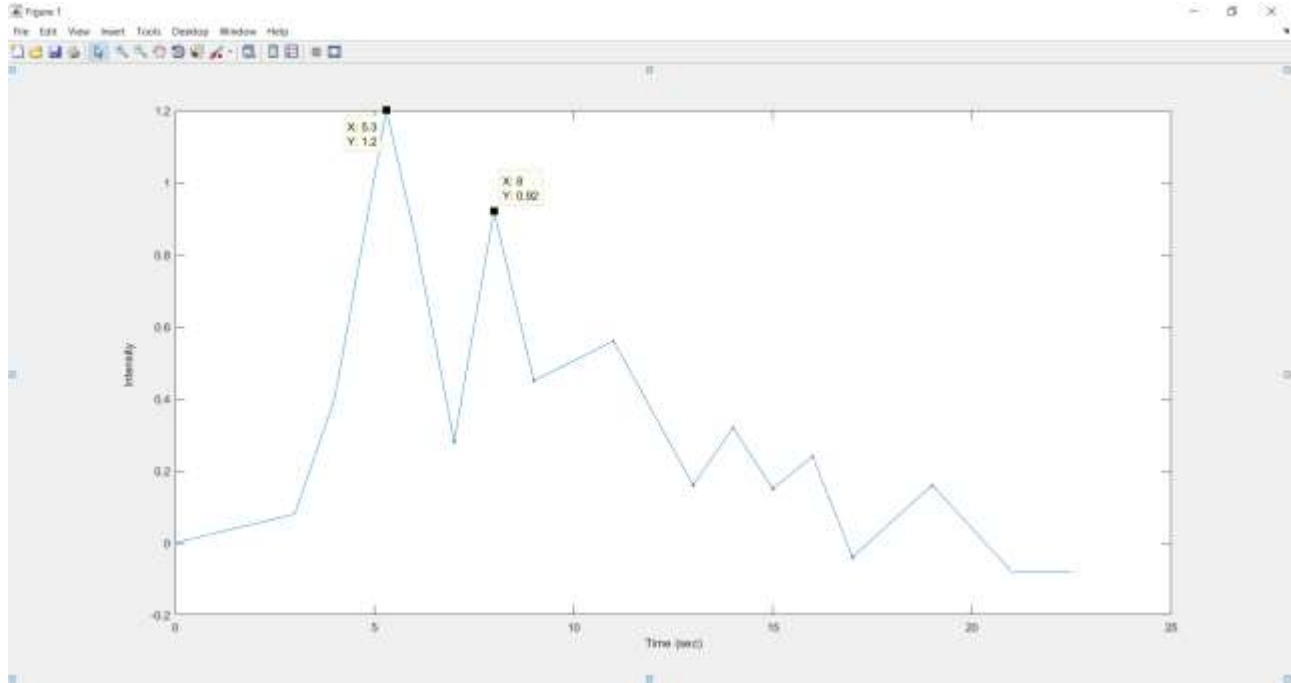


Figure (4.24): Fluorescence spectrum analyzes of TNT

E- Explosive Detection Program

Based on our tests, we have designed a program to detect explosive materials by comparing scanning data with an explosive material data. When the scanned signals are similar to explosive signals the program shows it is an explosive material and define the explosive materials with the matching percentage. If the scanned signal is not the same, the program shows no explosive signals. Figure 4.25 shows the flowchart of program algorithm.

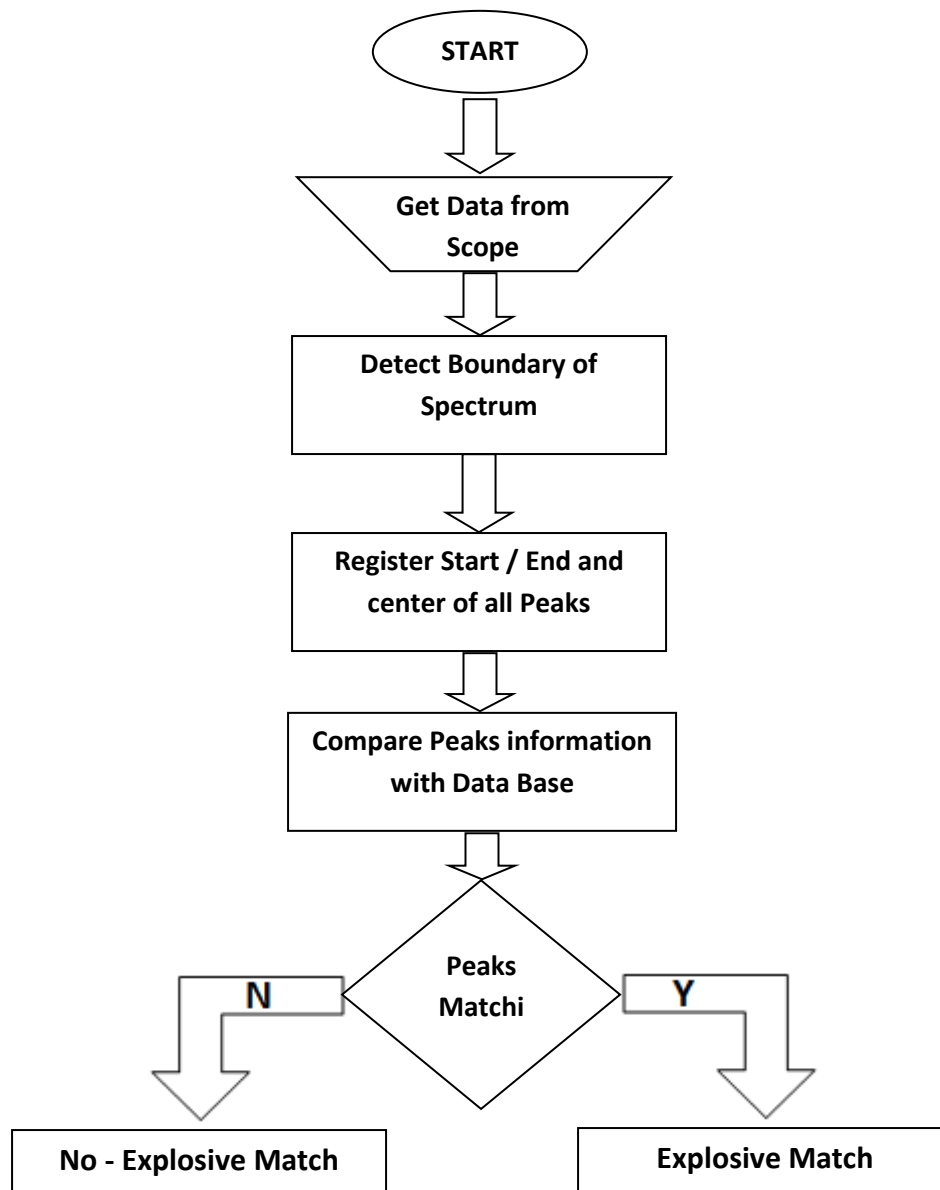


Figure (4.25): Algorithm scheme of explosive detection program

The program has been designed by using C# language, we designed a simple UI, figure 4.26 shows the program of UI.

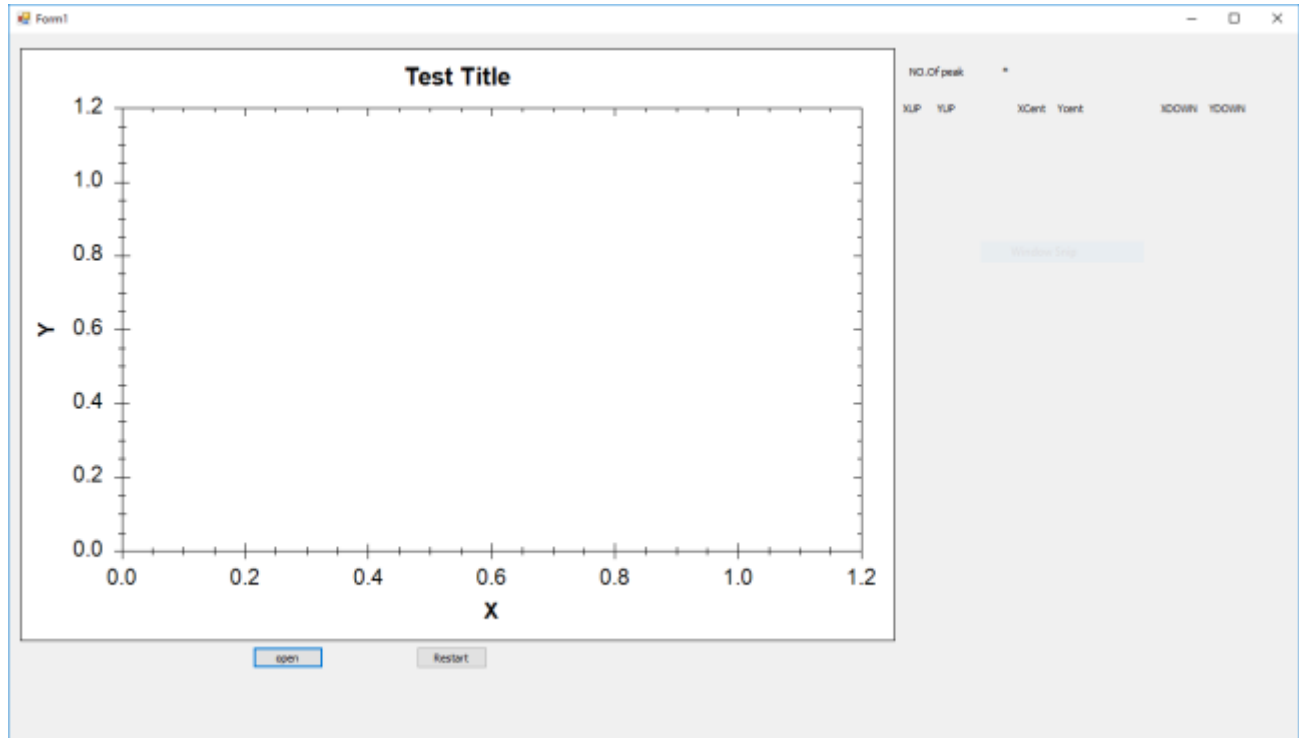


Figure (4.26): Explosive detection program UI

We can upload scanned peck data to it by pressing open then selecting it. The program will indicate the peak information and compare it with its database. When matching is found, the matching result will appear..

We have tested many spectra for different situations and the result shows that the program can detect an explosive material with high accuracy. Figure 4.27 shows some test results that identified C4, AN, TNT and when the sample has no explosive materials,

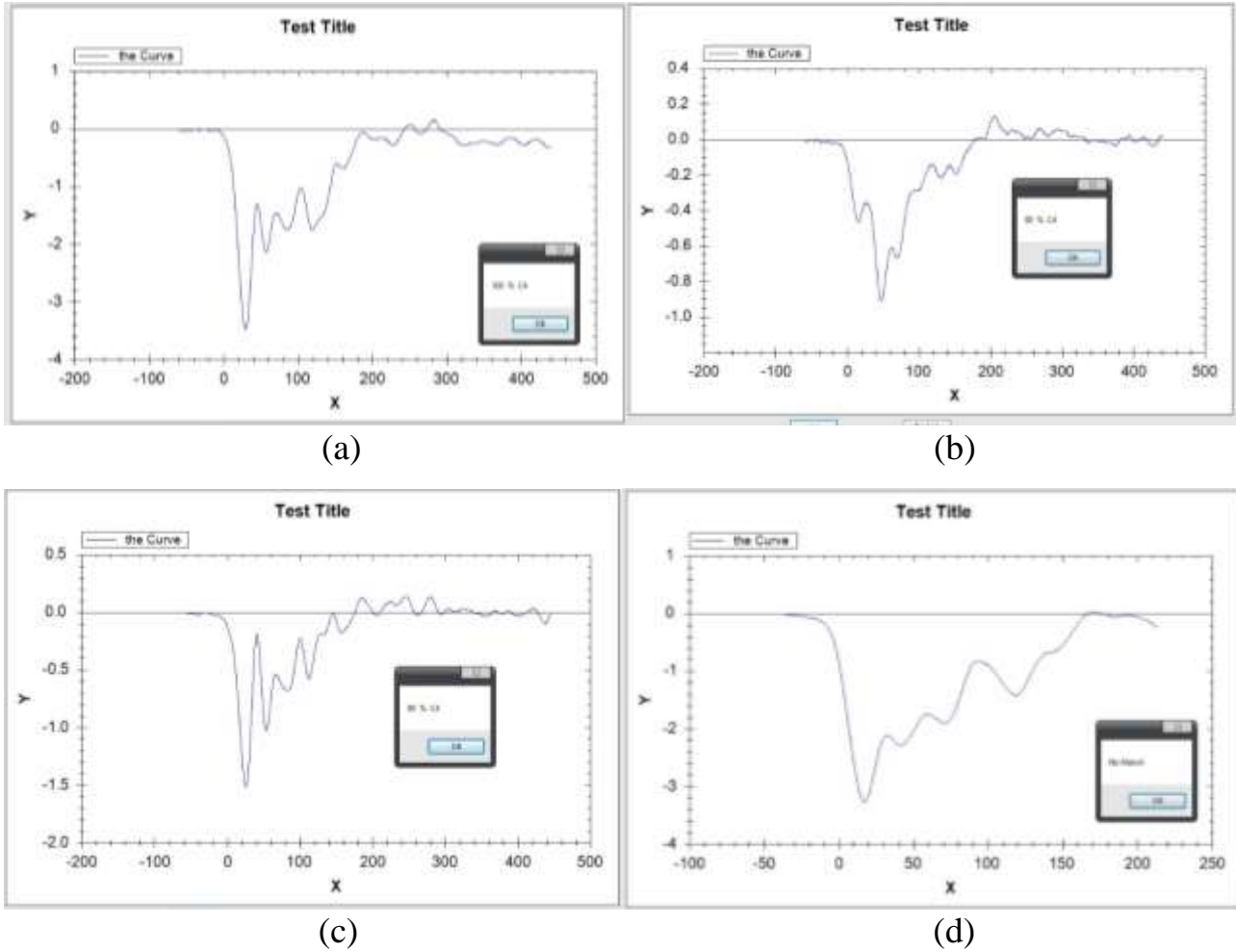


Figure (4.27): Explosive detection program result for (a, b and c) C4 with different situations, (d) non explosive material.

5.1 *Conclusions:*

- The LIBS spectroscopy which shows spectra contained the expected atomic and ionic C, H, N, and O emission lines, and other emissions resulting from the impurities, has some complications like the use of unsafe high laser energy leads to increased substrate penetration and damage the target surface, and the strongly depend upon the experimental condition like the surrounding atmosphere.
- LIF spectroscopy appears to be more promising in detecting explosive residues than LIBS measurements.
- Fluorescence imaging on a variety of substrates, like glass, silver and car paint ,the silver substrate shows the high absorption in the 266nm wave length which help us to reduce the back scattered laser from interference with the fluorescence signals.
- The explosives fluorescence signal is weak, but detectable, fluorescent peak occurring at wave length between 340-350 nm because of the structures of these molecules and tailing toward longer wavelengths, many other beaks are present at different wave length that is due to the impurities in the sample. Differences between our measurements and the previously reported values are due to various purification and preparation methods used by others.
- The fluorescence emission time information of the tested samples can be calculated and used as indicator for that samples
- Enhancements the ability of both spectrally and temporally LIF instrument to resolve long distance detection by developed un apparatus able to meet the standards of detection requirements.

5.2 *Suggested Future Works*

A qualitative study like the one described here, which tries to explain the fluorescence emission time domain for the explosive materials, is only a starting point to provide a good understanding for time domain fluorescence spectroscopy.

A) using 60 picosecond PMT rise time will enable us to detect a faster signal with more efficiency.

B) Choosing the specific wavelength of laser source (in the center peaked of the explosive material absorption spectrum) will give an improvement for the probability of interaction between laser photons and trace of explosive.

C) The Photo fragmentation (photo dissociation) followed by laser induced fluorescence [PF-LIF] is a relatively new technique which is based on decomposition (dissociation) of molecules into characteristic fragments Under UV laser irradiation.

D) The three phase diagrams can be realized for future work as a dual technique to combine two systems of detection together, one in time domain and the other in frequency domain, for laser induced fluorescence technique.

References

- 1- Paul K. D., Walter L. P., Ryan A. B., Douglas Y., Parisa R. and Phoenix V., ***“Using Behavioral Indicators to Help Detect Potential Violent Acts: A Review of the Science Base”***, Prepared for the United States Navy, RAND Corporation, ISBN 978-0-8330-8092-9, 2013.
- 2- Trip wire , ***“Introduction to Explosives”***, U.S. Public Intelligence report, Homeland report, 2013.
- 3- Hichem F. and Michel L., ***“Ethylene Glycol Dinitrate (EGDN): from Commercial Precursors, Physicochemical and Detonation Characterization”***, Central European Journal of Energetic Materials, Vol.12, No.2, pp. 287-305, ISSN 2353-1843, 2015.
- 4- Defense Department, ***“Homemade Explosives Recognition Guide”***, Book, Spiral-bound, Government Printing Office, First Edition, May 2010.
- 5- Katie L. G., Kyle T. H., Sergei V. B. And Sanford A. A., ***“Review of explosive detection methodologies and the emergence of standoff deep UV resonance Raman”*** Journal of Raman Spectroscopy, John Wiley & Sons, Ltd., DOI 10.1002/jrs.4868, 2016.
- 6- Anzano J. M., Gornushkin I. B., Smith B. W. and Winefordner, J. D., ***“Laser-Induced Plasma Spectroscopy for Plastic Identification”***, Polym. Eng. Sci., Vol.40, pp.2423–2429, 2000.
- 7- Portnov A., Rosenwaks S. and Bar I., ***“Emission Following Laser-Induced Breakdown Spectroscopy of Organic Compounds in Ambient Air”***, Applied Optics, Vol. 42, pp.2835–2842, 2003.

References

- 8- Ferioli F. and Buckley S. G., “*Measurements of Hydrocarbons Using Laser-Induced Breakdown Spectroscopy*”, Combust. Flame, Vol.144, pp.435–447, 2006.
- 9- Lopez-Moreno C., Palanco S., Laserna J. J., De Lucia F. C., Miziolek A. W., Rose J., Walters R. A., and Whitehouse A. I., “*Test of a stand-off laser-induced breakdown spectroscopy sensor for the detection of explosive residues on solid surfaces Spectrom*”. Journal of Analytical Atomic Spectrometry (J. Anal. At. Spectrom), Vol. 21, Issue 1, pp.55-60 2006.
- 10- Gondal M.A., Hussain T., Yamani Z.H. and Baig M.A., “*The role of various binding materials for trace elemental analysis of powder samples using laser-induced breakdown spectroscopy*”, Talanta, Vol.72No.2 ,pp.642–649, 2007.
- 11- Gondal M.A., Hussain T., Yamani Z.H. and Baig M.A., “*Optimization of the LIBS parameters for detection of trace metals in petroleum products*”, Talanta, Energy Source Part A, Vol 30, pp.441-451, 2008.
- 12- Dennis K. K., Susan D. A., Robert D. W., Chris S.,and Edwin L. D., “*LIBS Plasma Enhancement for Standoff Detection Applications*”, Proc. of SPIE Vol. 6954 695403-1 doi: 10.1117/12.77694,2008.
- 13- Gottfried J. L., De Lucia F. C., Munson C. A., and Miziolek A.W., “*Laser-induced breakdown spectroscopy for detection of explosives residues: a review of recent advances, challenges, and future prospects*”, Analytical and Bioanalytical Chemistry, Springer-Verlag, Vol. 395, Issue 2, ISSN: 1618-2650, pp. 283–300, 2009.

References

- 14- González R., Lucena P., Tobaría L. and Laserna J., “*Standoff LIBS detection of explosive residues behind a barrier*”, Journal of Analytical Atomic Spectrometry, Vol. 24, pp.1123-1126, 2009.
- 15- Moros J., Lorenzo J. A., Laserna J. J., “*Standoff detection of explosives: critical comparison for ensuing options on Raman spectroscopy-LIBS sensor fusion*”, Analytical and Bioanalytical Chemistry, Springer-Verlag, Vol. 400, Issue 10, ISSN: 1618-2650, pp.3353–3365, 2011.
- 16- Lucena P., Gaona I., Moros J. and Laserna J. J., “*Location and Detection of Explosive-Contaminated Human Fingerprints on Distant Targets Using Standoff Laser-Induced Breakdown Spectroscopy*”, Spectrochimica Acta Part B: Atomic Spectroscopy, Elsevier B.V., Vol. 85, Pages 71–77, July 2013.
- 17- Abel B., Kirmse B., and Troe J., “*Specific rate constants $k(E,J)$ for the dissociation of NO_2 I. Time-resolved study of rotational dependencies*”, Journal of Chemical Physics, Vol. 115, No. 14, doi: 10.1063/1.1398305, pp. 6522- 6530, October 2001.
- 18- Tonghun L., Jay B. J., and Ronald K.H., “*Experimental evaluation of strategies for quantitative laser-induced-fluorescence imaging of nitric oxide in high-pressure flames (1-60bar)*” Proceedings of the Combustion Institute, Vol 31pp757-764, 2007.
- 19- Charles M. W., Stephen P., Roderick R. K., and Mordechai R., “*A Novel Method for Remotely Detecting Trace Explosives*”, Lincoln Laboratory Journal, Vol. 17, No.2, November 2008.
- 20- Shiou jyh(puck)Ja. “*Explosives Detection and Identification Using Surface Plasmon-Coupled Emission*”, SPIE Defencesensing and security conference,2012.

References

- 21- Heinz G. and Thierry M., ***“Detectors for Synchrotron Tomography”***, Book, Oxford University Press, ISBN: 9780191707582, 2008.
- 22- Larry E. A., ***“Electronic portal imaging devices: a review and historical perspective of contemporary technologies and research”***, Institute of Physics Publishing Physics in Medicine and Biology, R31–R65 PII: S0031-9155 (02)07073-2, 2002.
- 23- Anna P., Sara W., Birgit B., Carina E. and Erik H., ***“Explosives Detection – A Technology Inventory”***, Weapons and Protection, FOI, FOI-R--2030—S, ISSN 1650-1942, 2006.
- 24- Mahmoud T. and Vahideh I., ***“Detection of explosives by positive corona discharge ion mobility spectrometry”***, Journal of Hazardous Materials, Elsevier B.V., Vol.176, Issues 1–3, pp. 692–696, April 2010.
- 25- Zuhai L. and Youjun Y., ***“A Concise Colorimetric and Fluorimetric Probe for Sarin Related Threats Designed via the Covalent-Assembly Approach”***, Journal of American Chemical Society (JACS), 136 (18), p 6594–6597, DOI: 10.1021/ja502945q, 2014.
- 26- National Academy of Sciences, ***“Existing and Potential Standoff Explosives Detection Techniques”***, Book, Committee on the Review of Existing and Potential Standoff Explosives Detection Techniques, the National Academies Press, ISBN: 0-309-52959-X, 2004.
- 27- Zbigniew B., Jacek J., Adam K., Janusz M., Norbert P., Mateusz P., Tadeusz P., Tadeusz S. and Jacek W., ***“Sensors and Systems for the Detection of Explosive Devices - An Overview”***, Metrology and Measurement Systems Index 330930, Vol. XIX, No. 1, pp. 3-28 ISSN: 0860–8229, 2012.

References

- 28- Furstenberg R., Kendziora C. A., Stepnowski J., Stepnowski S. V., Rake M., Papantonakis M. R., Nguyen V., Hubler G. K., and McGill R. A., ***“Stand-off detection of trace explosives via resonant infrared photothermal imaging”***, Applied Physics Letters Vol.93, 224103, ISBN: 9780080555805, 2008.
- 29- Christopher K., Andrew M., Robert F., Michael P., Viet N. and Jeff B. ***“Detecting traces of explosives”*** Defense & Security, SPIE Newsroom. DOI: 10.1117/2.1201503.005835, Vol.47, pp.124–141, 2015.
- 30- Balakishore Y., Hai-Shan W., William M., Mikhail S., Robert M., Robert I. and Brian E. L., ***“Sensitive Algorithm for Multiple-Excitation-Wavelength Resonance Raman Spectroscopy”***, WVHTC Foundation, 1000 Technology Drive, Suite 1000, Fairmont, WV, USA 26554.
- 31- Larry S. and Thomas G. T., ***“Nanosensors for trace explosive detection”***, Elsevier B.V., Vol. 11, Issue 3, pp.28–36, March 2008.
- 32- Abhijeet S., ***“Standoff Raman Spectroscopy Detection of Trace Explosives”***, MSc. Thesis, Missouri University of Science and Technology, 2010.
- 33- Usha S., Sathish Kumar A. S., and Boopathybagan, K., ***“LIDAR for Detection of Chemical and Biological Warfare Agents”***, Defence Science Journal, Vol. 61, No. 3, pp. 241-250, DOI: 10.14429/dsj. 61.556, 2011.
- 34- Jennifer L. G., Frank C. D., Russell S. H., Chase A. M., Raymond J. W., and Andrzej W. M., ***“Detection of Energetic Materials and Explosive Residues with Laser-Induced Breakdown Spectroscopy: I. Laboratory Measurements”***, Army Research Laboratory, Aberdeen Proving Ground, MD 21005-5066, 2007.

References

- 35- Leonid A. S., "*Laser Methods for Detecting Explosive Residues on Surfaces of Distant Objects*", Quantum Electronics Vol.42 No.1, pp.1–11, 2012.
- 36- Carol C. P., Randal L. S., Lawrence R. T., Philip H. and John E. P., "*Studies of the Laser-Induced Fluorescence of Explosives and Explosive Compositions*", Sandia National Laboratories, United States Department of Energy's, 2006.
- 37- Angel S. M., Nathaniel R. G., Shiv K. S., and Chris M., "*Remote Raman Spectroscopy for Planetary Exploration: A Review*", focal point review, Applied Spectroscopy Vol. 66, No. 2, 2012.
- 38- Pavel M. "*Inverse Spatially Offset Raman Spectroscopy for Deep Noninvasive Probing of Turbid Media*", Applied Spectroscopy Vol. 60, Issue 11, pp.1341-1347, 2006.
- 39- Munson C. A., Gottfried J. L., De Lucia F. C., McNesby K. L., and Miziolek A. W., "*Laser-Based Detection Methods for Explosives*", Army Research Lab Aberdeen Proving Ground MD Weapons and Materials Research Directorate, ReP. No. ADA474060, 2007.
- 40- Gary B., "*Novel Systems Detect Explosives*", Photonics Spectra, may, 2010.
- 41- Anna M. F., "*Investigation of Select Energetic Materials by Differential Reflection Spectrometry*", Phd Thesis, University of Florida, 2007.
- 42- Appendix E6, "*Chemical Properties, Toxicity, and Fate and Transport*", E6-1 Explosives, Idaho National Laboratory.

References

- 43- Andrew S. J. and Clayton H. H., ***“Introduction to Organic Chemistry”***, 2nd Edition, Book, Macmillan, New York, ISBN: 9780024180506, 2012.
- 44- Katie L. G., Sergei V. B., Bhaskar G., Sanford A. A. ***“Solution and Solid Trinitrotoluene (TNT) Photochemistry: Persistence of TNT-like Ultraviolet (UV) Resonance Raman Bands”*** APPLIED SPECTROSCOPY, Volume 68, Number 1, 2014.
- 45- Alim A. F., Richard A. J., Joseph A. M., Charlotte H. L., Michael H. and Martin H., ***“Guide for the Selection of Explosives Detection and Blast Mitigation Equipment for Emergency First Responders”***, Office of Law Enforcement Standards, National Institute of Standards and Technology, 2008.
- 46- Jim B., Roger N. and Jerry W., ***“Gunner’s Mate 1 & C: Explosives and Pyrotechnics”***, Naval Education and Training Professional Development and Technology Center, NLTN: 0504-LP-026-7760, 1996.
- 47- Kazafy H S., ***“Synthetic Fertilizers; Role and Hazards”***, Fertilizer Technology Vol. 1: Synthesis, DOI: 10.13140/RG.2.1.2395.3366, pp.110-133, 2016.
- 48- Timothy W. T., ***“History, Design, and Manufacture of Explosives”***, Scientific Principles of Improvised Warfare and Home Defense, Scientific and Technical Intelligence Press, Vol.3, 1997.
- 49- Steven L. B., ***“Smokeless Propellants as Vehicle Borne IED Main Charges: An Initial Threat Assessment”***, MSc. Thesis, United States Marine Corps, Command and Staff College, Marine Corps University, 2008.

References

- 50- Hummel R. and Dubroca T., ***“Laser- and Optical-based Techniques for the Detection of Explosives”***, Encyclopedia of Analytical Chemistry, John Wiley & Sons, Ltd., DOI: 10.1002/9780470027318.a0716.pub2, 2013.
- 51- Rudolf M. Josef K. and Axel H., ***“Explosives”***, Book, Wiley-VCH Verlag GmbH, Weinheim, ISBN: 978-3-527-31656-4, 2007.
- 52- Itamar M., Alona P., Salman R., and Ilana B., ***“Detection of explosives and latent fingerprint residues utilizing laser pointer-based Raman spectroscopy”***, Appl. Phys. B, Vol. 113, NO.4, P511–518, 2013.
- 53- Zbigniew B., Jacek J., Adam K., Janusz M., Norbert P., Mateusz P., Tadeusz P., Tadeusz S. and Jacek W., ***“Sensors and Systems for the Detection of Explosive Devices: An Overview”***, Metrology and Measurement Systems, Metrol. Meas. Syst., Vol. XIX, No. 1, pp. 3-28, ISSN 0860–8229, 2012.
- 54- David H., ***“Analytical Chemistry: Spectroscopic Methods”***, Saylor.org, 2012.
- 55- David D. T., Aleksandr V. M., Brian E. L., and Sanford A. A., ***“Deep Ultraviolet Resonance Raman Excitation Enables Explosives Detection”***, Society for Applied Spectroscopy, Vol. 64, No. 4, pp. 425-432, 2010.
- 56- Ann M. F., ***“Investigation of Select Energetic Materials by Differential Reflection Spectrometry”***, Ph.D. Thesis, University of Florida, 2007.

References

- 57- Digambar D. G., *“Electronic Spectroscopy”*, Dept. Of Chemistry, Govt. College Of Arts & Science, Aurangabad, 2003.
- 58- David S. M., *“Instrumentation for trace detection of high explosives”*, Review of Scientific Instruments, 75(8), pp.2499-2512, DOI: 10.1063/1.1771493, 2004.
- 59- John. M. H., *“MODERN SPECTROSCOPY”* Fourth Edition by John Wiley & Sons Ltd England ISBN 0 470 84416 7, 2004.
- 60- James,R.,B., *“A note on the Beer-Lambert lawanalytica chimica acta”* Published by Elsevier B.V. Volume 27 , Pages 95-97 1962.
- 61- Beb A.,B.,Smirne G.,Godun R.,M.,Foot C. G., *“ A method of state selective transfer of atoms between microtraps based on the franck condon principal ”*journalof physics BV40,NO21,2007.
- 62- Craig C. B., *“Enhanced Detection of Induced Fluorescence from Residual Radioactive Materials”*, PhD thesis, University of Nevada, Las Vegas, 2008.
- 63- Bhartia R., Hugh W., and Reidb R., *“Improved sensing using simultaneous deep UV Raman and fluorescence detection”* SPIE-The International Society for Optical Engineering, 2012.
- 64- Mohammad S. M., Zeyad A. S., Talib Z. T., *“Laser-Induced Breakdown Spectroscopy (Libs): An Innovative Tool for Elemental Analysis of Soils”*, International Journal of Modern Trends in Engineering and Research (IJMTER), Vol. 03, Issue 04, ISSN (Online):2349–9745, ISSN (Print): 2393-8161, 2016.
- 65- YONGJUN L. *“Photophysics Of Conjugated Organometallic Systems: Photoinduced Electron And Energy Transfer, Triplet Exciton Dleocalization, And Phosphorescent Organogelators”*, PhD thesis,. University of FLORIDA, 2009.

References

- 66- XI Jiang, *“Dual-Pulse Laser Induced Breakdown Spectroscopy in the Vacuum Ultraviolet with Ambient Gas: Spectroscopic Analysis and Optimization of Limit of Detection of Carbon and Sulfur in Steel”*, PhD thesis, School of Physical Sciences and Technology, Dublin City University, 2012.
- 67- Joachim N. and Alfred V., *“Laser-Induced Plasma Formation in Water at Nanosecond to Femtosecond Time Scales: Calculation of Thresholds, Absorption Coefficients, and Energy Density”*, IEEE Journal of Quantum Electronics, Vol. 35, No. 8, August 1999.
- 68- Jennifer G. and Frank CD. L., *“Laser-Induced Breakdown Spectroscopy for the Standoff Detection of Explosive Residues”*, Applied Industrial Optics: Spectroscopy, Imaging and Metrology, ISBN: 1-55752-947-7, 2012.
- 69- De Lucia F.C., Gottfried J. L., Munson C. A., and Miziolek A. W., *“Double Pulse Laser Induced Breakdown Spectroscopy of Explosives: Initial Study towards Improved Discrimination”*, Spectrochim. Acta, Part B, 62, pp.1399-1404, 2007.
- 70- Cristina L., Santiago P., Javier L., Frank D., Andrzej W., Jeremy R., Roy A. and Andrew I. *“Test of a stand-off laser-induced breakdown spectroscopy sensor for the detection of explosive residues on solid surfaces”*, Journal of Analytical Atomic Spectrometry, V. 21, P. 55–60, 2006.
- 71- Sara W., Anna P., Henric Ö., and Alison H., *“Laser-based standoff detection of explosives: a critical review”*, Springer-Verlag, Analytical and Bioanalytical Chemistry, Vol. 395, Issue 2, pp.259–274, 2009.

References

- 72- Robert D. W., Avishekh P., Dennis K. K., Jeremy R., Edwin L. D., and Guy O., “ *Standoff LIBS measurements of energetic materials using a 266nm excitation laser*”, SPIE, Vol 6954, 2008.
- 73- Sauer M., Hofkens J. and Enderlein J., “ *Handbook of Fluorescence Spectroscopy and Imaging: From Ensemble to Single Molecules*”, Wiley, 2011.
- 74- Paul M. P., Ellen L. H., Mikella E. F. “ *Laser – Based Optical Detection Of Explosive*”,Book, CRC Press,ISBN: 978-1-4822-3328-5,2016.
- 75- Guuichetea A., Eric D. E“*Detection of Explosive Threats*”, Applied Spectroscopy, Vol. 68, Num. 8, 2014.
- 76- Qiyin F., Thanassis P., Javier A., Russel V., Laura M., Kumar Sh. “ *Time-domain laser-induced fluorescence spectroscopy apparatus for clinical diagnostics*”,Review of Scientific Instruments , VOL., 75, N. 1 , 2004.
- 77- Alessandro E., Beyond Range: “ *Innovating Fluorescence Microscopy Remote Sens*” ,VOL. 4, Issue (1), P 111-119; oi: 10.3390/Rs 4010111 ,2012.
- 78- Julia M.H., Amanda P. S., Fredrick M.P., and Rechard N.D. “*Monitoring biosensor activity in living cells with fluorescence lifetime imaging microscopy*”, INT.J.MOL.SCI, Nov 7;13 (11): 14385-400. Do: 10.3390/ijms131114385, 2012.

References

- 79- M.J.Booth, T. WILSON “*Low-cost, frequency-domain fluorescence lifetime confocal microscopy*” Journal of Microscopy, Vol. 214, Pt 1 April 2004, pp. 36–42 ,November 2003.
- 80- Michael W., “ *Time-Correlated Single Photon Counting*”, Technical Note , v. 2, No.1,2009.

المُلخَص :

من أجل تطوير أسلوب كفوء للكشف عن وجود متفجرات، تمت دراسة تقنيات عديدة قادرة على كشف المتفجرات، الدراسة الحالية توفر عرضاً للتقنيات الحالية مثل التحليل الطيفي للبلازما المحتثة بالليزر (LIBS) التي هي تحليل الطيف الذري، ودراسة تقنية جديدة للكشف عن تسمى الفلورة المحتثة بالليزر (LIF).

(LIF) تقيس الانبعاث البصري للمواد المتفجرة المثارة بالليزر، وان استعمال (LIF) ادى الى اكتشاف خصائص ضوئية غير مسجلة لبعض المركبات التي تكون خاصه لهذه للمواد، مثلًا ازاحه الطور وتغير العمق لإشارة الفلورة.

مقياس طيفي له قدرة تحليل عاليه يتم استخدامه لتسجيل الاطوال الموجيه لانبعاث الفلورة لثلاثة أنواع من المواد المتفجرة، وهذه الخصائص البصرية تتألف من انحناءات في طيف طول موجة بين (300-370) نانومتر للثلاث عينات.

باستخدام مضخم ضوئي (photomultiplier) له وقت ارتفاع سريع ومكبر خاص لإشارة الفلورة تمكننا من قياس المجال الزمن لطيف الفلورة لثلاثة أنواع من المواد المتفجرة (AN)، (TNT)، (C₄) وغيرها من المواد غير المتفجرة، هذه الطريقة المستخدمة بعناية للكشف عن بعد لمسافه 8 متر.

تم فحص انواع مختلفه من القواعد لمحاكاة التفحص الحقيقي، وتم قياس مجال الزمن و مجال التردد لكفاءة التحليل الطيفي باستعمال (LIF) التي تعطينا تكوين إجمالي للعينة المفحوصه.

مكتبة للوصف الزمني الكلي لطيف عده انواع من المواد تمكننا من وضع خوارزميه للتمييز بين المواد المتفجرة وغير المتفجرة. والتي استعملت لوضع برنامج لتحقيق نظام الكشف عالي الحساسية.



جمهورية العراق
وزارة التعليم العالي
والبحث العلمي
جامعة النهرين
كلية العلوم
قسم الفيزياء

تطوير واستخدام منظومه كشف المواد المتفجرة عن بعد

أطروحة

مقدمة الى كلية العلوم / جامعة النهرين

وهي جزء من متطلبات نيل درجة الدكتوراه في فلسفه الفيزياء

من قبل

ولدان محمد عواد

بكالوريوس علوم فيزياء-كلية العلوم للبنات /جامعة بغداد (1999)

ماجستير علوم فيزياء- كلية العلوم للبنات /جامعة بغداد (2004)

اشراف

د.كمال حسين لطيف
رئيس باحثين

د. سهى موسى خورشيد
استاذ مساعد

تشرين الأول 2016 م

محرم 1437 هـ